

การสังเคราะห์พอลิไมด์ที่นำกระแสไฟฟ้าด้วยวิธีการต่อกิ่งด้วยพอลิเมอร์ที่นำกระแสไฟฟ้า

นายสุทธิศักดิ์ ศรีสุวรรณ

วิทยานิพนธ์นี้เป็นส่วนหนึ่งของการศึกษาตามหลักสูตรปริญญาวิทยาศาสตรดุษฎีบัณฑิต

สาขาวิชาวิศวกรรมเคมี ภาควิชาวิศวกรรมเคมี

คณะวิศวกรรมศาสตร์ จุฬาลงกรณ์มหาวิทยาลัย

ปีการศึกษา 2555

ลิขสิทธิ์ของจุฬาลงกรณ์มหาวิทยาลัย

บทคัดย่อและแฟ้มข้อมูลฉบับเต็มของวิทยานิพนธ์ตั้งแต่ปีการศึกษา 2554 ที่ให้บริการในคลังปัญญาจุฬาฯ (CUIR)

เป็นแฟ้มข้อมูลของนิสิตเจ้าของวิทยานิพนธ์ที่ส่งผ่านทางบัณฑิตวิทยาลัย

The abstract and full text of theses from the academic year 2011 in Chulalongkorn University Intellectual Repository(CUIR) are the thesis authors' files submitted through the Graduate School.

SYNTHESIS OF CONDUCTIVE POLYIMIDE VIA GRAFT CONDUCTIVE POLYMER

Mr. Suttisak Srisuwan

A Dissertation Submitted in Partial Fulfillment of the Requirements
for the Degree of Doctor of Engineering Program in Chemical Engineering

Department of Chemical Engineering

Faculty of Engineering

Chulalongkorn University

Academic Year 2012

Copyright of Chulalongkorn University

Thesis Title SYNTHESIS OF CONDUCTIVE POLYIMIDE VIA
GRAFT CONDUCTIVE POLYMER
By Mr. Suttisak Srisuwan
Field of Study Chemical Engineering
Thesis Advisor Associate Professor M.L. Supakanok Thongyai, Ph.D.

Accepted by the Faculty of Engineering, Chulalongkorn University in
Partial Fulfillment of the Requirements for the Doctoral Degree

.....Dean of the Faculty of Engineering
(Associate Professor Boonsom Lerthirunwong, Dr.Ing.)

THESIS COMMITTEE

.....Chairman
(Professor Piyasan Prasertdam, Dr.Ing.)

.....Thesis Advisor
(Associate Professor M.L. Supakanok Thongyai, Ph.D.)

.....Examiner
(Associate Professor Bunjerd Jongsomjit, Ph.D.)

.....Examiner
(Associate Professor Artiwan Chotipruk, Ph.D.)

.....External Examiner
(Assistant Professor Sirirat Wacharawichanant, D.Eng.)

สุทธิศักดิ์ ศรีสุวรรณ: การสังเคราะห์พอลิอิมิด์ที่นำกระแสไฟฟ้าด้วยวิธีการต่อกิ่งด้วยพอลิเมอร์ที่นำกระแสไฟฟ้า (SYNTHESIS OF CONDUCTIVE POLYIMIDE VIA GRAFT CONDUCTIVE POLYMER) อ.ที่ปรึกษาวิทยานิพนธ์หลัก: รศ.ดร.ม.ล.ศุภกนก ทองใหญ่, 144 หน้า.

พอลิอิมิด์เป็นพอลิเมอร์ที่ได้มีการศึกษากันอย่างกว้างขวาง โดยเฉพาะอย่างยิ่งในด้านอุปกรณ์ทางไฟฟ้าต่างๆ เนื่องจากมีคุณสมบัติในการทนความร้อนและสารเคมีได้เป็นอย่างดี รวมถึงมีความทนทานและขึ้นรูปได้ง่าย ซึ่งในงานวิจัยนี้ได้เน้นศึกษาและพัฒนาพอลิอิมิด์ให้มีคุณสมบัติในการนำไฟฟ้าและสามารถละลายน้ำได้ เพื่อนำไปปรับใช้กับแผงวงจรไฟฟ้า จอโอแอลอีดีและจอแสดงผลของอุปกรณ์ไฟฟ้าต่างๆ รวมไปถึงตัวรับประจุในเซลล์แสงอาทิตย์แบบอินทรีย์ โดยการทดลองแบ่งออกเป็น 4 ส่วนดังนี้ ในส่วนแรกได้ทำการศึกษาการสังเคราะห์พอลิอิมิด์นำไฟฟ้าโดยใช้วิธีต่อกิ่งด้วยพอลิเออนินิลิน และฟิล์มที่ได้มีค่าการนำไฟฟ้าอยู่ในช่วง 2.96-16.20 ซีเมนต์ต่อเซ็นติเมตร ซึ่งขึ้นอยู่กับปริมาณของพอลิเออนินิลินในสายโซ่ของโคพอลิเมอร์ ส่วนในด้านของการทนความร้อนนั้น โคพอลิเมอร์มีคุณสมบัติที่ดีกว่าพอลิเออนินิลิน ในส่วนที่สองได้ทำการสังเคราะห์ฟิล์มพอลิอิมิด์นำไฟฟ้าที่มีความแข็งแรงทนทาน โดยทำการเปรียบเทียบการขึ้นรูปฟิล์ม 2 แบบ ระหว่างการเคลือบส่วนที่นำไฟฟ้าไว้บนผิวของพอลิอิมิด์กับการผสมส่วนที่นำไฟฟ้าในเนื้อฟิล์มของพอลิอิมิด์ ซึ่งฟิล์มที่ผ่านการขึ้นรูปด้วยการเคลือบส่วนที่นำไฟฟ้าไว้ที่ผิวของพอลิอิมิด์ มีค่าการนำไฟฟ้า ความแข็งแรงทนทาน และสามารถทนต่อความร้อนได้ดีกว่า ในส่วนที่สามได้ทำการสังเคราะห์และเปรียบเทียบพอลิเมอร์นำไฟฟ้า 3 ชนิด ได้แก่ พอลิ(3,4-เอทิลีนไดออกซีไทโอปีน) พอลิเออนินิลิน พอลิไพโรโรลโดยใช้ซัลโฟเนตพอลิเอมิกแอซิด 2 ชนิดเป็นเติมเพลด พบว่าพอลิเออนินิลิน-ซัลโฟเนตพอลิเอมิกแอซิด1 มีค่าการนำไฟฟ้าสูงที่สุดที่ 7.74 ซีเมนต์ต่อเซ็นติเมตร ในภาวะปราศจากการอบหรือการเติมสารปรับปรุงใดๆ ในขณะที่พอลิเออนินิลิน-ซัลโฟเนตพอลิเอมิกแอซิด2 มีค่าการนำไฟฟ้าสูงที่สุดที่ 1.47 ซีเมนต์ต่อเซ็นติเมตร ที่ภาวะการเติมโดเมทิลฟอร์มาไมด์ 0.1 เปอร์เซ็นต์โดยน้ำหนัก ระบบของพอลิไพโรโรลมีค่าการนำไฟฟ้าเพิ่มขึ้นเมื่อเติมสารปรับปรุงและอบในระยะเวลาสั้นๆ อย่างไรก็ตามยังพบว่าระบบของพอลิเออนินิลินมีความเสถียรทางความร้อนต่ำกว่าระบบของพอลิ(3,4-เอทิลีนไดออกซีไทโอปีน) และพอลิไพโรโรล ในส่วนสุดท้ายได้ทำการสังเคราะห์พอลิเมอร์นำไฟฟ้า พอลิ(3,4-เอทิลีนไดออกซีไทโอปีน) โดยใช้เติมเพลด 3 ชนิด คือ พอลิ(สไตรีน ซัลโฟนิค แอซิด), ซัลโฟเนตพอลิเอมิกแอซิด1 และซัลโฟเนตพอลิเอมิกแอซิด 2 ซึ่งพบว่าพอลิเมอร์ที่ได้จากการเตรียมโดยการใส่ใบพัดกวนในการกวนผสม ใช้เวลาในการเตรียมที่น้อยกว่าและมีค่าการนำไฟฟ้าที่มากกว่าพอลิเมอร์ที่ได้จากการเตรียมโดยการใส่แท่งแม่เหล็กกวนสารในการกวนผสม นอกจากนี้พอลิเมอร์ที่สังเคราะห์ได้ยังสามารถเพิ่มค่าการนำไฟฟ้าได้โดยการเติมสารตัวเติม (เป็นโซ-1,4-ไดออกซาน, อิมิดาโซล และควิน็อกซาไลน์) และนำไปผ่านกระบวนการทรีทเม้นท์ด้วยความร้อน

ภาควิชา..... วิศวกรรมเคมี..... ลายมือชื่อนิสิต.....
 สาขาวิชา..... วิศวกรรมเคมี..... ลายมือชื่อ อ.ที่ปรึกษาวิทยานิพนธ์หลัก.....
 ปีการศึกษา..... 2555.....

5171858321: MAJOR CHEMICAL ENGINEERING

KEYWORDS: CONDUCTIVE POLYIMIDE/ CONDUCTING POLYMERS/
TEMPLATE POLYMERIZATION/ WATER-DISPERSIBLE

SUTTISAK SRISUWAN: SYNTHESIS OF CONDUCTIVE POLYIMIDE
VIA GRAFT CONDUCTIVE POLYMER. ADVISOR: ASSOC. PROF.
M.L.SUPAKANOK THONGYAI, Ph.D., 144 pp.

Polyimide has been widely studied, especially in terms of electronic devices due to their high thermal resistance, excellent chemical resistance, dimensional stability and ease of fabrication. This research was studied to improve polyimide properties in terms of conductive and water soluble materials for applications in printed circuit board (PCB), electrochromic displays, organic light emitting diodes (OLEDs) and organic photovoltaic devices (OPVs). The experimental consisted of 4 parts. The first part was studied the preparation of conductive polyimide-graft-polyaniline. Polyimide copolymer molecules can be made conductive by cooperation of grafted polyaniline. The conductivities of polyimide copolymers were in the range of 2.96-16.20 S/cm, depended on the chain length of graft polyaniline. The thermal stability of the polyimides copolymer was higher than the nascent polyaniline. The second part was studied the synthesis of the high strength surface-conductive polyimide film via comparison with polyimide/polyaniline-g-polyimide composite film. The conductivities, thermal stabilities and mechanical properties of surface-conductive polyimides were higher than conductive polyimide composites. The third part was studied comparison on three conducting polymers (PEDOT, PANI, PPy) with two sulfonated poly(imide)s. PANI-SPAA1 had the highest conductivity of 7.74 S/cm, which was without heat treatment and secondary doping. PANI-SPAA2 had the highest conductivity of 1.47 S/cm, which was doped with 0.1 wt.% of DMF. For PPy systems, the result showed the similar trends to the PEDOT systems. The conductivities were increased after doped with a secondary dopant and annealed for a short time. However, PANI system showed the lower thermal stability than PEDOT and PPy systems. The forth part was studied the preparation of high conductivities conducting polymers (PEDOT-PSS, PEDOT-SPAA1 and PEDOT-SPAA2) by using new method for the polymerization (SPAA1, SPAA2). The new method (mechanical stirring) to synthesis PEDOT with sulfonated poly(amic acid) template was undertaken and caused less reaction time and more conductivity than our earlier systems (magnetic stirring). The conductivities of PEDOT-SPAAs could be further enhanced by using the new secondary dopants (Benzo-1,4-dioxan, imidazole and quinoxaline) and heat treatment.

Department: Chemical Engineering Student's signature.....
Field of study: Chemical Engineering Advisor's signature.....
Academic Year: 2012

ACKNOWLEDGEMENTS

I would like to express my deeply gratitude to my advisor, Associate Professor Dr. M.L. Supakanok Thongyai to his continuous guidance, enormous number of invaluable discussions, helpful suggestions, warm encouragement and patience to correct my writing. I would like to thank Professor Dr. Piyasan Prasertdam, Associate Professor Dr. Bunjerd Jongsomjit, Assistant Professor Dr. Artiwan Chotipruk, and Assistant professor Dr. Sirirat Wacharawichanant from the Department of Chemical Engineering, Faculty of Engineering and Industrial Technology, Silpakorn University for serving as chairman and thesis committees, respectively, whose comments were constructively and especially helpful.

Sincere thanks are made to Mektec Manufacturing Corporation (Thailand) Limited for supporting the materials and the characterize equipments, and most important the scholarship for my Doctorate in Chemical Engineering.

I would like to thank Professor Gregory A. Sotzing from the Institute of Materials Science and the Polymer program, University of Connecticut, USA for his kindness, very good advice and being very helpful. I also would like to thank to Michael A. Invernale, Yujie Ding and Donna Mamangun for the supplied the new knowledge, good advices in the laboratory and their helpful friendship during my study in USA.

Sincere thanks to all my friends and all members of the Center of Excellent on Catalysis & Catalytic Reaction Engineering (Petrochemical Engineering Research Laboratory), Department of Chemical Engineering, Chulalongkorn University for their assistance and friendly encouragement.

Finally, I would like to dedicate this thesis to the memory of my parents and my families, who generous supported and encouraged me through the year spent on this study. I hope they would have been proud.

CONTENTS

| | Page |
|--|------|
| ABSTRACT (THAI) | iv |
| ABSTRACT (ENGLISH)..... | v |
| ACKNOWLEDGEMENTS..... | vi |
| CONTENTS..... | vii |
| LIST OF TABLES | ix |
| LIST OF FIGURES | xi |
| CHAPTER | |
| I INTRODUCTION | 1 |
| 1.1 Objectives of the research..... | 5 |
| 1.2 Scope of the research | 5 |
| II THEORY..... | 7 |
| 2.1 Polyimides..... | 7 |
| 2.2 Sulfonated polyimides | 14 |
| 2.3 Conducting polymer..... | 16 |
| 2.4 Template polymerization | 24 |
| 2.5 Conductive Polymers versus Metals and Insulators | 24 |
| 2.6 Commercial Conducting Polymers | 26 |
| III LITERATURE REVIEWS | 37 |
| 3.1 Conductive polyimide..... | 37 |
| 3.2 Poly(styrene sulfonic acid) template..... | 41 |
| 3.3 Other templates | 46 |
| 3.4 Sulfonated polyimide | 47 |
| IV EXPERIMENT..... | 51 |
| 4.1 Materials and Chemicals..... | 51 |
| 4.2 Equipments | 53 |

| CHAPTER | Page |
|---|------|
| 4.3 Synthesis | 57 |
| 4.4 Characterization instruments | 66 |
| V RESULTS AND DISCUSSION | 71 |
| 5.1 Preparation and characterization of conductive polyimide-graft-polyaniline | 71 |
| 5.2 Organic surface conductive polyimide | 80 |
| 5.3 Comparison of the thermally stable conducting polymers PEDOT, PANI, and PPy using sulfonated poly(imide) templates via poly(amic acid)..... | 86 |
| 5.4 Secondary dopants modified PEDOT-sulfonated poly(imide)s for high temperature range application..... | 110 |
| VI CONCLUSIONS AND RECOMMENDATIONS | 117 |
| 6.1 Conclusions..... | 117 |
| 6.2 Recommendations..... | 119 |
| REFERENCES | 120 |
| APPENDICES | 131 |
| APPENDIX A..... | 132 |
| APPENDIX B | 139 |
| APPENDIX C | 142 |
| APPENDIX D..... | 143 |
| VITA..... | 144 |

LIST OF TABLES

| | | Page |
|------------|---|-------------|
| Table 2.1 | Sulfonated diamines..... | 15 |
| Table 2.2 | Typical commercial PEDOT-PSS grades and their characteristics | 30 |
| Table 2.3 | Additives and their effect on the conductivity of PEDOT-PSS films | 32 |
| Table 2.4 | Typical conducting polymer structures (undoped form) | 36 |
| Table 3.1 | Chemical structures of the monomers used in preparation of polyimides..... | 40 |
| Table 5.1 | Molar ratio of compositions on the reaction mixtures..... | 73 |
| Table 5.2 | Films compositions on the reaction mixtures | 81 |
| Table 5.3 | Conductivities of PEDOT-PSS (in house) and PEDOT-SPAA | 90 |
| Table 5.4 | Conductivities of secondary-doped PEDOT-SPAA1 at various processing temperatures..... | 91 |
| Table 5.5 | Conductivities of secondary-doped PEDOT-SPAA2 at various processing temperatures..... | 92 |
| Table 5.6 | Conductivities of PANI-PSS (in house) and PANI-SPAA | 93 |
| Table 5.7 | Conductivities of secondary-doped PANI-SPAA1 at various processing temperatures..... | 94 |
| Table 5.8 | Conductivities of secondary-doped PANI-SPAA2 at various processing temperatures..... | 95 |
| Table 5.9 | Conductivities of PPy-PSS (in house) and PPy-SPAA | 96 |
| Table 5.10 | Conductivities of secondary-doped PPy-SPAA1 at various processing temperatures..... | 97 |
| Table 5.11 | Conductivities of secondary-doped PPy-SPAA2 at various processing temperatures..... | 98 |
| Table 5.12 | Comparison conductivities of conducting polymers before and after annealing at 180°C, 10 minutes | 115 |
| Table A-1 | Conductivities of PEDOT-PSS (in house) and PEDOT-SPAA | 132 |

| | Page |
|---|-------------|
| Table A-2 Conductivities of secondary-doped PEDOT-PSS at various processing temperatures..... | 133 |
| Table A-3 Conductivities of secondary-doped PEDOT-SPAA1 at various processing temperatures..... | 135 |
| Table A-4 Conductivities of secondary-doped PEDOT-SPAA2 at various processing temperatures..... | 137 |

LIST OF FIGURES

| | | Page |
|-------------|---|-------------|
| Figure 2.1 | Aromatic Polyimide Repeat Unit..... | 7 |
| Figure 2.2 | Reaction of dicyanomethylidene phthalide with aniline..... | 8 |
| Figure 2.3 | Polymerization of bisdicyanomethylidene derivative of PMDA with ODA | 9 |
| Figure 2.4 | Preparation of Kapton polyimide..... | 9 |
| Figure 2.5 | Reaction mechanism of imide formation..... | 11 |
| Figure 2.6 | Commonly used diamine monomers | 11 |
| Figure 2.7 | Commonly used dianhydride monomers | 12 |
| Figure 2.8 | Mechanism involved in chemical dehydration of amic acid (R=ethyl, Ar=phenyl) | 13 |
| Figure 2.9 | chemical structure of some conjugated polymers | 19 |
| Figure 2.10 | Conductivity of some metals and doped conjugated polymers | 20 |
| Figure 2.11 | Energy band in solid | 22 |
| Figure 2.12 | Synthesis of EDOT from oxalic acid ester and thiodiacetic acid ester | 27 |
| Figure 2.13 | Transesterification as a synthetic route to EDOT derivatives..... | 28 |
| Figure 2.14 | Structure of PEDOT-PSS..... | 29 |
| Figure 2.15 | Polypyrrole polymerization | 35 |
| Figure 3.1 | Synthesis of the imide macromonomer of oligoaniline and electroactive polyimide..... | 41 |
| Figure 3.2 | Structure of poly(styrene sulfonic acid) (PSSA)..... | 42 |
| Figure 3.3 | Chemical structure of the PEDOT-DNA template..... | 47 |
| Figure 3.4 | Structure of the PHMPS template | 47 |
| Figure 4.1 | Glove box..... | 54 |
| Figure 4.2 | Schlenk line..... | 54 |
| Figure 4.3 | Schlenk tube..... | 55 |

| | Page |
|-------------|---|
| Figure 4.4 | Inert gas supply system.....55 |
| Figure 4.5 | Vacuum pump56 |
| Figure 4.6 | Scheme for the 4,4'-ODADS reaction60 |
| Figure 4.7 | Synthesis of sulfonated poly(amic acid) (SPAA1)61 |
| Figure 4.8 | Fourier transform infrared spectroscopy (FT-IR) equipment.66 |
| Figure 4.9 | Thermogravimetric analysis (TGA) equipment.....67 |
| Figure 4.10 | Current generator, multimeter and four-point probe (gold wires)68 |
| Figure 4.11 | Current generator and nanovoltmeter equipped with four-point probe (platinum wires).....69 |
| Figure 4.12 | Tensile testing machine Equipment70 |
| Figure 5.1 | ¹ H NMR spectrum of DHBD(a), BA(b) and DHBD-BA(c)74 |
| Figure 5.2 | (a) ¹ H NMR spectrum of Main Chain Polyimide before grafting, (b) ¹ H NMR spectrum of Graft Copolymer Obtained76 |
| Figure 5.3 | FTIR spectra of each PANI-g-PI samples in comparison with pure PI and pure PANI for comparison77 |
| Figure 5.4 | GPC of PI, PI-PANI(1), PI-PANI(2), and PI-PANI(3)78 |
| Figure 5.5 | TGA of PI, PANI, PI-PANI(1), PI-PANI(2), and PI-PANI(3) as a function of annealing temperature in air79 |
| Figure 5.6 | FTIR spectra of PI, PI/PI-PANI_10, PI/PI-PANI_10(2)B, and PI/PI-PANI_10(2)F.....81 |
| Figure 5.7 | Isothermal TGA at 300 °C for PI, PI/PI-PANI_5, PI/PI-PANI_10, PI/PI-PANI_10(2) and PI/PI-PANI_20(2).....82 |
| Figure 5.8 | Conductivities of PI[A], PI/PI-PANI_2.5[B], PI/PI-PANI_5[C], PI/PI-PANI_7.5[D], PI/PI-PANI_10[E], PI/PI-PANI_10(2)[F], PI/PI-PANI_15(2)[G], PI/PI-PANI_20(2)[H]83 |

| | | |
|-------------|---|-----|
| Figure 5.9 | Tensile stresses of PI[A], PI/PI-PANI_2.5[B], PI/PI-PANI_5[C], PI/PI-PANI_7.5[D], PI/PI-PANI_10[E], PI/PI-PANI_10(2)[F], PI/PI-PANI_15(2)[G], PI/PI-PANI_20(2)[H] | 84 |
| Figure 5.10 | SEMs of PI [a], PI/PI-PANI_10 [b], PI/PI-PANI_10(2) [c], PI/PI-PANI_20(2) [d] and cross section of PI/PI-PANI_10(2) [e]..... | 85 |
| Figure 5.11 | Chemical structures of the various conducting polymers and the various templates used in this study, with their corresponding abbreviations | 86 |
| Figure 5.12 | (I) FTIR spectrum of a) SPI1, b) SPAA1. (II) FTIR spectrum of a) SPI2, b) SPAA2..... | 88 |
| Figure 5.13 | Conductivities of PEDOT-SPAA1 | 99 |
| Figure 5.14 | Conductivities of PEDOT-SPAA2 | 99 |
| Figure 5.15 | Conductivities of PANI-SPAA1..... | 100 |
| Figure 5.16 | Conductivities of PANI-SPAA2..... | 100 |
| Figure 5.17 | Conductivities of PPy-SPAA1 | 101 |
| Figure 5.18 | Conductivities of PPy-SPAA2 | 101 |
| Figure 5.19 | Conductivities of each system..... | 102 |
| Figure 5.20 | Overlaid TGAs of a) PEDOT, PANI, PPy with SPI1 and b) PEDOT, PANI, PPy with SPI2..... | 104 |
| Figure 5.21 | Isothermal TGA of PEDOT-PSS..... | 105 |
| Figure 5.22 | Isothermal TGA of PEDOT-SPI1 | 105 |
| Figure 5.23 | Isothermal TGA of PEDOT-SPI2 | 106 |
| Figure 5.24 | Isothermal TGA of PANI-PSS | 106 |
| Figure 5.25 | Isothermal TGA of PANI-SPI1 | 107 |
| Figure 5.26 | Isothermal TGA of PANI-SPI2..... | 107 |
| Figure 5.27 | Isothermal TGA of PPy-PSS..... | 108 |
| Figure 5.28 | Isothermal TGA of PPy-SPI1 | 108 |

| | Page |
|-------------|--|
| Figure 5.29 | Isothermal TGA of PPy-SPI2109 |
| Figure 5.30 | FTIR spectrum of 4,4'-ODADS110 |
| Figure 5.31 | ¹ H NMR spectrum of 4,4'-ODADS111 |
| Figure 5.32 | (I) FTIR spectrum of SPAA1 and SPI1, (II) SPAA2 and SPI2, (III) PEDOT-SPAA1 and PEDOT-SPI1, (IV) PEDOT-SPAA2 and PEDOT-SPI2112 |
| Figure 5.33 | Conductivities of each system at 20°C, 180°C and 300°C114 |
| Figure 5.34 | TEM images of PEDOT-PSS (a), PEDOT-SPAA1 (b) and PEDOT-SPAA2 (c)116 |
| Figure A-1 | Log conductivity of PEDOT-PSS.....134 |
| Figure A-2 | Log conductivity of PEDOT-SPAA1136 |
| Figure A-3 | Log conductivity of PEDOT-SPAA2.....138 |
| Figure B-1 | TGA of Poly(styrene sulfonic acid) (PSSA) in air139 |
| Figure B-2 | TGA of Poly(3,4-ethylenedioxythiophene) (PEDOT) in air139 |
| Figure B-3 | TGA of sulfonated poly(amic acid) (SPAA) in air140 |
| Figure B-4 | Isothermal TGA of PEDOT.....140 |
| Figure B-5 | Isothermal TGA of SPAA141 |

CHAPTER I

INTRODUCTION

Polyimide (PI) is one of the most utilized polymer substrates in electronic industry. Because of its excellent thermo-mechanical properties, good dielectric properties, dimensional stability, ease of fabrication, and excellent chemical resistance. Polyimide is appropriate for a variety of applications in electronic appliances. Normally, polyimide is utilized as a substrate in flexible circuits that are becoming more and more important for miniature size electrical devices [1]. Moreover, Polyimides can be made as conductive materials by combined with conducting polymers especially polyaniline (PANI), and can be utilized as sensor [2], gas separation membrane [3-5] and photoconductive surface in photocopy machine [6]. Polyaniline is one of the most frequently investigated electronically conductive polymers because of its great advanced applications due to its low cost, excellent environmental stability and ease to synthesis. Moreover, many methods were attempted to make high temperature material that was conductive via composited polyaniline in polyimide matrix. Du Pont company was claimed the preparation of composited polyaniline micro-particles in polyimide, which can make the flat conductive freestanding film, with high temperature resistibility, in US patent 7,316,791 [6]. Moon and Seung prepared PANI-DBSA/polyamic acid (PAA) blends via blending PANI-DBSA with pyromellitic dianhydride (PMDA) and 4,4'-oxydianiline (ODA) in a co-solvent and subsequently obtained PANI-DBSA/PI blends through thermal imidization [7]. However, the conductivity was according to the distribution of particles and the durability of the composites and still needed to be improved. The electrochemical behaviors of electroactive polyamides with amine-capped aniline pentamer prepared by oxidative coupling polymerization have also been demonstrated by Zhang and Wei et al [8]. Moreover, Kuan-Yeh Huang et al [9] reported the effects of amine-capped aniline trimer (AT) on the corrosion protection efficiency of as-prepared electroactive polyimide. However, the practical applications of Huang's electroactive aniline oligomer-derivative polymers have seldom been

mentioned because they have low conductivities. If we can equally distribute polyaniline in polyimide, the advanced conductive properties of materials are expected. Normally polyaniline cannot be prepared as freestanding film, so the incorporation with polyimide will enable the preparation of freestanding film for high temperature conductivity application. The possibility to improve and optimize the conductivity, thermal stability and strength of the composite simultaneously may be based on the direct grafting of polyaniline to polyimide main chains. This technique is an easy method to control polyaniline distribution in polyimide matrix while achieving higher conductivities in the same time, but their mechanical properties were quite low. To improve the weakness, we need to use polyimide as polymer matrix to synthesize polyimide/polyaniline-g-polyimide composite films or use as the substrate layer of surface-conductive polyimide films.

On the other hand, conducting polymers can be improved their mechanical properties by using polyimide as the template in the process of template polymerization. Poly(styrene sulfonic acid) (PSSA) is the traditional template for synthesis of viable aqueous dispersions of conducting polymers, such as PEDOT-PSS, PANI-PSS and PPy-PSS, which have achieved popularity for applications in electrochromic displays [10], organic light emitting diodes (OLEDs) [11], organic photovoltaic devices (OPVs) [12], and transparent electrode [12], due to their advantageous properties (excellent transparency in the doped state, high conductivity, good film formation). However, the temperature threshold for these materials is low, less than 200°C before conductivity decreases, which limits its usage in high temperature processing especially when cooperated with metal oxide. For certain high temperature processes (incorporated with metal oxide) and applications (high-heat areas such as deserts); an improvement for different template is needed. Moreover, in an application for organic electronic as transparent electrode, the sulfonate acid groups can cause high acidity which is detrimental to the lifetime of organic electronic component. An improvement to reduce acidity by destroying sulfonate group at above 180°C while maintaining high conductivity is crucially needed. Sulfonated poly(amic acid) was the best choice to use as the new templates for conducting polymers which can be dissolved in water, can be resisted higher temperatures for annealing and also can be annealed for longer times than traditional templates.

This research will be divided into 4 parts. The first part will show the preparation of conductive polyimide-graft-polyaniline. Polyimide copolymer molecules can be made conductive by cooperation of grafted polyaniline. The conductivities of polyimide copolymers were in the range of 2.96-16.20 S/cm, depended on the chain length of graft polyaniline. The thermal stability of the polyimides copolymer was higher than the nascent polyaniline. At high temperature, polyaniline lost its conductivity but copolymer still conducted. The TGA and GPC predicted the similar amount of cooperated polyaniline in copolymer, which proved the success of preparation of graft-copolymer.

The second part will further explain the synthesis of the high strength surface-conductive polyimide (one conductive layer, one substrate layer) via comparison with conductive polyimide composite (mixture of polyimide and polyaniline-g-polyimide). The mechanical properties of polyaniline-g-polyimide films that synthesized with the method from the first part are improved. The conductivities, thermal stabilities and mechanical properties of surface-conductive polyimides were higher than conductive polyimide composites. This modification method can further make conductive photolithographic polyimide.

The third part included the study on various conducting polymers (PEDOT, PANI, and PPy) using sulfonated poly(amic acid) templates (SPAA1, SPAA2). Conducting polymers using SPAA2 template had higher thermal stability than using SPAA1 template with slightly lower conductivity. PANI system had higher conductivities than PPy and PEDOT systems. In term of thermal stability, PEDOT system had more thermally stable than PPy and PANI systems. Moreover, the conductivities of PEDOT and PPy systems are enhanced by addition of various secondary dopants and/or using thermal treatment.

The final part will show the preparation of high conductivities conducting polymers (PEDOT-PSS, PEDOT-SPAA1 and PEDOT-SPAA2) by using new method for the polymerization (SPAA1, SPAA2). Moreover, this part will present the effect of new dopants to increase conductivities of conducting polymers. The new method (mechanical stirring) to synthesis PEDOT with sulfonated poly(amic acid) template was undertaken and caused less reaction time and more conductivity than our earlier systems (magnetic stirring). The conductivities of PEDOT-SPAAs could be further

enhanced by using the secondary dopants and heat treatment. After heat treatment, the structures of PEDOT-SPAAs were changed to PEDOT-SPIs and their conductivities were increased as the same time. Benzo-1,4-dioxan, imidazole and quinoxaline were investigated as the new dopants and could be used as well as surfynol to improve the conductivity (better than DMF dopant). However, the condition of secondary doping with new dopants could be further improved in term of concentration and annealing time to enhance the maximum conductivity. Finally, the high thermal stability and highly conductivity PEDOT-SPI have successfully been synthesized in order to apply for higher application temperature or higher processing temperature without detrimental to the conductivity.

1.1 Objectives of the research

1.1.1 To synthesize conductive polyimide-graft-polyaniline.

1.1.2 To synthesize conductive polyimide composite and surface-conductive polyimide using polyimide-graft-polyaniline as conducting agent.

1.1.3 To synthesize and compare the thermal properties and conductivities of conducting polymers (PEDOT, PANI, PPy) using different sulfonated poly(imide) templates upon heating.

1.1.4 To study the new method and new secondary dopants for increasing conductivities of conducting polymers.

1.2 Scope of the research

1.2.1 Synthesize conductive polyimide-graft-polyaniline from 4,4'-hexa fluoro isopropylidene diphthalic anhydride (6FDA), 3,3'-dihydroxybenzidine (DHBD), 4,4'-oxydianiline (ODA), 3-bromoaniline and Aniline.

1.2.2 Synthesize polyimide from pyromellitic dianhydride (PMDA) with 4,4'-oxydianiline (ODA) to use as polymer matrix of conductive polyimide composite and to use as substrate layer of surface-conductive polyimide.

1.2.3 Synthesize sulfonated polyimide from 4,4'-diaminodiphenyl ether-2,2'-disulfonic acid (4,4'-ODADS) and 4,4'-oxydiphthalic anhydride (O-DPDA), in case SPAA1 and SPI1.

1.2.4 Synthesize sulfonated polyimide from 4,4'-diaminodiphenyl ether-2,2'-disulfonic acid (4,4'-ODADS) and 4,4'-Hexafluoroisopropylideneoxydiphthalic anhydride (6FDA), in case SPAA2 and SPI2.

1.2.5 Synthesize conducting polymers; poly(3,4-ethylene dioxythiophene) (PEDOT), polyaniline (PANI) and polypyrrole (PPy) with the sulfonated poly(imide) templates.

1.2.6 Increase the conductivity of conducting polymers using sulfonated poly(amic acid) as a template with secondary dopants as follows; 5 wt.% of d-sorbitol, 0.1 wt.% DMF, 0.1 wt.% Surfynol®2502, 0.1 wt.% benzo-1,4-dioxan, 5 wt.% imidazole, 0.1 wt.% quinoline, 5 wt.% methyl viologen and 0.1 wt.% quinoxaline.

This thesis is divided into six chapters as follows:

Chapter I provide an overview of polyimide, conductive polyimide, conducting polymers and objective and scope of this research.

Chapter II explains the basic theory about the synthesis of conductive polyimide, synthesis of synthesis sulfonated polyimide and synthesis of conducting polymers.

Chapter III presents literature reviews of the previous works related to conductive polyimide composite, the conventional template (PSSA), the modern template and the method of sulfonated poly(imide) synthesis.

Chapter IV shows the experimental equipments and experimental procedures to synthesis conductive polyimide, sulfonated diamine monomer, conducting polymer, template polymerization, secondary dopant studies, including the preparation of films, also instruments and techniques used for characterizing the resulting polymers.

Chapter V exhibits the experimental results, which was divided to four parts.

- i) Preparation and characterization of conductive polyimide-graft-polyaniline.
- ii) Organic surface conductive polyimide.
- iii) Comparison of the thermally stable conducting polymers PEDOT, PANI, and PPy using sulfonated poly(imide) templates via poly(amic acid).
- iv) Secondary dopants modified PEDOT-sulfonated poly(imide)s for high temperature range application.

Chapter VI shows overall conclusions of this research and recommendations for future research.

CHAPTER II

THEORIES

2.1 Polyimides

Polyimides are classified as one of organic materials known as “high performance” polymers due to their excellent high thermal stability [13]. The structural composition of aromatic polyimides consists primarily of five-membered heterocyclic imide units and aromatic rings, which are linked sequentially by simple atoms or groups, as shown in the generic repeating unit below.

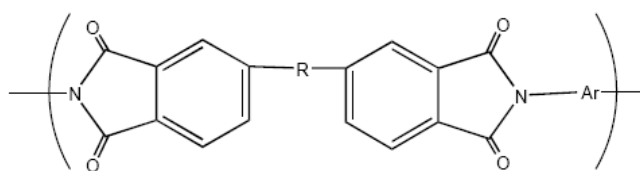


Figure 2.1 Aromatic Polyimide Repeat Unit.

The rigid structure of polyimides provides high glass transition temperatures (T_g) more than 300°C with a good mechanical strength and high modulus. The linearity and stiffness of the cyclic backbone allow for molecular ordering and lead to lower coefficients of thermal expansion (CTE) than those found for thermoplastic polymers having coiled, flexible chains. Additionally, the morphology of long, linear ordered chains provides solvent resistance to the aromatic polyimides [13].

2.1.1 Synthesis Method

2.1.1.1 One-step method

High-Temperature Solution Polymerization

One-stage homogeneous solution polymerization technique can be utilized to synthesis polyimides, which are soluble in organic solvents at the temperatures of polymerization. The mixtures of monomers are heated in a high boiling solvent or a mixture of solvents in a temperature range between 140 to 250°C leading to the

imidization reaction proceeds rapidly. Solvents that commonly used are nitrobenzene, benzonitrile, o-dichlorobenzene, trichlorobenzenes, α -chloronaphthalene, and phenolic solvents such as chlorophenols and m-cresol in addition to dipolar aprotic amide solvents. Toluene is usually used as a cosolvent to accommodate the removal of the water of condensation during polymerization by azeotropic distillation. Water is distilled off continually as an azeotrope along with the solvent while imidization continues to perform via amic acid intermediate. During the polymerization, the concentration of amic acid group become negligible at any time because it is unstable at high temperature and rapidly imidizes, or reverts to amine and anhydride. Because of water, as by-product during the formation of imide, some of the anhydride groups are rapidly hydrolyzed to o-dicarboxylic acid. When a mixture of dianhydride, diamine, and a solvent is heated, a viscous solution is formed at intermediate temperature of 30-100°C resulting in poly(amic acid) [13].

Low-Temperature Solution Polymerization

Kim and Moore [13] were investigated the synthesis of dicyanomethylidene derivative of phthalic anhydride, as shown in Figure 2.2. The resulting compound was reacted with aniline in NMP to produce an intermediate of amic acid that gradually transformed during 24 h at room temperature to N-phenylphthalimide, co producing malonitrile as condensation byproduct. Further, bis(dicyanomethylidene) derivative of PMDA and ODA were reacted in NMP to afford poly(amic acid) intermediate, which underwent partial imidization at room temperature in the homogeneous solution, as shown in Figure 2.3.

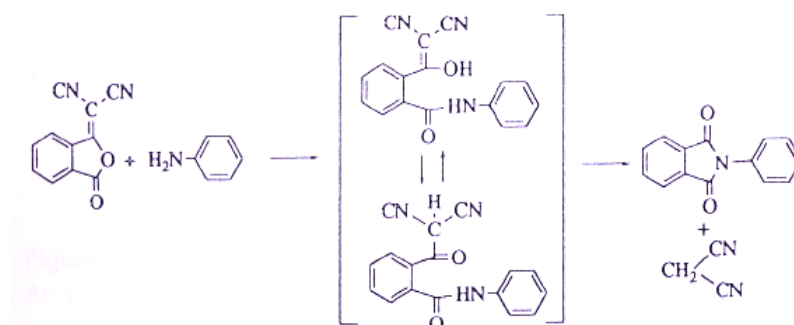


Figure 2.2 Reaction of dicyanomethylidene phthalide with aniline.

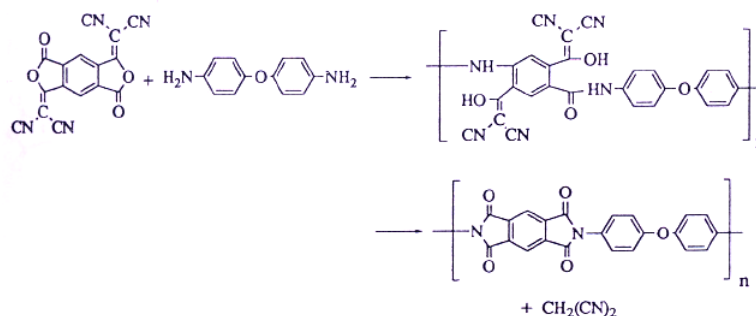


Figure 2.3 Polymerization of bisdicyanomethylidene derivative of PMDA with ODA.

The extent of imidization was reached over 24 h with approximately 75%, after that the polymer began to precipitate. The solid-state imidization of films prepared from the poly(amic acid) analog intermediate behaved similarly to that of poly(amic acid). However, the imidization could be accomplished at lower temperature; it was nearly complete at 120°C in 20 h.

2.1.1.2 Two-step method via poly(amic acids)

The majority problems of polyimides are rigid planar aromatic and heteroaromatic structures which leading to infusible and insoluble. Dupont Company was coped with this problem by synthesizing the soluble polymer precursor, namely “poly(amic acid)” and converting it to the final polyimide [14]. An example of the synthesis of Kapton polyimide as show in Figure 2.4 is the highly elegant process made it possible to bring the first significant commercial polyimide products into the market namely Du Pont’s Kapton™.

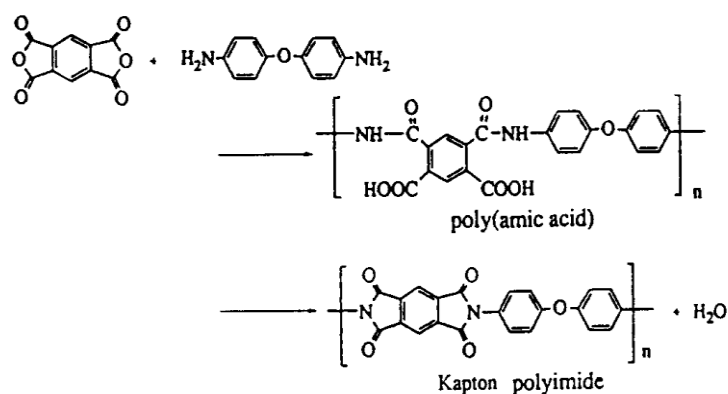


Figure 2.4 Preparation of Kapton polyimide.

The process of two-step poly(amic acid) is the most commonly procedure to synthesis polyimides. In this procedure, a dianhydride is reacted with a diamine in a dipolar aprotic solvent such as N-methyl-2-pyrrolidinone (NMP) or N,N-dimethylacetamide (DMAc) at ambient temperature resulting in a poly(amic acid), which is then convert into the polyimide product. The reaction between 3,3',4,4'-biphenyltetracarboxylic dianhydride (s-BPDA) and 4,4'-diaminodiphdiphenylether (ODA) proceed rapidly at room temperature to make a viscous solution of poly(amic acid), which is an ortho-carboxylated aromatic polyamide.

Poly(amic acid)s can be shaped as films and fibers by removing solvent. The poly(amic acid) films are thermally or chemically converted to form the polyimide and produced water as a by-product. Because water need to be removed during in-situ imidization, the process is generally suitable only for the preparation of thin object such as films.

Formation of poly(amic acid)

When a dianhydride and a diamine are added together into a dipolar aprotic solvent, poly(amic acid) is rapidly formed at ambient temperatures. Figure 2.5 shows the reaction mechanism includes the nucleophilic attacked of the amino group on the carbonyl carbon of the anhydride group, followed by the opening of the anhydride ring to form amic acid group and finally thermally converting to imide structure.

An equilibrium reaction is the most important aspect of this process [15-18]. A high-molecular-weight poly (amic acid) is readily formed in most cases as long as pure reagents are consumed due to the forward reaction is much faster than that the reverse reaction. The high-molecular-weight poly(amic acid) is not formed if the large reaction rate difference is not met. For this reason, it is important to keep the driving forces that favor the forward reaction over the reverse reaction. Because of the acylation reaction of amines is an exothermic reaction, the equilibrium is favored at lower temperatures and the high monomer concentrations leads to the higher molecular-weight poly (amic acids).

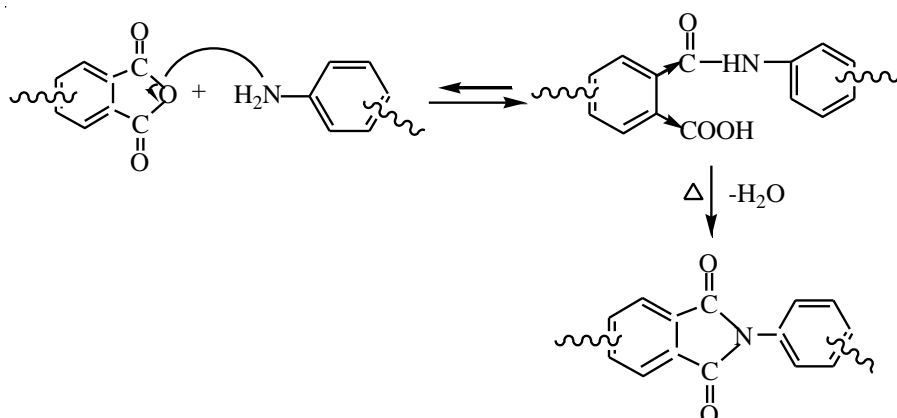


Figure 2.5 Reaction mechanism of imide formation.

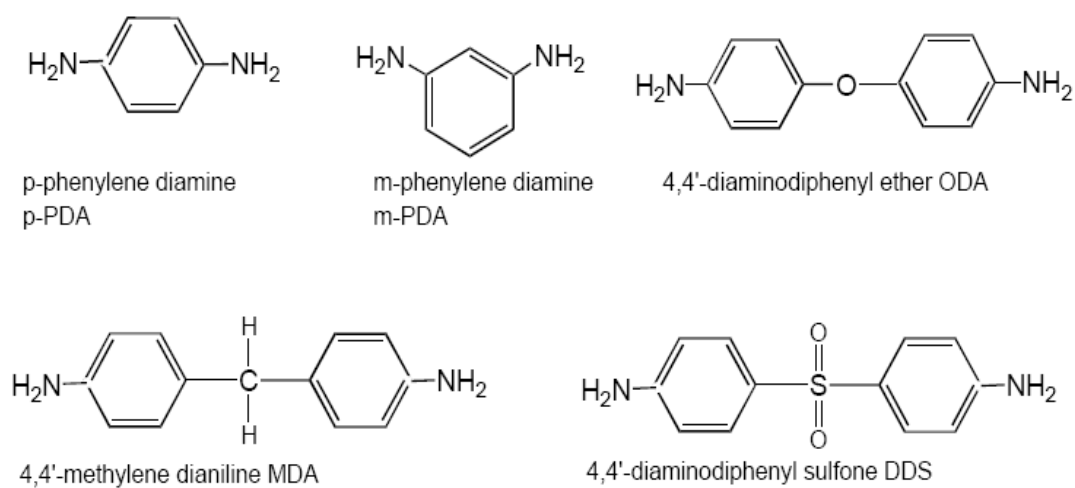


Figure 2.6 Commonly used diamine monomers.

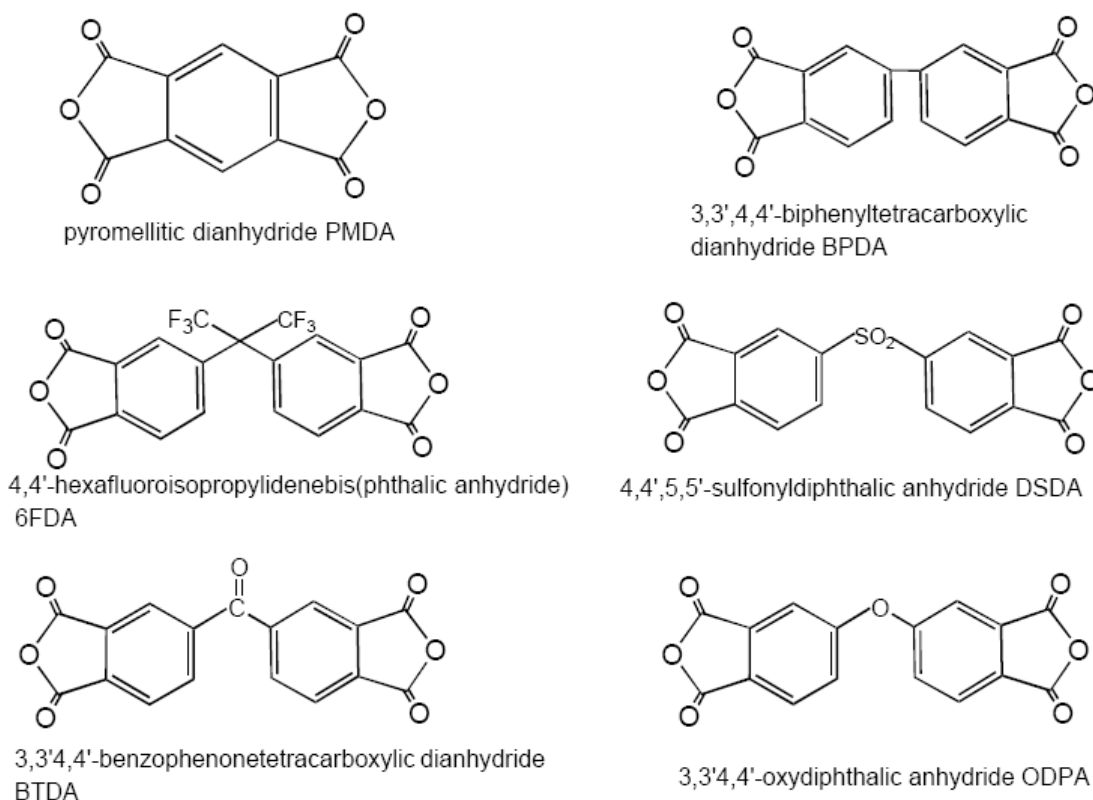


Figure 2.7 Commonly used dianhydride monomers.

Thermal Imidization of Poly (amic acid)

The most common conversion of poly(amic acid)s to the corresponding polyimides is performed thermally in “solid state”. This process is suitable for preparation of thin objects such as films, fibers, coatings, and powders, which allow the diffusion of solvent and by-product out from the thin products without forming voids and brittles in the final polyimide products. The casted films are dried and heated slowly up to 250-350 °C, depending on the stability and glass transition temperature (T_g) of the polymer. The fast heating may cause the formation of bubbles in the sample. After heating, imidization reaction takes place not in a true solid state but rather in a very concentrated sticky solution, at least during the initial and the intermediate stages of thermal imidization. The possession of residual solvent plays an important role in the film forming behaviors. The imidization conducts with faster rate in the possession of dipolar amide solvents. The observance is ascribed as the specific solvation to allow the favorable conformation of amic acid group to cyclize [19]. It may also be clarified by the plasticizing effect of the solvent to increase the

mobility of the reacting functional groups. The likable property of amide solvent also suggests that its basicity to accept protons may be responsible for the specific effect. The proton of the carboxylic group is strongly hydrogen-bonded to the carbonyl group of the amide solvent. Thermal imidization process of poly(amic acid)s is rather complex. It is normally impossible and unlikely to explain the thermally imidized reaction by basic kinetic expression as the process typically includes several interrelated elementary reactions.

Mechanism of Chemical Imidization

The kinetic study of model compounds exposed that imides and isoimides are formed via a mixed-anhydride intermediate (7), which is formed by acylation of the carboxylic group of amic acid (6), as shown in Figure 2.8.

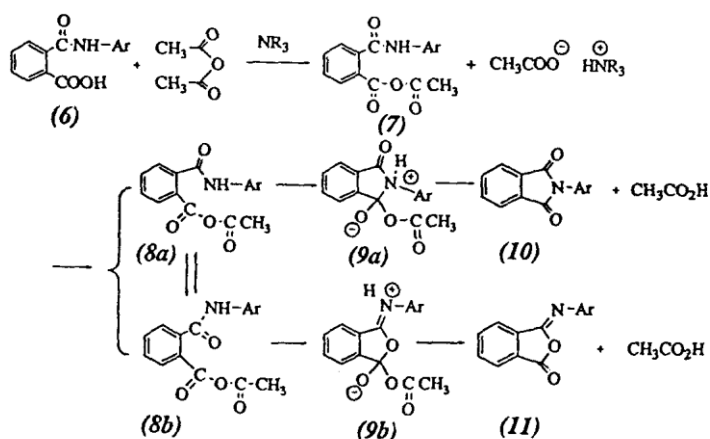


Figure 2.8 Mechanism involved in chemical dehydration of amic acid (R=ethyl, Ar=phenyl).

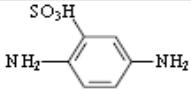
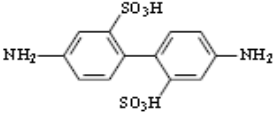
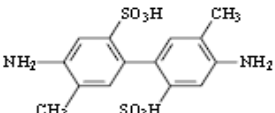
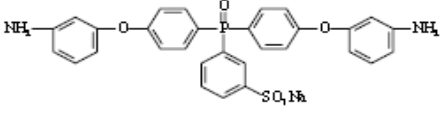
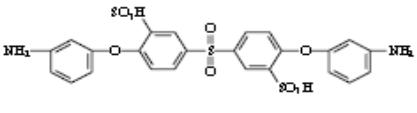
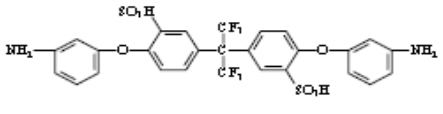
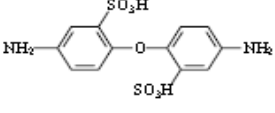
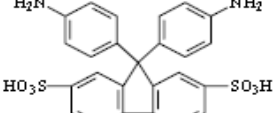
The possession of the intermediate mixed-anhydride could be detected by IR as supplements of proton nuclear magnetic resonance (NMR) [20]. Di-functional acid chloride such as sebacoyl chloride is used instead of acetyl chloride for cyclization of poly(amic acid) [20]. The viscosity of solution temporarily increased during the reaction because of the interchain mixed-anhydride formation. The viscosity slowly decreased back to the normal level as the cyclization proceeded. Imides are formed by intramolecular nucleophilic substitution at the anhydride carbonyl by the amide

nitrogen atom (*8a-9a*), while isoimides are formed as a result of substitution by the amide oxygen (*8b-9b*). The cyclization of N-phenylphthalamic acids with acetic anhydride smoothly conducts at room temperature in DMAc in the presence of a tertiary amine. The amine acts as a catalyst as well as an acid acceptor. Using a less than stoichiometric amount of amine still leads to completion of the reaction, only at a slower rate. Using triethylamine (pK_a 10.6) as a catalyst produced exclusively normal imides. However, a mixture of isoimide and imide was formed when less basic pyridine (pK_a 5.2) was used as a catalyst [20].

2.2 Sulfonated Polyimides

Nowadays, the synthesis of sulfonated polyimide copolymers has been classified as a direct copolymerization process. This approach requires that a sulfonated monomer should involve in the copolymerization, as opposed to sulfonation of the parent polymer. Stoichiometric contents of sulfonated diamine relative to nonsulfonated diamine, and naphthalenic dianhydride (NDA) as the dianhydride, were used for sulfonated copolyimide synthesis. A stoichiometric ratio between total diamine and dianhydride of 1:1 is usually used in order to obtain the highest molecular weight polymer. The degree of sulfonation could be varied by changing the ratio between sulfonated and nonsulfonated diamine that comprised polyimide. The copolymerizations were a one-step high temperature polycondensation in *m*-cresol; however, the catalysts employed could be varied. The triethylammonium salt form of the sulfonated diamine is always used for synthesis of high molecular weight polyimides. The sodium sulfonate forms of most diamines and acid are insoluble in *m*-cresol. After adding triethylamine to a sulfonated diamine in *m*-cresol at room temperature for about 4 hours, the triethylammonium salt form of the sulfonated diamine was occurred, which was soluble in the reaction media and also the free uncomplexed aromatic amine would be more reactive. Isoquinoline or benzoic acid are used as catalysts for imide formation [21].

Table 2.1 Sulfonated diamines.

| Structure | Name | Abbreviation |
|---|--|--------------|
|  | 2,5-Diaminobenzenesulfonic acid | DAB |
|  | 4,4'-Diamino-2,2'-biphenyl disulfonic acid | BDA |
|  | 4,4'-Diamino-5,5'-dimethyl-2,2'-biphenyl disulfonic acid | 6TS |
|  | 3-Sulfo-4,4''-bis(3-aminophenoxy)triphenyl phosphine oxide sodium salt | SBAPPO |
|  | 3,3'-Disulfonate-bis[4-(3-aminophenoxy)phenyl]sulfone | SA-DADPS |
|  | 2,2-Bis[4-(4-aminophenoxy)phenyl]hexafluoropropane disulfonic acid | BAHFDS |
|  | 4,4'-Diaminodiphenylether-2,2'-disulfonic acid | ODADS |
|  | 9,9'-Bis(4-aminophenyl)fluorine-2,7-disulfonic acid | BAPFDS |

2.2.1 Direct sulfonation of polymer

The most simple and widely used procedure to synthesis sulfonated polysulfones or polyimide concerns the direct sulfonation of the main chain using fuming sulphuric acid or chlorosulfonic acid in chlorinated solvents [22]. Since this is an electrophilic substitution reaction, positions ortho to the ether groups are favoured. As claimed earlier, these positions are electrophilically activated by the oxygen atoms giving an electron-rich character to the arylene ether segments, which in turn make them the most appropriate sites for substitution. However, the ease of sulfonation also implies that these positions are activated for desulfonation under acidic aqueous conditions due to the sulfonation reaction is a reversible reaction. This might prove detrimental for the successful use of such polymers in PEMFCs. Of particular concern to the polymer chemists are the harsh conditions needed for the sulfonation of the polymer main chain, leading to partial cleavage of the polymeric main chain. The Directly sulfonated polymers characteristically show extensive swelling and lose their mechanical stability when a certain critical degree of sulfonation, or temperature, is exceeded under immersed conditions. For example, directly sulfonated polysulfones with a degree of sulfonation of 80% were found to be water-soluble at room temperature, therefore limiting the IEC of the polymers that can be used as membranes in fuel cells without dissolved by water.

2.3 Conducting Polymer

2.3.1 Classification of Conducting Polymer

The idea that plastics could be made to conduct electricity was considered to be absurd. Indeed, plastics have been extensively used by the electronics industry because of insulator property, which utilized as inactive packaging and insulating material. Intrinsically conducting polymer (ICP) is rapidly changing as a new class of polymer. These properties are intrinsic to the doped form of the polymer, which have the higher conductivity than that of insulators and extends well into the region of common metals and also they are often referred to as “synthetic metals”. The common nature of most ICPs is the possession of alternating single and double bonds along the polymer chain, which enable the delocalization or mobility of charge along the polymer backbone. The conductivity is assigned to the delocalization of π -bonded

electrons over the polymeric backbone, indicating the unusual electronic properties, such as low ionization potentials, low energy optical transitions and high electron affinities [23]. ICPs are classified as doped conjugated polymers and are fundamentally different from conducting polymer composites [24], redox polymers [25], and ionically conducting polymers such as polymer/salt electrolytes [26].

Conducting Polymer Composites are a physical mixture of a conducting material and a nonconductive polymer. For example, a metal or carbon powder distributed throughout the matrix of polymer. Conducting materials such as short graphite fibers, conductive carbon blacks, and metal-coated glass fibers, metal particles or flakes, were usually used in previous experiments. Their conductivity is explained by percolation theory, the movement of electrons is occur between metallic phases and show a sudden drop in conductivity at the point where the dispersed conductive phases are discontinuous path for the transport of electrons through the materials. The conductivity of these materials with the conductive filler of 10-40 wt% can be as high as 10^{-1} S/cm [27, 28]. However, there are a number of drawbacks associated with such composite materials (fillers), such as (i) their conductivity is highly dependent on processing conditions, (ii) there is often an insulating surface layer formed on the conductor and (iii) the composite may become mechanically unstable due to heavy loading of the conducting particles. More recently, composites as well as blends and grafting of ICP materials were utilized in order to impart processability and improve the mechanical properties of these materials [29].

Redox Polymers consist of electrostatically and spatially localized redox sites that can be reduced or oxidized and they can transport the electrons by an electron exchange reaction (electron hopping) between neighboring redox sites if the segmental motions enable this. Redox polymers can be classified into several subclasses:

- Polymers that contain covalently attached redox sites, either built into the chain, or as pendant groups; the redox centers are mostly organic or organometallic molecules.

- Ion exchange polymeric systems (polyelectrolytes) were the materials where the redox active ions (mostly complex compounds) are held by electrostatic binding.

Ionically Conducting Polymers are great interesting because they show ionic conductivity in a flexible but solid membrane. Ionic conductivity is carried through the movements of ions, which different from the electronic conductivity of conjugated conducting polymers and metals. They have been important in development of devices such as all-solid-state lithium batteries. In 1973, Wright et al. [30] found ion conductivity in a PEO-alkaline metal ion complex (10^{-7} S/cm at room temperature), which influenced the beginning of the research and development of solid polymer electrolytes. Since then many salts, including those containing di- and trivalent cations, were combined with a variety of polymers in order to form polymer electrolytes [31-33]. The considerable potential of these materials as solid ionic conductors was first recognized by Armand in 1979 [34]. Since then, there has been interested in the synthesis and characterization of this class of material, as well as substantial emphasis on their potential consumption as solid electrolytes in electrochemical equipments such as smart window, rechargeable lithium batteries and electrochromic displays [35]. Polymer electrolytes also substitute a tempting class of coordination compounds such as the oxo-crown ethers [36]. Amorphous polymer electrolyte has been researched continuously for 30 years, and although the conductivities significantly increased over that period, they remain too low ($<10^{-4}$ S/cm) for various applications. The latest discovery, the crystalline polymer electrolytes, was shown the new class of solid ionic conductors and presented a different method for ionic conductivity in solid state. There is only in latest years that develop significantly in understanding the structure of materials became possible through the methods of determining crystal structure of powder [37, 38]. Normally, polymer electrolytes are lower conductivity than liquid electrolytes and cannot generate high power at room temperature, preferably, batteries at low temperatures. Polymer electrolytes have many excellent properties such as better safety than conventional organic liquid electrolytes or ease of manufacture, in various shapes.

Intrinsically Conducting Polymers (ICPs) propose a unique integration of ion exchange characteristics and optical properties that make them special. They are easily reduced and oxidized at relatively low potentials, and the redox process is attended and reversible by great transform of composition, conductivity and color of material. Polymers are made with proceeded, or doped, semiconducting polymers conjugated with a reducing agent, oxidizing agents, protonic acid, polyanions or higher polycations delocalized [39]. Conductivity of these materials can be adjusted by chemical manipulation of the polymer backbone, by the level of doping, by the nature of the dopant and by blending with other polymers. In addition, polymeric materials are flexible, lightweight and processability.

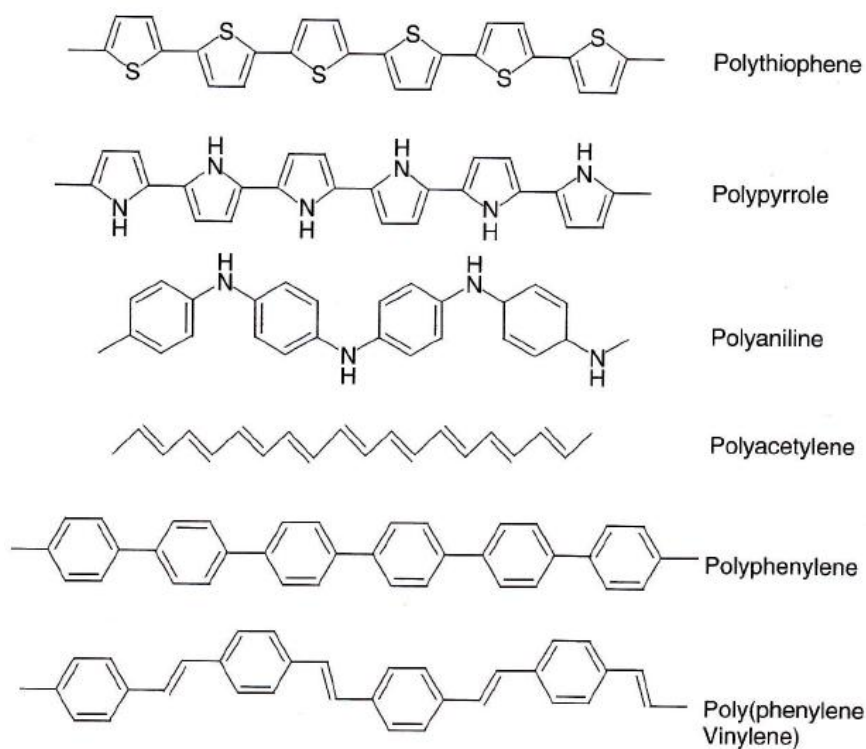


Figure 2.9 chemical structure of some conjugated polymers.

Many concerned conducting polymers have been researched over the past 30 years, those based on polypyrroles, polyanilines, polyphenylenes, polythiophenes and poly(*p*-phenylene vinylene)s have attracted the most attention. Figure 2.9 show the structure of some conjugated polymers in their neutral insulated form. In order that make them electronically conductive, it is necessary to introduce mobile carriers into

the conjugated system; this is achieved by oxidation or reduction reactions and the insertion of counterions (called “doping”). Dedoped conjugated polymers are performed as semiconductors with band gaps ranging from 1 to several eV, therefore their room temperature conductivities are very low, typically 10^{-8} S/cm or lower. However, by doping, conductivity can increase by many orders of magnitude. The concept of doping is unique and distinguishes conducting polymers from all other types of polymer [40]. During the doping process, an organic polymer, either an insulator or semiconductor having small conductivity, typically in the range of 10^{-10} to 10^{-5} S/cm, is converted to a polymer, which is in a metallic conducting regime (1 to 10^4 S/cm). The highest value reported to date has been obtained in iodine-doped polyacetylene ($> 10^5$ S/cm) and the predicted theoretical limit is about 2×10^7 , more than an order of magnitude higher than that of copper. Conductivity of other conjugated polymer reaches up to 10^3 S/cm [41,42] as shown in Figure 2.10.

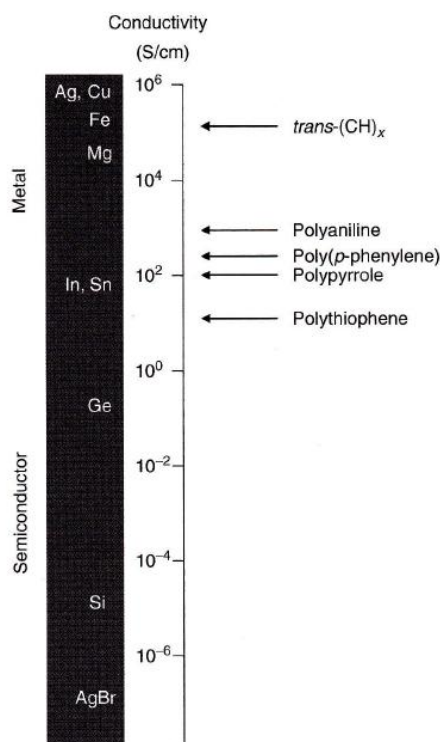


Figure 2.10 Conductivity of some metals and doped conjugated polymers.

2.3.2 Concept of Doping in Intrinsically Conducting Polymers

Doping in a conventional semiconductor such as silicon is very different from that in a conjugated organic polymer. In conventional semiconductors, the dopant is a small amount of a donor or acceptor that is introduced into the atomic lattice resulting in a change in the occupancy of electronic states in the solid as a result of thermal ionization of the dopant. The band structure and the density of states are essentially unchanged by the introduction of the dopant [43].

Doping of a conducting polymer, on the other hand, involves the introduction of a large amount of a donor or acceptor (in the range of a few up to 30 wt%). The presence of such a large amount of dopant and structural changes in the polymer resulted in a material that is significantly different from the nondoped material. The dopant perturbs the polymer extensively not only because of its significant physical size and the fact that it does not incorporate into the molecular structure, but also because of the extensive charge transfer that takes place between the polymer chain and the dopant, causing both to become ionic and leading to changes in the geometry of the chain. The doping level can also be reversibly controlled to obtain conductivities anywhere between the insulating nondoped form to the fully doped, highly conducting form of the polymer.

Doping involves either oxidation or reduction of the polymer backbone. Oxidation removes electrons and produces a positively charged polymer and is described as p-doping. Similarly, reduction produces a negatively charged backbone and is known as n-doping. The oxidation and reduction reactions can be induced either by chemical species (e.g., iodine, sodium amalgam or sodium naphthalene) or electrochemically by attaching the polymer to an electrode. The electrochemical doping process proceeds in much the same way as with chemical doping, with the exception that the driving force for the oxidation and reduction is provided by an external voltage source (i.e., by the electrochemical potential of the working electrode). Electrochemical p- and n- doping can be accomplished under anodic and cathodic conditions by immersing polymer film in contact with an electrode in an electrolyte solution. In these p- and n-doping processes, the positive and negative charges on polymers remain delocalized and are balanced by the incorporation of counterions (anions or cations), which are referred to as dopants.

2.3.3 Conduction Mechanism

The electronic properties of any material are determined by its electronic structure. The theory that most reasonably explains electronic structure of materials is band theory. Quantum mechanics stipulates that the electrons of an atom can only have specific or quantized energy levels. However, in the lattice of a crystal, the electronic energy of individual atoms is altered. When the atoms are closely spaced, the energy levels are formed bands. The highest occupied electronic levels constitute the valence band and the lowest unoccupied levels, the conduction band as shown in Figure 2.11. The electrical properties of conventional materials depend on how the bands are filled. When bands are completely filled or empty no conduction is observed. If the band gap is narrow, at room temperature, thermal excitation of electrons from the valence band to the conduction band gives rise to conductivity. This is what happens in the case of classical semiconductors. When the band gap is wide, thermal energy at room temperature is insufficient to excite electrons across the gap and the solid behaves as an insulator. In conductors, there is no band gap since the valence band overlaps the conduction band and hence enhancing their high conductivity.

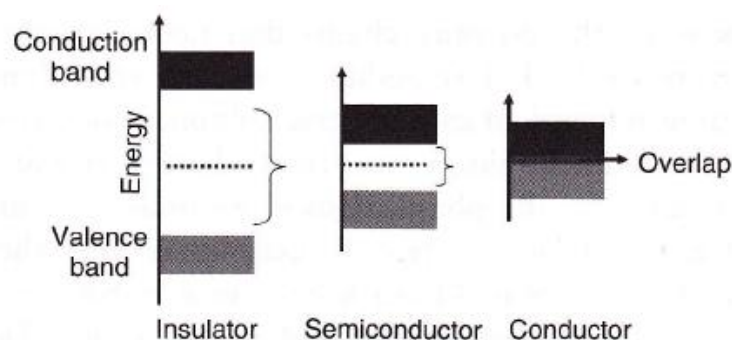


Figure 2.11 Energy band in solid.

2.3.4 Synthesis

Intrinsically conducting polymers are generally synthesized via chemical or electrochemical oxidation of a monomer where the polymerization reaction is stoichiometric in electrons. However, several other synthetic approaches exist, such as photochemical-initiated or biocatalytic oxidative polymerizations using naturally occurring enzymes. The method of synthesis can be divided to 2 methods as follows;

2.3.4.1 Chemical Synthesis

Chemical synthesis has the advantage of being a simple process capable of producing bulk quantities of ICPs on a batch basis. To date it has been the major commercial method of producing such materials. Chemical polymerization is typically carried out with relatively strong chemical oxidants like ammonium peroxydisulfate, ferric ions, permanganate or bichromate anions, or hydrogen peroxide. These oxidants are able to oxidize the monomers in solution, leading to the formation of cation radicals. These cation radicals further react with other monomers or n-mers, yielding oligomers or insoluble polymer. There are two main limitations of the chemical oxidation technique, both related to the limited range of chemical oxidants available. The counterion of the oxidants ultimately ends up as a dopant or co-dopant in the polymer. Hence it is difficult to prepare ICPs with different dopants. The limited range of oxidants also makes it difficult to control the oxidizing powder in the reaction mixture and in turn the degree of over oxidation during synthesis. Both the type of dopant and the level of doping are known to impact upon final properties of the polymer such as molecular weight, crosslinking and conductivity.

2.3.4.2 Electrochemical Synthesis

The electrochemical synthesis of conducting polymers, first demonstrated with polypyrrole [44], has proven important in the development of the field. Using this approach, semiconducting polymers have been obtained from a wide variety of monomers including thiophene, furan, carbazole, aniline, indole, azulene and polyaromatic monomers such as pyrene and fluoranthene. In general, chemical oxidation provides ICPs as powders, while electrochemical synthesis leads to films deposited on a working electrode. A wide range of anodes may be employed, including platinum, gold, carbon and indium-doped tin oxide (ITO)-coated glass. The ITO-coated glass electrodes, being transparent in the visible/near-infrared region, are very useful for in situ spectral investigations involving absorption or circular dichroism of the deposited polymer films.

The advantage of electrochemical polymerization is due to the method of selecting an appropriate electrolyte, a much wider choice of cations and anions for use as dopant ions is possible. Also, in electrochemical polymerization, doping and

processing take place simultaneously with polymerization. However, in conventional methods, first polymer synthesis and doping are carried out, followed by processing. The electrochemical oxidation route also has greater control over the electrochemical potential of the system (thereby limiting over-oxidation) and it alters the rate of polymerization as well as the film thickness.

2.4 Template Polymerization

In this study, we have utilized the difference of various templates such as poly(styrene sulfonic acid), poly(amic acid) and poly(imide) to react with conducting polymers via template polymerization. Template or matrix polymerization can be defined as a procedure of polymer synthesis in which specific interactions between preformed macromolecules (template) and a growing chain are utilized. These interactions affect structure of the polymerization product (daughter polymer) and the kinetics of the process [45]. Template polymerization usually refers to one phase system in which monomer, template, and the reaction product are soluble in the same common solvent.

The template polymerization can be observed in living organism. The growth of living organisms is associated with very complicated processes of template polymerization. Low molecular weight substrates, such as sugars, amino acids, fats, and water in animals and carbon dioxide in plants are precursors of polymers (polypeptides, polynucleic acids, polysaccharides, etc.). They are organized in tissues and can be reproduced. In many biological reactions such as DNA replication or polypeptide creation, low molecular weight substrates and polymeric products are present in the reaction medium together with the macromolecular compounds called matrices or templates controlling the process.

2.5 Conductive Polymers versus Metals and Insulators

This part explains the origin of the conductivity in intrinsically conducting polymers. The properties of metals, semiconductors, and insulators are first explained in general [46].

The properties of metals, semiconductors, and insulators can be most easily explained using simple, non-polymeric solids as an example. The changes in orbitals

and energy levels starting from individual atom to small molecules and then to three-dimensional solids are well understood [47]. In small molecules with a well-defined number of atoms, the atomic orbitals merge to form molecular orbitals with discrete and well-defined energy levels. The low lying orbitals are filled with electrons and typically have a bonding character, whereas high lying orbitals are often unfilled and have an antibonding character.

If a very large number of atoms are arranged in a three-dimensional lattice, the energy levels of neighboring states rearrange into bonding and antibonding states, and a continuous band is formed. In certain solids such as metals, the orbitals in the bands are continuous and electrons close to the top of the filled orbitals can be excited into unoccupied levels requiring hardly any energy. To describe the energy levels in such metals, it is useful to consider the distribution of electron firstly at temperature $T=0$ without thermal energy. The highest occupied energy level in these metals at $T=0$ is called the Fermi level. The extension of electronic states is defined by the boundaries of the crystalline domains and the charge carrier transport is only limited by scattering processes.

The electrical conductivity of metallic solids decreases with increasing temperature although more electrons are excited. This is because of the thermal motion of the atoms that lead to collisions between electrons and atoms. Because of these collisions the electrons become less efficient in transporting charge.

In semiconductors and insulators, the relevant bands for charge transport are separated by an energy gap. At $T=0$ the electronic states of the energetically lower lying band, called the valence band, are completely filled, whereas the states forming the conduction band are empty. As the temperature is increased, certain electrons gain enough that they can occupy empty orbitals in the conduction band. These electrons are now mobile and the solid becomes electrically conductive. It can now be described as a semiconductor. If the energy gap is very large, only a few electrons will reach the conductive band and the overall conductivity will be close to zero, and the material is described as an insulator. The distinction between insulator and semiconductor is therefore a gradual distinction, which depends on the band gap. The distinction between a semiconductor and an insulator is, therefore, less well defined as that between a metal (incomplete bands at $T=0$) and a semiconductor (complete bands

at $T=0$). In semiconductors the conductivity increases with increasing temperature since more electrons are able to reach the valence band when heated, which contradicts to metallic materials that the conductivity decreases with increasing temperature.

2.6 Commercial Conducting Polymers

The fundamental discovery by Shirakawa, MacDiarmid and Heeger of polymeric organic conductors in 1977 [48, 49] marked the beginning of an era of dramatic growth in a field that earned its pioneers the Nobel Prize in Chemistry in 2000 [50-52]. The first examples of ICPs, based on oxidatively doped polyacetylenes (PACs), faced several intrinsic obstacles that prevented their industrial commercialization. The materials degrade readily in air and no known good methods exist for making easily processable PAC polymers. These drawbacks led to the investigation of alternative polymer backbone structures in the search for stable, processable, high-conductivity ICPs. Over the years, several promising polymer types have emerged as potentially useful alternatives to PACs for commercial applications, including polythiophenes (specifically, poly(3,4-ethylenedioxythiophene or PEDOT), polyanilines (PANI) and polypyrroles (PPy). The details of these conducting polymers are described in this part.

2.6.1 Poly (3,4-ethylenedioxythiophene) (PEDOT)

PEDOT plays a dominant role in antistatic and conductive coatings, electronic components and displays. In its p-doped state, PEDOT combines high conductivity, optical transparency and stability properties that are very suitable for several applications. PEDOT is widely used as antistatic coatings and as hole-injecting/electron-blocking layers in light-emitting diodes and solar cells and has been explored as a potential conductor for transparent electrodes. In particular, widespread applications have been developed using the conducting properties of both the PEDOT complex with poly(styrenesulfonic acid) (PEDOT-PSS) and the in situ-polymerized layers of the EDOT monomer. Antistatic coating applications for PEDOT-PSS include photographic films, electronic packaging, CRT screens and LCD polarizer films. Conductive films of PEDOT-PSS are found in inorganic electroluminescent devices and all-organic field effect transistors and PEDOT-PSS layers function as the

material of choice for hole injection in polymeric organic light-emitting diodes (LEDs) and polymer photovoltaic cells. In situ-PEDOT is also well established in industry and is used as a polymeric cathode material for solid aluminum, tantalum and niobium capacitors and as a conductive template for Cu-through-hole plating of printed wiring boards.

2.6.1.1 EDOT Synthesis

EDOT chemistry started as early as the 1930s, when corresponding 2,5-dicarboxylic acid esters were first described [53,54]. A detailed synthesis description for 3,4-ethylenedioxy-thiophene-2,5-dicarboxylic acid was given by Gogte et al. in 1967 [55]. Decarboxylation of this intermediate led to EDOT [56] and since its introduction into the chemistry of ICPs its industrial manufacture has been based on the Gogte pathway with minor changes, utilizing a copper-catalyzed decarboxylation in the last step [57] as shown in Figure 2.12.

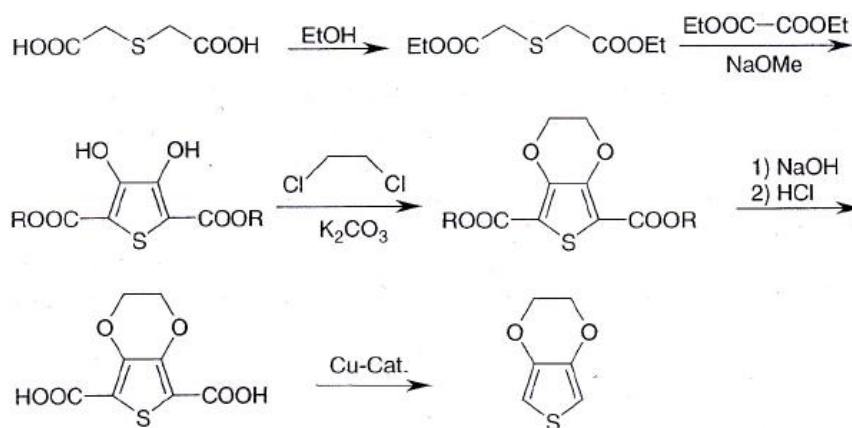


Figure 2.12 Synthesis of EDOT from oxalic acid ester and thiodiacetic acid ester.

Several alternative routes have been suggested, which in some cases are especially useful for preparing derivatives of EDOT. One of the highest preparative values of these other pathways seems to be associated with the transesterification of 3,4-dimethoxythiophene (or other lower alkoxythiophenes) with vicinal diols [58,59]. The Williamson ether synthesis step sometimes suffers from low yields with long-chain 1,2-dibromoalkanes due to competing elimination reactions, making

transesterification the synthetic strategy of choice. For several EDOT derivatives (benzo-EDOT), the transesterification reaction provides the best synthetic access. Transesterification proved to be especially useful in synthesizing enantionmerically pure chiral disubstituted EDOTs as shown in Figure 2.13.

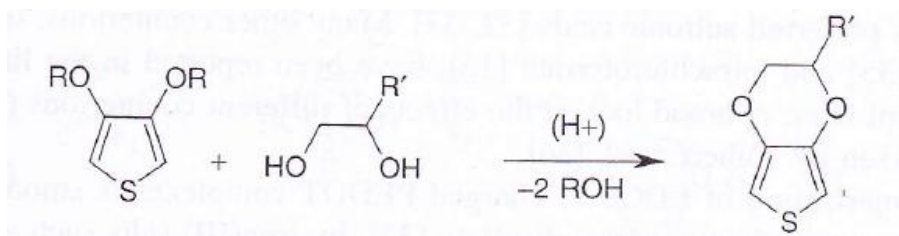


Figure 2.13 Transesterification as a synthetic route to EDOT derivatives.

2.6.2 PEDOT-PSS Complex

The industrially useful PEDOT-PSS is made by aqueous oxidative polymerization of the EDOT monomer in the presence of the template polymer PSS. PSS is a commercially available, water-soluble polymer and can serve as a good dispersant for aqueous PEDOT. Polymerization with the oxidant sodium peroxodisulfate yields the PEDOT-PSS complex in a conductive, cationic form.

The PSS in this complex has two functions. The first is to serve as the charge-balancing counterion to the PEDOT cation. The second is to disperse the PEDOT segments in water. Although the resulting PEDOT-PSS complex is not truly water soluble, the reaction forms a stable, easy to process, deep blue microdispersion of polymer gel particles.

Two key factors are important for understanding the nature of the PEDOT-PSS complex. First, the PEDOT segments formed during polymerization are most likely an oligomeric rather than polymeric. It has not been possible to observe high molecular weight PEDOT polymers directly and analyses of various PEDOT containing polymers via MALDI-TOF mass spectrometry strongly support this assumption. Several measurements with PEDOT-PSS or with substituted PEDOT derivatives, including neutral PEDOT molecules indicated that the molecular weights of the individual PEDOT molecules do not exceed 1000-2500 Da or about 6-18 repeating units [60, 61]. Second, the PEDOT-PSS complex has high stability. Ghosh

and Ingnas demonstrated that the ionic species PEDOTⁿ⁺ and PSSⁿ⁻ could not be separated by standard capillary electrophoresis methods [62].

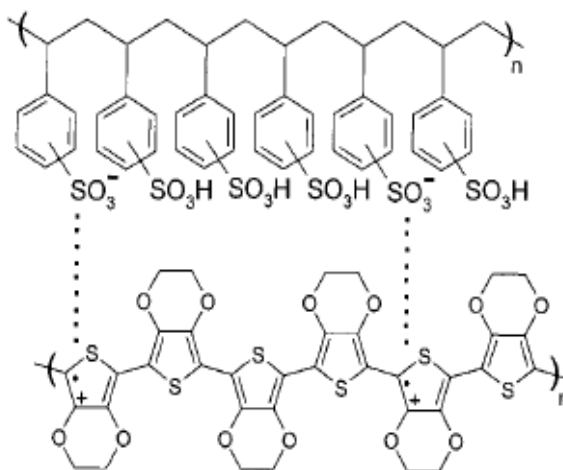


Figure 2.14 Structure of PEDOT-PSS.

2.6.2.1 Synthesis of a PEDOT-PSS Complex

Poly (styrenesulfonic acid) (PSS) was the first polyelectrolyte used for a polyelectrolyte complex (PEC) with PEDOT in 1990 and has remained the industrial standard ever since. PSS is commercially available in a large range of molecular weights with different polydispersities. Further to its commercial availability and its solubility in water, PSS forms durable films and shows no absorption in the visible range of light, resulting in transparent films. The sulfonic acid group is strongly acidic and hence highly polar. Sulfonic acids typically have a low pK_a value, for example, for benzenesulfonic acid the pK_a is 0.70 [63].

PSS as a counterion for PEDOT is always used in excess, that is, as host polyelectrolyte (HPE). The molar ratio of thiophene groups to sulfonic acid groups in standard PEDOT-PSS dispersions is in the range of 1:1.9 to 1:15.2, which corresponds to a weight ratio range of 1:2.5 up to 1:20. Since only one charge is found for every three to four thiophene rings [64, 65], the charge excess of PSS is between 6-fold and 46-fold.

Due to the delocalization of positive charges in PEDOT, the resulting weak polar groups and the different spacing of charges in PEDOT compared to PSS, it is

reasonable to assume that the structure of PEDOT-PSS shows the form of a scrambled egg type. A pairing of charges as required in the ladder type is not possible.

The solvent of choice for the synthesis of PEDOT-PSS complex is water. Water is inert with respect to most oxidation or reducing agents. It is highly polar and a good solvent for PSS. However, water is a poor solvent for the monomer EDOT. At 20°C, 0.21 g of EDOT can be dissolved in 100 mL of water. The solubility increases in the presence of PSS to 0.30%. An important parameter for the EDOT polymerization is the pH value. The presence of PSS leads to a low pH of less than 3. This is beneficial since acid acts as a catalyst for the reaction. In the absence of acid, the oxidation of EDOT can result in keto-functionalized side products. The reaction turns out more acidic as it progresses since further protons are released. Furthermore, the presence of stoichiometric amounts of iron (III) or iron (II) ions leads to the precipitation of the PEDOT-PSS complex in the latest stages of the reaction. This is because multivalent cations such as Fe (III) form a complex with PSS and reduce the stability of the PEDOT-PSS complex.

Typically properties of PEDOT-PSS polymers that depend on the PEDOT-PSS ratio are summarized in Table 2.2. To meet the requirements for conductivity, antistatic grades of PEDOT-PSS have relatively low PSS contents and therefore higher conductivity values. In contrast, PEDOT-PSS grades designed for hole injection in polymer OLEDs have larger PSS contents, smaller particles and lower conductivity. Specifically, PEDOT-PSS grades useful for passive matrix OLED displays have the lowest conductivity in order to prevent cross-talk in multi-pixel devices. Increasing the PSS content logically reduces the electrical conductivity.

Table 2.2 Typical commercial PEDOT-PSS grades and their characteristics.

| PEDOT-PSS ratio | Approximate conductivity (S/cm) | Typical application |
|-----------------|------------------------------------|---------------------------------|
| 1:2.5 | 1-500 | Conductive coatings Antistatics |
| 1:6 | 10^{-3} | OLEDs |
| 1:20 | 10^{-5} | Passive matrix displays |

2.6.2.2 Secondary Doping

MacDiarmid and Epstein have used the term primary doping for the addition of small non-stoichiometric quantities of a material to conductive polymers that lead to a strong increase in conductivity of these polymers [66]. This can be brought about by a redox agent that either oxidizes (p-doping) or reduces (n-doping) the polymer chain. Alternatively, the protonation of polyaniline is also referred to as doping. The term secondary doping as used by MacDiarmid and Epstein refers to an additive that further increases the conductivity of an already doped polymer by up to several orders of magnitude. The main difference between primary and secondary doping is that the first has a reversible effect, whereas the effect of the latter is permanent and remains even when the additive is removed.

Table 2.3 shows a range of chemicals and their effect on the conductivity of PEDOT-PSS films. It includes many organic solvents, sugars, polyols, ionic liquids, surfactants, and salts. Some chemicals have no or only small effects, others increase the conductivity by several orders of magnitude. A very important class of additives for formulations is high-boiling solvents and other polar, water-miscible compounds. Particularly useful are amides such as N-methylpyrrolidone and dimethylformamide, polyhydroxy compounds such as ethylene glycol or sugar alcohols and sulfoxides such as DMSO. These solvents, often called “secondary dopants”, are used in small amounts to increase the conductivity of the films. The effects of these additives are independent of whether they remain in the film after drying, which is contradictory to the explanation of the conductivity enhancement as a screening effect by remaining solvents. The favored reasons are polar solvents at least partly dissolve the PEDOT stacks in the PEDOT-PSS complex, thereby creating an opportunity for a favorable morphological rearrangement and clustering of gel particles. The rearrangement leads to a decreased resistance between dried gel particles, thus increasing the overall conductivity of the film by up to more than two orders of magnitude.

Table 2.3 Additives and their effect on the conductivity of PEDOT-PSS films.

| Substance | Example | Conductivity enhancement factor (Maximum values) |
|------------------------------------|-----------------------|--|
| Monovalent alcohols | Methanol | None |
| | Ethanol | |
| | Heptanol | |
| Polyols | Glycerol | 5 |
| | Ethylene glycol | 500 |
| | Sorbitol | 45 |
| | meso-Erythritol | 100 |
| Alcohols with a second polar group | 2-Nitroethanol | 100 |
| | Methoxyphenol | 50 |
| Hydroxylated ethers | Diethylene glycol | 5 |
| Hydroxylated thioethers | Thiodiethanol | 5 |
| Ethers | Tetrahydrofurane | 5 |
| Amines | Pyridine | None |
| Amides | N,N-Dimethylformamide | 40 |
| | N,N-Dimethylacetamide | 100 |
| | N-Methylpyrrolidone | 100 |
| Imide | Succinimide | 330 |
| Sulfoxides | Dimethyl sulfoxide | 800 |
| Ketones | Cyclohexanone | None |
| Nitriles | Acetonitrile | None |
| Nitromethane | Nitromethane | None |

2.6.3 Polyaniline

PANI is one of the most promising conducting polymers with enhanced conductivity, good environmental stability, and diverse color change corresponding to different redox states. It has been known that PANI nanomaterials can be applied for many practical fields such as chemical sensor, supercapacitor, corrosion protection, battery and energy storage, and antistatic coating. Therefore, there have been

prodigious research papers concerning the synthesis and application of PANI nanomaterials.

2.6.3.1 Polyaniline Nanoparticle

The processability of PANI is relatively poor because it is infusible and insoluble in common solvent. In order to improve its processability, the alternative approach is achieved by preparing PANI nanoparticles and dispersing them uniformly in aqueous/organic solvent. The PANI nanoparticle has been synthesized using polymer surfactant, and the diameter of the PANI nanoparticle is controlled by different surfactants. The amphiphilic polymer molecule such as hydrophobically end-capped poly (ethylene oxide) was used to form micelle, and the micelle dimensions could be tuned by changing the spacer group of the hydrophilic block. The size of the PANI nanoparticle was distributed in the range of 5–40 nm. Chemical oxidation polymerization of aniline has been performed in DBSA isooctane–water reverse micelle system. It was reported that the PANI nanoparticle exhibited needle-like shape (diameter: 10 nm, length: 20–30 nm) and had a uniform dispersion in solvent. It is a feasible and attractive method to readily prepare DBSA-PANI nanoparticle in the reverse micelle system. Another approach to fabricate PANI nanoparticles was reported with aqueous/ionic liquid interfacial polymerization. Interfacial polymerization involves the step polymerization of two reactive monomers or agents, which are respectively dissolved into two immiscible phases. The polymerization reaction takes place at the interface of the two liquids. Green PANI nanoparticle was formed at the interface and gradually diffused into the aqueous phase. The entire water phase was homogeneously filled with dark-green PANI, while the ionic liquid layer showed a color of orange stemming from the formation of aniline oligomers. The yield of PANI nanoparticles was ca. 25 wt%. PANI nanoparticles with the diameter of ca. 30–80 nm could be obtained in environmentally benign solvent. Chemical oxidation polymerization in dilute and semi-dilute solutions of poly(sodium 4-styrenesulfonate) (PSS) was demonstrated for the synthesis of PANI nanocolloids (particle size: ca. 2–3 nm). A similar approach was performed to synthesize PANI nanoparticles using ammonium peroxydisulfate in aqueous medium comprising poly(ϵ -caprolactone)-PEOpoly(ϵ -caprolactone) amphiphilic triblock copolymer

micelle. Micelle size conspicuously affects the morphology of the PANI nanoparticle, and the PANI nanoparticle size is strongly dependent on PEO molecular weight. The diameter of the nanoparticle increased from 30 nm to 100 nm as the PEO molecular weights decreased. Electropolymerization was performed using constant potential of 0.7 V and obtained a PANI nanoparticle with diameter of ca. 80 nm.

2.6.4 Polypyrrole

Among the conducting polymers, polypyrrole (PPy) has attracted great attention because of its high electrical conductivity and good environmental stability. PPy has been considered as the key material to many potential applications such as electronic devices, electrodes for rechargeable batteries and supercapacitors, solid electrolytes for capacitors, electromagnetic shielding materials, sensors, corrosion-protecting materials, actuators, electrochromic devices, or membranes. PPy consisting of five-membered heterocyclic rings and it is one of the most promising conducting polymers. PPy has been extensively explored because of their easy synthesis, tunable conductivity, reversible redox property, an environmental stability. PPy can be easily prepared by chemical or electrochemical polymerization via the oxidation of pyrrole monomers. In general, chemical polymerization leads to intractable powder, whereas electrochemical polymerization results in film deposited on the electrode. PPy may be prepared by either chemical or electrochemical oxidation of pyrrole monomer

Electrochemical oxidation method, pyrrole and an electrolyte salt are dissolved in a suitable solvent and then the solution is subjected to oxidation, resulting in the growth of a conducting PPy film on the anodic working electrode. The electrochemical polymerization is a fast, easy, and clean method to obtain highly conductive PPy films. There are some difficulties in correlating the properties of the materials with the synthetic conditions and expanding the reaction system over a laboratory scale.

In Chemical Polymerization method, an oxidizing agent such as lead dioxide, quioines, ferric chloride or persulfates is added to the pyrrole and a dopant dissolved in a suitable solvent, resulting in the precipitation of doped PPy powder. In general, the electrical conductivities of chemically prepared PPy are a little lower than those of PPy films prepared electrochemically. Nevertheless, the chemical oxidation method is

suitable for commercial mass production of PPy and may produce processible PPy since the method has much greater feasibility to control the molecular weight and structural feature of the resulting polymer than the electrochemical oxidation method. It is well known that various properties such as the electrical conductivity, stability, and morphology of synthesized PPy strongly depend on various reaction conditions such as the kinds and concentrations of oxidant and dopant, polymerization temperature and time, stoichiometry, and solvent. For example, pyrrole can be polymerized using FeCl_3 , one of the most common oxidizing agents as indicated in below:

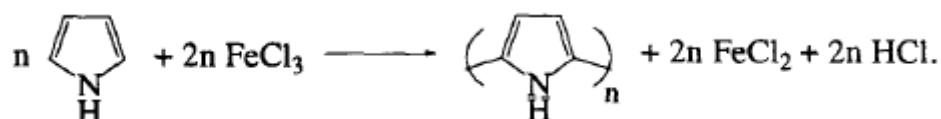


Figure 2.15 Polypyrrole polymerization.

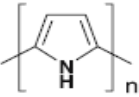
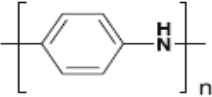
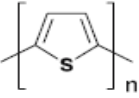
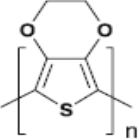
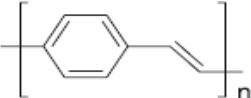
Chemical Polymerization with Surfactants To improve conductivity, stability or solubility in organic solvents, various kinds of surfactants have been used as additives in the chemical polymerization of pyrrole. When PPy was prepared in aqueous solution containing $\text{Fe}_2(\text{SO}_4)_3$ as an oxidant and anionic surfactants such as sodium dodecylbenzenesulfone, sodium alkylnaphthalenesulfonate, or sodium alkylsulfonate, the resulting PPy exhibited enhanced conductivity and polymerization yield with an accelerated polymerization reaction rate.

2.6.4.1 Polypyrrole Nanoparticle

Spherical PPy nanoparticles have been prepared by chemical oxidation polymerization with the aid of surfactant or stabilizer in an aqueous solution. Microemulsion polymerization has been extensively utilized to synthesize various nanometer-sized conducting polymer particles. A typical example is the synthesis of PPy nanoparticles with diameter of several nanometers using low temperature polymerization. Low temperature polymerization is appropriate for reducing the inner space of micelles by virtue of deactivating the chain mobility of the surfactant. Thus PPy nanoparticles as small as 2 nm in diameter could be prepared through chemical

oxidation polymerization inside the micelles made of cationic surfactants at low temperature. As the polymerization temperature increased, PPy nanoparticle grew as a result of the enhanced chain mobility of the surfactant. In addition, the size of PPy nanoparticle decreased with shortening the chain length of the surfactant. The micelle aggregation number, which is defined as the number of surfactant molecules required to form a micelle, becomes smaller as the chain length of surfactant decreases. The reduced micelle aggregation number gives rise to the formation of smaller particles. On the other hand, the longer surfactant chains provide more free volume inside micelle, which lead to the increment of particle size. Importantly, the thermodynamically stable micelle successfully acted as a nanoreactor in synthesizing PPy nanoparticles. Another approach to synthesize PPy nanoparticles was performed in a microemulsion system; ferric chloride (FeCl_3) was employed as an oxidizing agent, and dodecylbenzenesulfonic acid (DBSA) and butanol were used as a surfactant and a co-surfactant, respectively. It was reported that microemulsion polymerization system increased not only the yield of the resultant PPy but the extent of conjugation length in the polymer as compared with solution and conventional emulsion polymerization.

Table 2.4 Typical conducting polymer structures (undoped form) [67].

| Name | Structure |
|----------------------------------|--|
| Polypyrrole |  |
| Polyaniline |  |
| Polythiophene |  |
| Poly(3,4-ethylenedioxythiophene) |  |
| Poly(para-phenylene vinylene) |  |

CHAPTER III

LITERATURE REVIEWS

This chapter describes the literature reviews of the previous works related to the field of conductive polyimide and conducting polymer, including synthesis method, application and improving the conductivity.

3.1 Conductive polyimide

Chatzidaki E.K. et al. [68] (2007) studied on the synthesis of new polyimide-polyaniline hollow fibers via dissolution of the polymers in NMP and dry/wet spinning of the resulting solution in a non-solvent (H₂O). The morphology and thermal properties of the fibers were characterized by SEM and TGA while FTIR spectroscopy was used for the study of their chemical structure. Selectivity measurements and permeability in different gases (He, CH₄, H₂, O₂, CO₂ and N₂) were studied to evaluate the performance of the membrane in gas separation applications. The results show that the novel membrane is a well structured hollow fiber with highly thermal stable up to 500°C. The addition of polyaniline into the polyimide matrix resulting in an enhancement in fiber permeability (60-600 times) possibly due to increasing of the total free volume due to the great distribution of shorter polyaniline molecules in the matrix which can be allowed larger quantities of gases to pass through the composite membrane. Perm-selectivity ratios for the composite membranes H₂/CH₄, H₂/N₂, He/N₂ and H₂/CO₂ when compared with membranes produced using only polyimide were found lower by a factor of 6.4, 7.7, 8.9 and 1.47, respectively. The opposite effect was observed for CH₄/CO₂ and N₂/CO₂ perm-selectivity ratios that showed an increase by a factor of 3.52 and 5.2, respectively. The ratio CH₄/CO₂ is of particular interest for natural gas purification purposes.

Han M.G. and Im S.S. [69] (1998) studied in order to use camphorsulfonic acid (CSA) to protonate polyaniline (PANI), the counterion enabled the PANI-CSA complex processable as a solution phase. The composite films between

camphorsulfonic acid (CSA)-doped polyaniline/polyimide (PANI/PI) were prepared by the solvent casting method using N-methylpyrrolidinone (NMP) as a cosolvent followed by thermal imidization. The conductivity of the PANI-CSA/PAA (50 wt % PANI) at room temperature is higher than the pure PANI. Molecular order of polymer chain structure was improved via the thermal imidization resulting in PANI-CSA/PI film. Because of the annealing effect of PANI chain, this PANI-CSA/PI film showed higher conductivity than PANI-CSA and PANI-CSA/PAA film. PANI-CSA/PI composite films had a great thermal stability of conductivity at high temperature.

Han M.G. and Im S.S. [70] (1999) studied the synthesis of dodecylbenzenesulfonic (DBSA)-doped polyaniline/polyimide (PANI/PI) blends with various compositions were prepared by solvent casting followed by a thermal imidization process. Physical and electrical properties of the resulting polymers were characterized by infrared spectroscopy, thermal analysis, X-ray diffraction technique, UV-vis spectrophotometer, conductivity measurements and dielectrometer. The polymer blends exhibited a relatively low percolation threshold of electrical conductivity at PANI content of 5 wt% and showed higher conductivity than pure DBSA-doped PANI when the PANI content exceeded 20 wt%. A lower compatibility and a lower percolation threshold were shown between the two components in the blends than those of PANI-camphorsulfonic acid/polyamic acid (PANI-CSA/PAA). A well-defined layered structure due to the alignment of the long alkyl chain dopant perpendicular to the PANI main chain was evidenced by WAXD spectra.

Han M.G. and Im S.S. [71] (2000) studied in order of the changes in protonation level ($[N^+]/[N]$ ratio), doping state, and conjugation condition for polyaniline-complexes/polyamic acid (PANI-complexes/PAA) blends. Their thermally cured polyaniline-complexes/polyimides (PANI-complexes/PI) have been performed by X-ray photoelectron spectroscopy and UV-Vis spectroscopy. It was indicated that the protonation levels were predominantly associated with dopants that show different protonation ability. From the XPS N1s peak convolution, it was shown that thermal treatment of blends led to dedoping when the curing temperature reached 250°C. However, the stability of protonation state of polymer blends against thermal

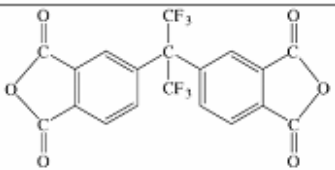
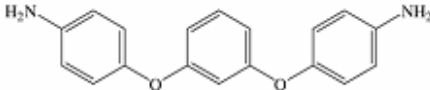
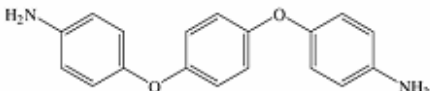
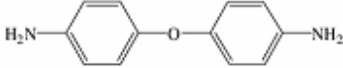
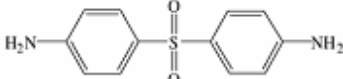
curing was higher than that of pure PANI-complexes. Dopants in the blends were affected the distribution of N^+ species and thermal stability to curing. Mild thermal treatment at 180°C led to the increase of conjugation length due to the increased order of polymer chain, although their protonation levels were not increased.

Han M.G. and Im S.S. [72] (2001) were synthesized polyaniline (PANI) complexes/polyimide (PI) blends using small-angle X-ray scattering patterns to analyze the compatibility between two components of the blends. As the experimental results, it indicated that the microphase separation or molecular level mixing, which was the reflection of compatibility, was dependent on the kinds of dopant (dodecylbenzene sulfonic acid (DBSA) and camphorsulfonic acid (CSA)), PANI content and the imidization state. On account of self-assembling nature of PANI-DBSA, PANI-DBSA/poly(amic acid) (PAA) shows phase-separated morphology. On the other hand, PANI-CSA/PAA blends show well-mixed and high compatible morphology. Thermal curing of polymer blends brought about the change of blend morphology, which was in correlation with altered chain structure from PAA into PI, and was also a function of PANI content. The conversion from PAA to PI by thermal curing processes led to enhancement of compatibility probably due to higher interaction between two components.

Lu X.H. et al [73] (2006) were described the effects of polyimide (PI) structure on electrical conductivity of dodecylbenzene sulfonic acid-doped polyaniline (PANI-DBSA)/PI blends, as good as its thermal degradation behavior. Four types of Polyimides with different molecular architecture were synthesized and subsequently solution blended with PANI-DBSA. From the four types of PIs, 4-4'-diaminodiphenyl sulfone (DADPS)-based PI was provided the highest conductivity to the blends. It is attributed to the rigid nature of DADPS, which may induce more extended conformation of PANI chains, and hence result in a more ordered structure. The conductivity of resulting polymer blends has significant higher thermal stability than PANI-DBSA. The thermal stability is independent on the polyimide structure. TGA results show that the PI matrix may have hindered the thermo-oxidative degradation

and evaporation of the dopants and slowed down the process of thermal degradation of the conductivity.

Table 3.1 Chemical structures of the monomers used in preparation of polyimides.

| Monomer | Abbreviation | Chemical structure |
|---------------------------------------|--------------|--|
| Hexafluorotetracarboxylic dianhydride | 6FDA |  |
| 1,3-Bis(4-aminophenoxy)benzene | 1,3-BAPB |  |
| 1,4-Bis(4-aminophenoxy)benzene | 1,4-BAPB |  |
| 4,4'-Oxydianiline | ODA |  |
| 4,4'-Diaminodiphenyl sulfone | DADPS |  |

Wang Z.Y. et al. [74] (1998) studied the synthesis of aniline trimer, *N,N'*-bis(4'-aminophenyl)-1,4-phenylenediamine, which was successfully used as a diamine monomer, together with 4,4'-oxydianiline and 4,4'-(hexafluoroisopropylidene)diphthalic anhydride, in the synthesis of high molecular weight polyimides. A series of film-forming polyimides containing a range of the electroactive component were obtained. Chemical redox reactions and electrochemical properties of these polyimides were studied.

Chao D.M. et al. [75] (2007) synthesized the imidic macromonomer of oligoaniline and *p*-phenylenediamine by oxidative coupling polymerization. They prepared an electroactive polyimide, exhibiting exciting molecular structure, electrochemical properties and excellent thermal stability. Fourier-transform infrared (FTIR) and X-ray powder diffraction (XRD) were used to study the polymerization characteristics and structure of the electroactive polyimide. Electrochemical activity of the polyimide was tested in 1.0 M H₂SO₄ aqueous solution and it shows two redox

peaks, which is the same as that of polyaniline. Moreover, the thermal properties of the polyimide were tested by thermogravimetric analysis (TGA). Its electrical conductivity is about $8.87 \times 10^{-6} \text{ S cm}^{-1}$ at room temperature upon preliminarily protonic-doped experiment.

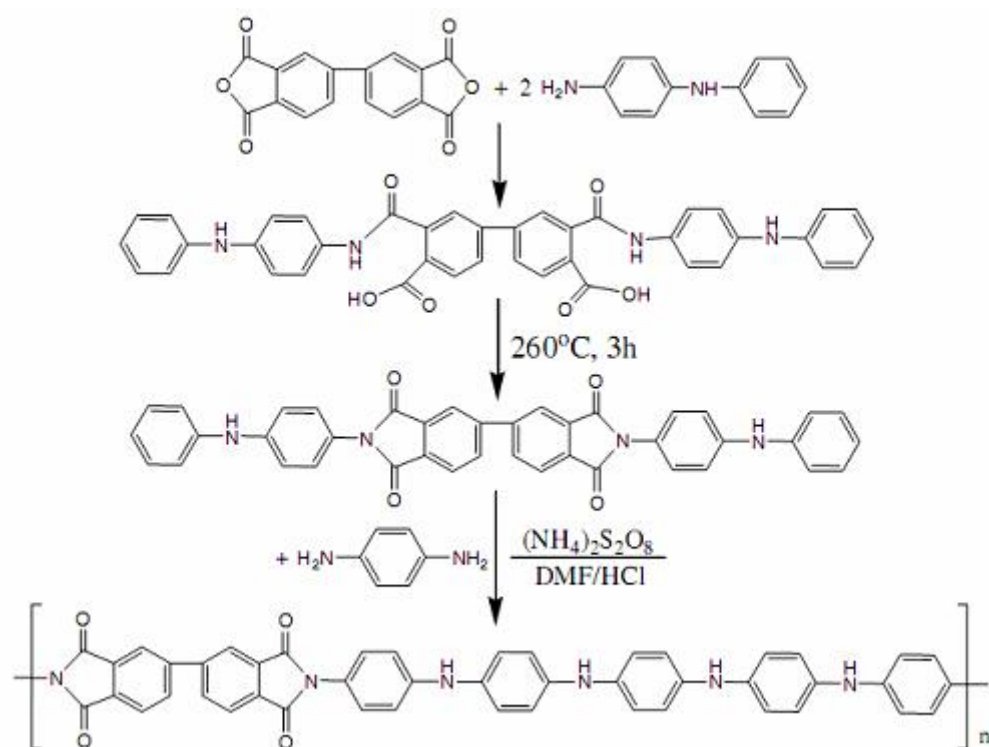


Figure 3.1 Synthesis of the imide macromonomer of oligoaniline and electroactive polyimide [75].

3.2 Poly (styrene sulfonic acid) Template

Poly(styrene sulfonic acid)(PSSA) is widely studied in order to use as the template of various conducting polymers via template polymerization. Moreover, during polymerization in water, PSSA is a charge-balancing dopant which allows for the formation of a colloidal dispersion. The structure of PSSA was shown in Figure 3.2. The previous works of this template are shown as follows:

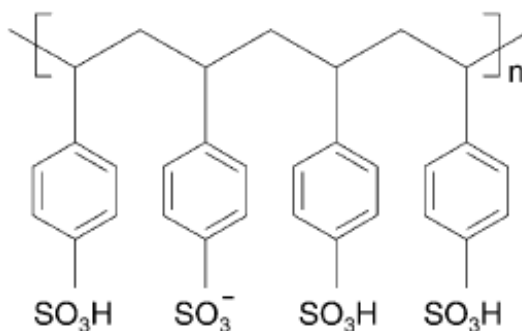


Figure 3.2 Structure of poly(styrene sulfonic acid) (PSSA).

Kim J.Y. et al. [76] (2002) were found the increase of conductivity in the PEDOT-PSS systems through the change of solvent from ~ 0.8 to 80 S/cm. The temperature dependence of the reduced activation energy exhibits that PEDOT-PSS system approaches the critical regime when organic solvents (DMF, THF, and DMSO) are used. As XRD and the absorbance experiments, the polymer chain conformation of the samples does not changed by the difference solvent used. EPR and XPS results show that the doping concentration of the systems with various solvents is almost the same. The screening effect due to the polar solvent between the polymer main chain and the dopant plays an important role for charge transport properties in term of conductivity and its temperature dependence.

Ouyang J. et al. [77] (2004) were studied on the enhancement of conductivity of PEDOT-PSS films which results from adding organic compounds to PEDOT-PSS aqueous solution or treating the PEDOT-PSS film with organic solvents, such as Ethylene glycol(EG), NMP, DMSO, 4-methoxyphenol, DMAc, cyclohexone, acetonitrile, methyl alcohol, nitromethane, and pyridine. After treatment with EG, the PEDOT-PSS film which is soluble in water becomes insoluble due to an increased interchain interaction among the PEDOT chains. This increased interchain interaction resulted from conformational changes of the PEDOT chains, which change from a coil to linear or expanded-coil structure was observed by Raman spectroscopy. The enhancement of conductivity was observed only when organic compounds with two or more polar groups in a molecule were used. They described that the driving force for the conformal changes in the PEDOT chains is the interaction between the dipoles

or the charges on the PEDOT chains and the dipole of one polar group of the organic compound.

Lee B. et al. [78] (2005) studied the preparation of the oxidative chemical polymerization of thieno [3,4-*b*]thiophene (T34bT) using several different oxidants including ammonium persulfate, ferric sulfate, and hydrogen peroxide in the presence of poly(styrenesulfonic acid) in water and properties of the resulting poly(thieno[3,4-*b*]thiophene)-poly-(styrenesulfonic acid) (PT34bT-PSS) dispersion. The resulting PT34bT-PSS is rendered a colloidal dispersion in water with a particle size diameter ranging of 180-220 nm depending on the oxidant used for polymerization. The neutral and oxidized forms of PT34bT-PSS which was prepared from ferric sulfate dispersed in water were blue and lime green, respectively, while the neutral and oxidized forms of PT34bT-PSS which were prepared from ammonium persulfate and hydrogen peroxide were blue and blue-green, respectively. Spectral properties of the PT34bT-PSS dispersion can be tuned by the combination of oxidants. Electrical conductivities for resulting polymers were found to be dependent on chemical oxidants used and varied from 10^{-2} to 10^{-4} S/cm.

Ouyang J. et al. [79] (2005) studied the conductivity of a PEDOT-PSS film, which can be increased by more than two orders of magnitude by adding a compound with two or more polar groups, such as ethylene glycol (EG), 2-nitroethanol and meso-erythritol (1,2,3,4-tetrahydroxybutane) into an aqueous solution of PEDOT-PSS. The results indicate that the conductivity enhancement depends on the chemical structure of the additive. When the alcohol solvents (heptanol, methanol or ethanol) were used, no conductivity enhancement was observed. And also, no conductivity enhancement was observed when acetonitrile or nitromethane was added into an aqueous solution of PEDOT-PSS. FTIR spectrums were represented that the additive induces a conformational change in the PEDOT chain in the PEDOT-PSS film. This conformational change results in an increase in the intrachain and interchain charge-carrier mobility.

Lee B. et al. [80] (2005) were prepared water dispersible conducting PT34bT with very low band gap by polymerizing T34bT in the presence of a polymeric charge compensating dopant (PSSA) and chemical oxidant in water. The spectral properties of these systems are highly dependent on chemical oxidants utilized. The resulting dispersions prepared utilizing hydrogen peroxide or persulfate ion have much better dispersibility than those prepared from ferric sulfate hydrate under normal laboratory conditions. Electrical conductivities for these polymers are dependent on chemical oxidants used and are varied from 0.01 to 10^{-4} S/cm.

Huang J. et al. [81] (2005) studied the influence of annealing conditions on the physical properties of thin films of PEDOT-PSS. In the experiments, they describe how annealing temperature, the ambient gas, and the choice of dopant affect the conductivity, morphology, and work function of the films. Two specific dopants, glycerol and sorbitol are used. The possession of O₂ and water in the ambient gas reduces the conductivity and work function of the undoped PEDOT-PSS films. Therefore, PEDOT-PSS films must be treated by inert gases such as N₂. The improvements in conductivity after thermal treatment are attributed to morphology changes led to larger grain sizes and lower inter-grain hopping barriers. The addition of dopants leads to substantial conductivity increasing up to a factor of about 500, depending on the exact doping ratio. The surface roughness is found to increase, with the degree of roughness at a given annealing temperature, apparently dependent on the rate of evaporation of the dopant molecules.

Jang J. et al. [82] (2007) were studied the synthesis of poly(aniline) with PSS template. The resulting water-dispersible PANI-PSS nanoparicles with an average diameter of 30 nm were fabricated by using chemical-oxidation polymerization. Water-dispersible PANI-PSS nanoparticles can be used in ink-jet-printed chemical sensors. Moreover, the chemical sensors thus-produced showed superior sensitivity and more rapid response time relative to conventional.

Nardes A.M. et al. [83] (2008) were studied and further clarified the role of sorbitol as a typical high-boiling processing additive on the conductivity of PEDOT-

PSS thin films under thermal annealing and exposure to humidity. The great conductivity enhancement of thin PEDOT-PSS films caused by adding sorbitol into the aqueous dispersion occurs during thermal annealing and coincides with the evaporation of sorbitol from the films. After thermal annealing, the increased conductivity is accompanied by a lowering of the work function and by a remarkable increase in environmental stability, as evidenced from a reduced water uptake, which we attribute to a denser packing of the PEDOT:PSS material.

Kang K.S. et al. [84] (2009) were found that the conductivity of PEDOT-PSS film enhanced nearly three orders of magnitude after HCl-methanol treatment. FTIR spectrums show the decreased characteristic peaks of PSS when increased duration of treatment in acidic methanol. After soaking PEDOT-PSS into the HCl-methanol solution for 10 min, the conductivity of PEDOT-PSS film was increased by approximately two orders of magnitude. The conductivity gradually increased up to 30 min but slightly decreased thereafter. After treatment, the surface of PEDOT-PSS was extremely smoother than before the solvent treatment. Removal of PSS from PEDOT-PSS film is beneficial for increasing the conductivity and protecting the electrode corrosion.

Chen Y. et al. [85] (2009) were studied in order to improve conductivity and transmittance of the PEDOT-PSS films after mixing MWCNT. Two-step modification processes of MWCNTs were performed to uniformly disperse MWCNTs in PEDOT-PSS. HNO_3 was used to form -OH and -COOH groups onto the MWCNT surface. For the second modification process using sorbitol, the carboxyl groups from FMWCNTs and hydroxyl groups from sorbitol molecule were reacted and formed covalent bonds between FMWCNTs and sorbitol molecules. The more sorbitol molecules on the FMWCNT showed the better uniform dispersion of FMWCNTSORS in a PEDOT-PSS solution without any precipitation, which means that FMWCNTSORS were well-dispersed in the PEDOT-PSS matrix.

Wang G.F. et al. [86] (2009) prepared PEDOT-PSS which was modified with DMSO and sequential thermal treatment. The mechanism for the conductivity

improvement was studied with particle size analysis, XPS and FESEM. The results show that the increased PEDOT concentration on the surface was enhanced electrical conductivity. In addition smaller size of electrical conductive particles exhibited better packing, bigger contact area facilitate in better electrical connection and three orders of magnitude conductivity enhancement.

Dimitriev O.P. et al. [87] (2009) were studied conductivity enhancement of PEDOT-PSS films, which contain different amounts of organic solvents, i.e., ethylene glycol (EG) or dimethyl sulfoxide (DMSO), and annealed at different temperatures. The maximum of conductivity of the resulting films was reached at about 5 wt.% of DMSO or EG in the solution. The residue solvent in the film also resulted in the poor control of the film morphology and conductivity. The author used an alternative method of the films exposure to the solvent vapors. The latter method has more advantages, because it preserves film morphology, and allows one to control conductivity as a function of the exposure time.

3.3 Other templates

Ner Y. et al. [88] (2010) were synthesized PEDOT using DNA as a polyelectrolyte template. The resulting material formed a stable and aqueous-dispersible system with higher conductivity than that of conventionally prepared PEDOT-PSS (ca. 1.0 S/cm versus ca. 0.15 S/cm). The material was redox active in the dispersed state and in the solid state. The DNA double helix was found to undergo changes in conformation upon redox switching, resulting in controllable variance of its ability to polarize light.

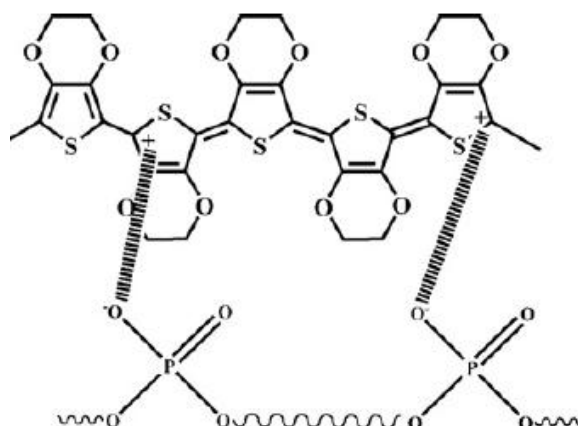


Figure 3.3 Chemical structure of the PEDOT-DNA template [88].

Yang C. et al. [89] (2010) were found that poly(2-hydroxy-3-(methacryloyloxy) propane-1-sulfonate) (PHMPS), a polyhydroxyl sulfonate, was used as both the template and the dopant in the in situ doping chemical oxidative polymerization of pyrrole. The size decreased and their dispersing stabilities in water increased with the increasing of the feeding ratio of PHMPS. The PPy/PHMPS nanoparticles possess high electrical conductivity at room temperature and the weak temperature dependence of the conductivity.

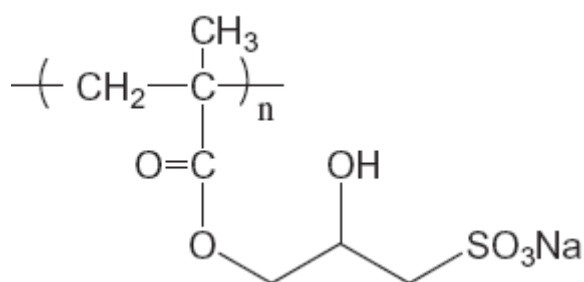


Figure 3.4 Structure of the PHMPS template [89].

3.4 Sulfonated Polyimide

Faure S. et al. [90] (1997) were synthesized the sulfonated five-membered and six-membered ring polyimides from 4,4'-oxydiphthalic anhydride (O-DPDA) and NTDA, respectively, which were practically tested in fuel cell systems. The results represented that ODPA-based polyimides were not stable enough in fuel cell

conditions while NTDA-based ones were fairly stable as long as the sulfonation degree was controlled to an appropriate level. The addition of sulfonic group into polymer structure was achieved by using a commercially available sulfonated diamine monomer, 2,2'-benzidinedisulfonic acid (BDSA).

Gunduz N. et al. [91] (2000) studied the synthesis of sulfonated polyimides using 2,5-diaminobenzene sulfonic acid sodium salt as the source of the sulfonated subunits. 4,4'-(9-fluorenylidene dianiline) and 4,4'-diaminodiphenyl sulfone were used as amine monomers. Two different tetracarboxylic acid anhydrides that used in the procedure were biphenyl-3,3',4,4'-tetracarboxylic acid dianhydride (BPDA) and 4,4' (hexafluoroisopropylidene)-bis-phthalic acid anhydride (6FDA). Polymers with high molecular weights and narrow molecular weight distributions were obtained by the ester–acid procedure in aprotic solvents. From the result of TGA, a first weight loss step upon heating in air was observed at 250 °C, due to degradation of sulfonic acid groups while the polymer backbone was stable to temperatures as high as 500 °C.

Genies C. et al. [92] (2001) were prepared the membrane materials from 1,4,5,8-naphthalene- tetracarboxylic acid dianhydride (NTDA), 4,4'-diaminobiphenyl-2,2'-disulfonic acid and various non-sulfonated diamines. A two-step process was employed, first synthesizing the sulfonated block oligomers with the desired length (DP = 19) bearing anhydride end groups. The final polymers were obtained by adding the predetermined amounts of NTDA and non-sulfonated-diamines for the adjustment of IEC. Polyimides based on bis-phthalic acid anhydride which gives five-membered imide rings are much more resistant to hydrolysis than the six-membered imide rings from naphthalenetetracarboxylic acid dianhydride.

Fang J. [93] (2002) was studied the preparation of sulfonated diamine monomer, 4,4'-diaminodiphenyl ether-2,2'-disulfonic acid (ODADS) by direct sulfonation of a commercially available diamine, 4,4'-diaminodiphenyl ether (ODA), using fuming sulfuric acid as the sulfonating reagent. A series of sulfonated polyimides were prepared from 1,4,5,8-naphthalenetetracarboxylic dianhydride

(NTDA), ODADS, and common nonsulfonated diamines. The resulting sulfonated polyimides indicated much better stability toward water than those derived from the widely used sulfonated diamine 2,2'-benzidinedisulfonic acid (BDSA) due to ODADS-based polyimide membranes have a more flexible structure than the corresponding BDSA-based.

Okamoto K. et al. [94] (2005) studied the synthesis of sulfonated copolyimides (co-SPIs) with ion exchange capacities of 1.83–2.32 meq/g from 1,4,5,8-naphthalenetetracarboxylic dianhydride (NTDA), two types of sulfonated diamines, namely, 4,4'-bis(4 sulfophenoxy) biphenyl-3,3'-disulfonic acid (BAPBDS) and bis(3-sulfopropoxy)benzidines (BSPBs), and common non-sulfonated diamines via polycondensation reaction. The results indicated that the BSPB-based co-SPI membranes had a clear microphase-separated structure composed of hydrophilic and hydrophobic domains but the connection of hydrophilic domains was rather poor while the BAPBDS-based co-SPI membranes did not show such a clear microphase separation. The co-SPI membranes showed the high proton conductivities of 0.10–0.16 S/cm in water at 323 K, which was comparable to that of Nafion 112 (0.13 S/cm).

Qiu Z. et al. [95] (2006) proposed the preparation of the primarily sulfonated aromatic dichloride monomer and hydrophobic dichloride monomers containing trifluoromethyl-substituted 1,8-naphthalimide or 1,4,5,8-naphthalimide moieties using as comonomers to generate oxidative and water stable copolymers for proton exchange membranes. The resultant copolymers with the SO₃H group in the side chain had high molecular weights due to their high viscosity and the formation of tough and flexible membranes. The copolymer membranes exhibited excellent oxidative and water stabilities due to the introduction of the hydrophobic CF₃ groups on the ortho-position of imido groups, which could protect the polymer main chains from being attacked by water molecules containing highly oxidizing radical species. The sulfonated copolyimides containing 1,8-naphthalimide moiety (I-x) exhibited better hydrolytic and oxidative stabilities, and higher proton conductivity than those containing 1,4,5,8-naphthalimide moiety with a similar IEC values. When considering

both water stability and proton conductivity, copolymer I-50 with IEC 1.67 has the best combination of properties for application in PEM for FC. Its proton conductivity reaches 2.6×10^{-1} S/cm, at 80 °C, which is higher than that of Nafion 117 (1.5×10^{-1} S/cm, at 80 °C). Therefore, these materials proved to be promising as proton exchange membranes.

CHAPTER IV

EXPERIMENT

The experimental works of this study were consisted in order to study the preparation of Conductive polyimide-graft-polyaniline, Organic surface conductive polyimide, Conducting polymers in the name of Poly(3,4-ethylenedioxythiophene) (PEDOT), Polyaniline (PANI) and Polypyrrole (PPy) with using Sulfonated poly(imide) as a template and Secondary dopants modified PEDOT-Sulfonated Poly(imide)s for high temperature range application. Moreover, this chapter will explicate the procedure for the step of synthesis, the detail of characterization techniques including FTIR, GPC, TGA, TEM, NMR, Four-point probe method, Tensile testing method, Current generator and Nanovoltmeter.

4.1 Materials and Chemicals

4.1.1 Chemicals 1 (As described in Paper 1, Paper 2)

The chemicals that used for the experiments, which carried out in the laboratory of the Center of Excellence on Catalysis and Catalytic Reaction Engineering, Bangkok, Thailand are listed as follows:

1. 4,4'-Hexafluoroisopropylidene diphthalic anhydride (6FDA) was purchased from Fluka.
2. Pyromellitic dianhydride (PMDA) was purchased from Merck.
3. 4,4'-Oxydianiline (ODA) was purchased from Fluka.
4. 3,3'-Dihydroxybenzidine (DHBD) was purchased from TCI America.
5. 3-Bromoaniline (BA) was purchased from Sigma-Aldrich.
6. Aniline was purchased from Sigma-Aldrich.
7. 4-Dodecylbenzenesulfonic acid (DBSA) was purchased from Sigma-Aldrich.
8. Potassium carbonate (K_2CO_3) was purchased from Fluka.
9. Ammonium persulfate (APS) was purchased from Sigma-Aldrich.
10. Methanol was purchased from Sigma-Aldrich.

11. N,N-dimethylformamide (DMF) was purchased from Sigma-Aldrich.
12. N-Methyl-2-pyrrolidinone (NMP) was purchased from Merck.
13. Toluene was purchased from Exxon Chemical Ltd., Thailand.
14. Hydrochloric acid (HCl) was purchased from Fisher.
15. Hexane was purchased from Fisher.

4.1.2 Chemicals 2 (As described in Paper 3, Paper 4)

The chemicals that used for the experiments, which carried out in the laboratory of the Polymer Program, the Institute of Materials Science at the University of Connecticut, USA are listed as follows:

1. 4,4'-diaminodiphenyl ether (4,4'-ODA) was purchased from Sigma-Aldrich.
2. 4,4'-oxydiphthalic anhydride (O-DPDA) was purchased from Sigma-Aldrich.
3. Triethylamine (Et₃N) was purchased from Sigma-Aldrich.
4. m-cresol was purchased from Sigma-Aldrich.
5. Fuming sulfuric acid (SO₃, 20%) was purchased from Sigma-Aldrich.
6. Poly(styrene sulfonic acid) (18 wt.% in water) was purchased from Sigma-Aldrich.
7. Iron (III) p-toluene sulfonate hexahydrate was purchased from Sigma-Aldrich.
8. 3,4-ethylenedioxythiophene (EDOT) was purchased from Sigma-Aldrich.
9. Lithium trifluoromethanesulfonate was purchased from Sigma-Aldrich.
10. N,N-dimethylformamide (DMF) was purchased from Sigma-Aldrich.
11. Aniline was purchased from Sigma-Aldrich.
12. Pyrrole was purchased from Fisher Scientific and was used as received.
13. Ammonium persulfate was purchased from Fisher Scientific.
14. Benzo-1,4-dioxan was purchased from Sigma-Aldrich.
15. Methyl viologen was purchased from Sigma-Aldrich.
16. Quinoxaline was purchased from Sigma-Aldrich.
17. 4,4'-Hexafluoroisopropylideneoxydiphthalic anhydride (6FDA) was purchased from TCI America.
18. Concentrated sulfuric acid (95%) was purchased from Fisher Scientific.

19. Sodium hydroxide (NaOH) was purchased from Fisher Scientific.
20. Hydrochloric acid (HCl) was purchased from Fisher Scientific.
21. Acetone was purchased from Fisher Scientific.
22. Surfynol® 2502 surfactant was purchased from Air Products, Inc.
23. d-Sorbitol 97% was purchased from Acros Organics.
24. Ion-exchange resin DOWEX 50WX8 50-100 mesh was purchased from Acros Organics.
25. ion-exchange resin Amberlite* IR-120 (Na⁺ form) was purchased from Acros Organics.
26. Quinoline was purchased from Acros Organics.
27. Imidazole was purchased from Acros Organics.
28. Sodium poly(styrene sulfonate) was purchased from Polysciences, Inc.
29. Glass beads (50-100 μm) was purchased from Polysciences, Inc.
30. Dialysis tubes (Molecular weight cut off [MWCO] = 3.5 to 5 kDa) was purchased from Spectrum Laboratories Inc.

4.2 Equipments

Because of the most of the reagents are very sensitive to oxygen and moisture, the special techniques are used in term of management and the loading of ingredient into the reactor. The devices used for this purpose are listed below.

(a) **Glove box** (Vacuum Atmospheres) with oxygen and moisture controller for handling and storing reagents under inert gas atmosphere. Oxygen and moisture contents are controlled to below 2 ppm. The glove box is shown in Figure 4.1.

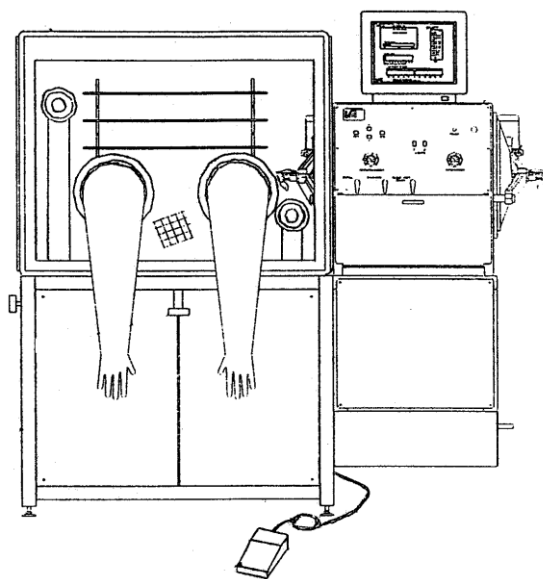


Figure 4.1 Glove box.

(b) **Schlenk line**, which included vacuum line that connected to vacuum pump and argon line for purging when reagents are transferred. The schlenk line is shown in Figure 4.2.

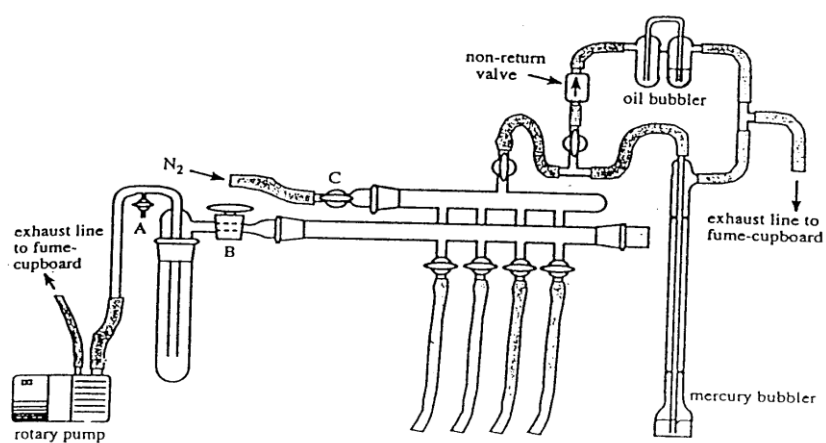


Figure 4.2 Schlenk line.

(c) **Schlenk tube** that used for keeping reagents under inert gas atmosphere is chosen the appropriated size that can be used together with the Schlenk line. Schlenk

tube was included a ground joint and a side arm which connected with three ways glass valve. The Schlenk tube is shown in Figure 4.3.

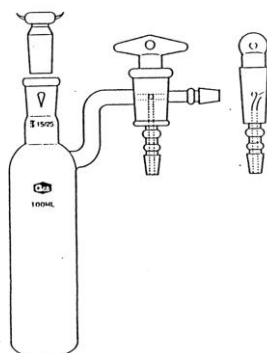


Figure 4.3 Schlenk tube.

(d) **The inert gas** (argon or nitrogen) from the cylinders was flowed through oxygen trap (BASF catalyst, R3-11G), moisture trap (molecular sieve), sodium hydroxide (NaOH) and phosphorus pentoxide (P_2O_5) columns to purifying the inert gas before entering Schlenk line and solvent distillation column. The inert gas supply system is shown in Figure 4.4.

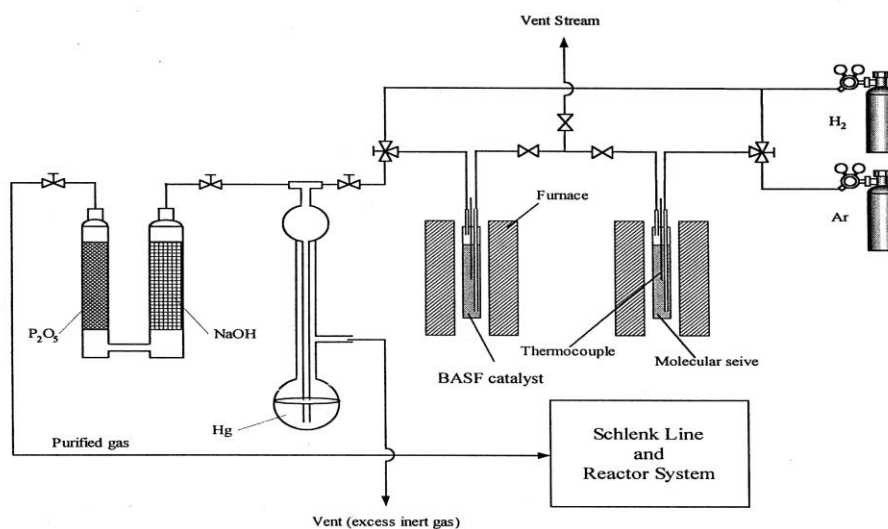


Figure 4.4 Inert gas supply system.

(e) **The vacuum pump** from Labconco Coporation, model 195 was used in as the vacuum supply to the vacuum line of the Schlenk line under the low pressure of

10^{-1} to 10^{-3} mmHg. The vacuum pump is shown in Figure 4.5.

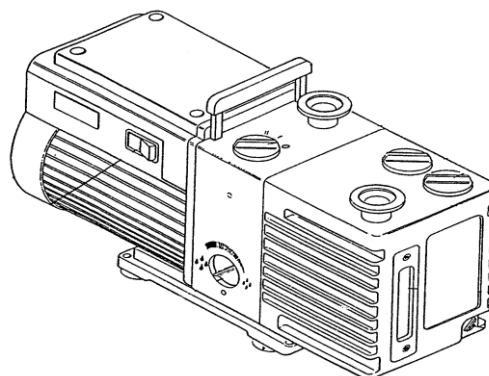


Figure 4.5 Vacuum pump.

(f) Magnetic Stirrer and Hot Plate

The hot plate model RCT and magnetic stirrer from IKA Labortechnik are used in these experiments.

(g) Syringe, Needle

The syringe of the volume 50 and 10 ml and the cooperated needles No. 17 and 20 are used in these experiments.

(h) Cooling System

The cooling system in the solvent distillation is needed in order to prevent the freshly evaporated solvent from the reactor during the synthesis.

4.2.1 Film Preparation Part

(a) Vacuum oven

A vacuum oven model 282A from Cole-Parmer was used for removing solvent from freshly cast films. The temperature, pressure and time can be controlled and set via digital panel and display their status on LCD.

(b) Temperature controlled oven

A Carbolite temperature controlled oven model LHT5/30 (201) which maximum working temperature of 500°C was utilized in these experiments. The oven was used for thermal treated the polyimide film.

4.3 Synthesis

4.3.1 Preparation and characterization of conductive polyimide-graft-polyaniline

4.3.1.1 Preparation of the polyimide

Polyimide was synthesized by the two steps reaction of 4,4'-hexafluoro isopropylidene diphthalic anhydride (6FDA), 4,4'-oxydianiline (ODA), and 3,3'-dihydroxybenzidine (DHBD) in DMF solutions. Firstly, the polyamic acid was made from the reacted solution of dianhydride and diamine. Lastly, polyimide film was made by imidization of polyamic acid to eliminate water molecules at high temperature. Thus, the polyamic acid solution were cast on glass plates, dried under vacuum for 1 hr at 70 °C, and cured by multi-step heating processes of 150, 200, 250, and 300 °C, for 30 min each in a high-temperature oven (Thickness *ca.* 20 μm, 86.46% yield). The polyimide films are crushed to be a powder before dissolved and proceeded in the reaction with 3-bromoaniline (BA).

4.3.1.2 Preparation of the polyimide-g-polyaniline

For synthesis example of PI-PANI(2), crushed polyimide films were dissolved in DMF solutions at 120 °C and stirred until dissolved completely. Then 3-bromoaniline (BA) and K₂CO₃ were added to the solution, refluxed at approximately 120 °C for 20 hrs, and the particles filtrated out to achieve the intermediate.

DBSA and APS were added in solutions, reacted at room temperature and stirred for 1 hr. Anilines were slowly added to the solutions and stirred for 12 hrs at room temperature. The solution was precipitated in methanol; the filtrated particles were washed with toluene to dissolve away the unreacted pure polyaniline, and finally under vacuum for 2 hrs at 50 °C. (Toluene is the normal solvent of neutral polyaniline but not polyimide) To dope the copolymer, dried particles were dissolved in DMF at room temperature and stirred until dissolved completely. HCl acid was added and the mixture stirred for 2 hrs. The solutions were then cast as films on glass plates and dried under vacuum for 2 hrs at 70 °C to achieve PI-PANI(2), (68.24% yield).

4.3.2 Organic Surface Conductive Polyimide

4.3.2.1 Preparation of the polyimide

Polyimide was synthesized via the reaction between PMDA and ODA with a one step polymerization technique. The mole ratio of dianhydride:diamine was 1:1 and the solid content of mixed solution was 15 wt%. Each of Pyromellitic dianhydride (PMDA) and 4,4'-Oxydianiline (ODA) were dissolve separately in N-Methyl-2-pyrrolidinone (NMP). The PMDA solution and ODA solution were added together to the flask via syringe, after that stirred and heat to 50 °C. The resulting homogeneous solution was reacted for 2 hrs at 180 °C in argon atmosphere and then added with toluene to remove water from imide condensation polymerization by azeotropic distillation. The mixture was stirred for 2 hrs at the same condition (temperature in argon atmosphere). The resulting polymer solution was cooled to room temperature and precipitated into water/methanol solution, filtered, and then vacuum-dried for overnight at 60 °C to obtain the polyimide solid (85.22% yield).

4.3.2.2 Preparation of the polyaniline-g-polyimide

Polyimide was synthesized by the two step reaction of 4,4'-hexafluoroisopropylidene diphthalic anhydride (6FDA), 4,4'-oxydianiline (ODA), and 3,3'-dihydroxybenzidine (DHBD) in DMF solutions in a mole ratio of 6FDA: ODA: DHBD = 10.03:9:1. Films of the poly(amic acid) solution were cast on glass plates, dried under vacuum for 1 hr at 70 °C, and cured by multi-step heating processes of 150, 200, 250, and 300 °C, for 30 min each in a high-temperature oven.

Polyimide films were dissolved in DMF solutions at 120 °C and stirred until dissolved completely. Then 3-bromoaniline (BA) and K₂CO₃ were added to the solution, reacted at 180 °C for 20 hrs, and the particles were filtrated out to achieve the intermediate. The Powder was redissolved in DMF. DBSA and APS were added in solutions, reacted at room temperature and stirred for 1 hr. Anilines were slowly added to the solutions and stirred for 12 hrs at room temperature. The solution was precipitated in methanol; the filtrated particles were washed with toluene to dissolve away the unreacted pure polyaniline, and finally under vacuum for 2 hrs at 50 °C to achieve PI-PANI particles (64.36% yield)

4.3.2.3 Preparation of conductive polyimide composite and surface-conductive polyimide (PI/PI-PANI)

For synthesis examples of PI/PI-PANI₁₀ and PI/PI-PANI₁₀₍₂₎, in cast of PI/PI-PANI₁₀ (conductive polyimide composite film); PI-PANI particles (10 wt%) were dissolved in DMF and mixed with pure polyimide particles (90 wt%) at room temperature and stirred until dissolved completely. HCl acid was added and the mixture stirred for 2 hrs. The solutions were then cast as films on glass plates and dried under vacuum for 2 hrs at 70 °C to achieve PI/PI-PANI₁₀. For synthesis of PI/PI-PANI₁₀₍₂₎ (surface-conductive polyimide film), polyimide particles (90 wt%) and PI-PANI particles (10 wt%) were dissolved separately in DMF at room temperature and stirred until dissolved completely. HCl acid was added in PI-PANI solution and stirred for 2 hrs. Polyimide solution was cast as film on glass plates, pre-baked under vacuum for 10 min at 80 °C and then, PI-PANI solution was cast on polyimide film and dried under vacuum for 2 hrs at 70 °C to achieve PI/PI-PANI₁₀₍₂₎.

4.3.3 Comparison of the Thermally Stable Conducting Polymers PEDOT, PANi, and PPy Using Sulfonated Poly(imide) Templates via Poly(amic acid).

4.3.3.1 Synthesis of 4,4'-diaminodiphenyl ether-2,2'-disulfonic acid (4,4'-ODADS)

To a 100 mL three-neck flask with a stirring device was added 2.00 g (10.0 mmol) of 4,4'-diaminodiphenyl ether (4,4'-ODA). The flask was cooled in an ice bath, and then 1.7 mL of concentrated (95%) sulfuric acid was slowly added with stirring. After 4,4'-ODA was completely dissolved, 10.5 mL of fuming (SO₃ 20%) sulfuric acid was slowly added to the flask. The reaction mixture was stirred at 0°C for 2 h and then slowly heated to 80°C and kept at this temperature for an additional 3 h. After cooling to room temperature, the slurry solution mixture was carefully poured onto 20 g of crushed ice. The resulting white precipitate was filtered off and then re-dissolved in a sodium hydroxide solution. The basic solution was filtered, and the filtrate was acidified with concentrated hydrochloric acid. The solid was filtered off,

washed with water and methanol successively, and dried at 80°C in vacuum oven overnight. (87.17% yield) [104-105].

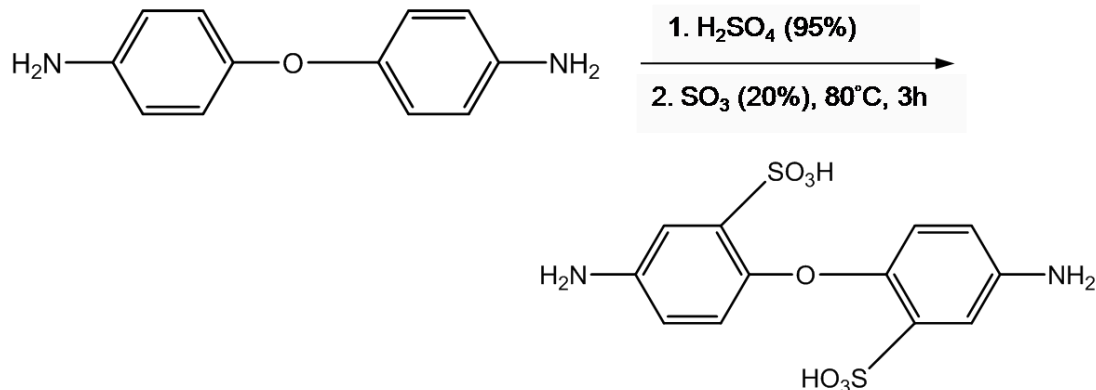


Figure 4.6 Scheme for the 4,4'-ODADS reaction [104-105].

4.3.3.2 Synthesis of sulfonated poly(amic acid)s (SPAA1, SPAA2)

To a 100 mL three-neck flask with N₂ inlet and outlet was added 0.5405 g (1.5 mmol) of 4,4'-ODADS, 6 mL of m-cresol, and 0.3643 g (3.6 mmol) of triethylamine. After 4,4'-ODADS was completely dissolved, 0.4653 g (1.5 mmol) of O-DPDA for SPAA1 or 0.6664 g (1.5 mmol) of 6FDA for SPAA2 were added and then stirred at room temperature for 24 h. When the reaction was complete, the reaction mixture was decanted into acetone (75 mL), filtered, washed with acetone (25 mL, 2 times), and dried at 50°C in a vacuum oven overnight. (1.1463 g, 83.66% yield for SPAA1 and 1.3404 g, 85.31% yield for SPAA2) [104-105].

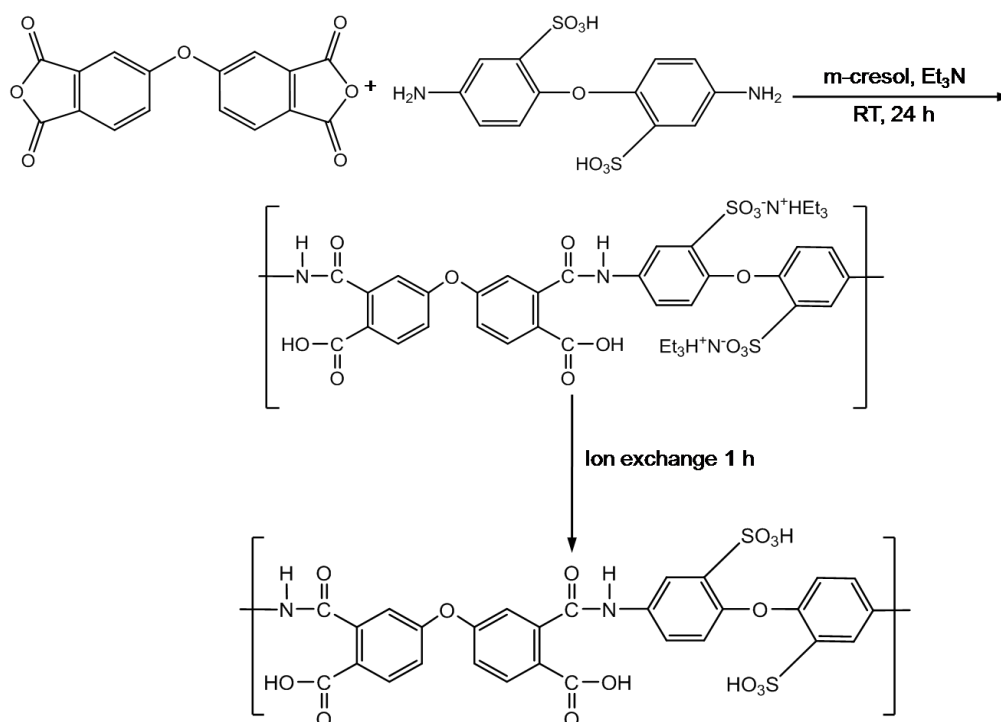


Figure 4.7 Synthesis of sulfonated poly(amic acid) (SPAA1) [104-105].

4.3.3.3 Purification

The sulfonated poly(amic acid)s were purified via dialysis tube. SPAAs dissolved in water were loaded inside the dialysis tube and soaked in DI water for 24 h, changing the water twice (2 times at 12 h each) [104-105].

4.3.3.4 Ion Exchange

The purified SPAAs salt form were changed to SPAAs acid form with an ion exchange resin of strong acid type DOWEX 50WX8 (cation exchange) in case using for polymerization with EDOT and purified with Amberlite* IR-120 (Na⁺ form) ion exchange resin in case using for polymerization with aniline. The SPAAs salt form were stirred in DI water with the ion exchange resin for 1 h to convert them to the free acid form (SO₃H) and sulfonated poly(amic acid) sodium form (Na⁺); they were centrifuged and filtered in a crucible filter and then dried at 50°C in vacuum oven overnight [104-105]. Molecular weight and molecular weight distributions of SPAA1 and SPAA2 were $M_{n1}=20,769$, $M_{w1}=35,502$, $PDI_1=1.71$ and $M_{n2}=18,627$, $M_{w2}=39,442$, $PDI_2 = 2.12$.

4.3.3.5 Template Polymerization of EDOT and poly(styrenesulfonic acid) (PEDOT-PSS)

To a 25 mL one neck flask, 21.3 mg (0.15 mmol) of EDOT and 290.4 mg of 18 wt.% PSSA aqueous solution were added. To this suspension 108.4 mg (0.16 mmol) of iron (III) p-toluene sulfonate hexahydrate was added. The total mass of all the reactants was adjusted to 10 g by adding an appropriate amount of de-ionized water. The reaction mixture was stirred vigorously for 24 h at room temperature leading to a dark blue dispersion [104-105].

4.3.3.6 Template Polymerization of EDOT and Sulfonated Poly(amic acid) (PEDOT-SPAA1, PEDOT- SPAA2)

To a 25 mL one neck flask, 21.3 mg (0.15 mmol) of EDOT and 200.0 mg (0.30 mmol) of SPAA1 or 230.6 mg (0.30 mmol) of SPAA2 were added. To this suspension 108.4 mg (0.16 mmol) of iron (III) p-toluene sulfonate hexahydrate was added for both polymerizations. The total mass of all the reactants was adjusted to 10 g by adding appropriate amount of de-ionized water. The reaction mixtures were stirred vigorously for 7 days, 5 days for PEDOT-SPAA1 and PEDOT-SPAA2, respectively at room temperature leading to a dark blue dispersion [104-105].

4.3.3.7 Template Polymerization of PANI and poly(styrenesulfonic acid) (PANI-PSS)

To a 100 mL one neck flask, 49.36 mg (0.53 mmol) of ANI was introduced dropwise in 0.5 M aqueous HCl solution 40 mL and was stirred for 1 h. Then, 600.0 mg (0.07 mmol) of PSS^-Na^+ was added to the mixed solution and was stirred for 1 h. The polymerization of ANI was conducted with 157.46 mg (0.69 mmol) of APS as an oxidizing agent. The reaction mixtures were stirred vigorously for 12 h at room temperature leading to a dark green dispersion [82,105].

4.3.3.8 Template Polymerization of ANI and sulfonated poly(amic acid) (PANI-SPAA1, PANI-SPAA2)

To a 100 mL one neck flask, 49.36 mg (0.53 mmol) of ANI was introduced dropwise in 0.5 M aqueous HCl solution 40 mL and was stirred for 1 h. Then, 47.34

mg (0.07 mmol) of SPAA1 Na⁺ form or 54.32 mg (0.07 mmol) of SPAA2 Na⁺ form were added to the mixed solution and were stirred for 1 h. The both polymerizations of ANI were conducted with 157.46 mg (0.69 mmol) of APS. The reaction mixtures were stirred vigorously for 12 h at room temperature leading to a dark green dispersion [105].

4.3.3.9 Template Polymerization of Py and poly(styrenesulfonic acid) (PPy-PSS)

To a 25 mL one neck flask, 10.06 mg (0.15 mmol) of Py and 290.4 mg of 18 wt.% PSSA aqueous solution were added. To this suspension 108.40 mg (0.16 mmol) of iron (III) p-toluene sulfonate hexahydrate was added. The total mass of all the reactants was adjusted to 10 g by adding an appropriate amount of de-ionized water. The reaction mixture was stirred vigorously for 24 h at room temperature leading to a black dispersion [105].

4.3.3.10 Template Polymerization of Py and sulfonated poly(amic acid) (PPy-SPAA1, PPy-SPAA2)

To a 25 mL one neck flask, 10.06 mg (0.15 mmol) of Py and 200.0 mg (0.30 mmol) of SPAA1 or 230.6 mg (0.30 mmol) of SPAA2 were added. To this suspension 108.40 mg (0.16 mmol) of iron (III) p-toluene sulfonate hexahydrate was added for both polymerizations. The total mass of all the reactants was adjusted to 10 g by adding appropriate amount of de-ionized water. The reaction mixtures were stirred vigorously for 5 days at room temperature leading to a black dispersion [105].

4.3.3.11 Preparation of PEDOT, PANI, PPy with SPAA1 and SPAA2 films

Films were prepared by drop casting pristine films and doped films onto glass slides at room temperature. The films were annealed at 180°C for 10 or 90 min, and 300°C for 10 min for improving conductivities with thermal treatment. Separate films of each material were evaluated for conductivity at room temperature after annealing. All films were also prepared with 5 wt.% of d-sorbitol, 0.1 wt.% DMF, 0.1 wt.% Surfynol® 2502, and with all three components simultaneously [105].

4.3.4 Secondary Dopants Modified PEDOT-Sulfonated Poly(imide)s for High Temperature Range Application

4.3.4.1 Synthesis of 4,4'-diaminodiphenyl ether-2,2'-disulfonic acid (4,4'-ODADS)

To a 100 mL three-neck flask with a stirring device, 5.00 g (25.0 mmol) of 4,4'-diaminodiphenyl ether (4,4'-ODA) was added. The flask was cooled in an ice bath, and then 5 mL of concentrated (95%) sulfuric acid was slowly added while stirring. After 4,4'-ODA was completely dissolved, 18 mL of fuming (SO₃ 30%) sulfuric acid was slowly added to the flask. The reaction mixture was stirred at 0°C for 2 h and then slowly heated to 80°C and kept at this temperature for additional 3 h. After cooling to room temperature, the slurry solution mixture was carefully poured onto 40 g of crushed ice. The resulting white precipitate was filtered off and then re-dissolved in a sodium hydroxide solution. The basic solution was filtered, and the filtrate was acidified with concentrated hydrochloric acid. The solid was filtered off, washed with water and methanol successively, and dried at 80°C in vacuum oven overnight [104-105]. (78.24% yield).

4.3.4.2 Synthesis of sulfonated poly(amic acid)s (SPAA1, SPAA2)

To a 100 mL three-neck flask with N₂ inlet and outlet, 3.5 g (9.71 mmol) of 4,4'-ODADS, 50 mL of m-cresol, and 1.96 g (19.42 mmol) of triethylamine were added. After 4,4'-ODADS was completely dissolved, 3.01 g (9.71 mmol) of O-DPDA for SPAA1 or 4.32 g (9.71 mmol) of 6FDA for SPAA2 were added and then stirred at room temperature for 3 days. When the reaction was complete, the reaction mixture was decanted into acetone (200 mL), filtered, washed with acetone (25 mL, 2 times), and dried at 50°C in a vacuum oven overnight [104-105]. (82.89% yield for SPAA1 and 77.56% yield for SPAA2).

4.3.4.3 Ion Exchange

The purified SPAAs in salt form were changed to SPAAs in acid form with an ion exchange resin of strong acid type DOWEX 50WX8 (cation exchange) before

polymerization with EDOT. The SPAAs in salt form were stirred in DI water with the ion exchange resin for 3 h to convert them into the free acid form (SO_3H). They were centrifuged and filtered in a crucible filter and then dried at 50°C in vacuum oven overnight [104-105]. Molecular weight and molecular weight distributions of SPAA1 and SPAA2 were $M_{n1}=43,457$, $M_{w1}=72,124$, $\text{PDI}_1=1.89$ and $M_{n2}=39,987$, $M_{w2}=68,322$, $\text{PDI}_2 = 2.67$.

4.3.4.4 Template Polymerization of EDOT and poly (styrenesulfonic acid) (PEDOT-PSS)

To a 1,000 mL LDPE bottle, 319.5 mg (2.25 mmol) of EDOT and 4,356 mg of 18 wt.% PSSA aqueous solution were mixed. To this suspension 1626 mg (2.4 mmol) of iron (III) p-toluene sulfonate hexahydrate was added. The total mass of all the reactants was adjusted to 150 g by adding an appropriate content of de-ionized water. The reaction mixtures were added glass beads 10 g and stirred at 4,000 rpm (using mechanical stirrer) for 3 days at room temperature leading to a dark blue dispersion. The solutions were purified according to literature procedure [104-105].

4.3.4.5 Template Polymerization of EDOT and Sulfonated Poly(amic acid) (PEDOT-SPAA1, PEDOT- SPAA2)

To a 1,000 mL LDPE bottle, 319.5 mg (2.25 mmol) of EDOT and 3,015.0 mg (4.5 mmol) of SPAA1 or 3,458.7 mg (4.5 mmol) of SPAA2 were added. To this suspension 1626 mg (2.4 mmol) of iron (III) p-toluene sulfonate hexahydrate was added for both polymerizations. The total mass of all the reactants was adjusted to 150 g by adding appropriate content of de-ionized water. To reaction mixtures, glass beads 10 g were added. The reaction was stirred vigorously at 4,000 rpm (using mechanical stirrer) for 3 days for both of PEDOT-SPAA1 and PEDOT-SPAA2 at room temperature leading to a dark blue dispersion. The solutions were purified according to literature procedure [104-105].

4.3.4.6 Preparation of conducting polymer films

Both pristine films and doped films were prepared by drop casting onto glass slides at room temperature. The films were annealed at 180°C for 10 or 90 min, and

300°C for 10 min in order to improve conductivities by thermal treatment. Each film from each material was evaluated for conductivity at room temperature after annealing [104-105]. To investigate the secondary doping, all of the films were also prepared with 0.1 wt.% Benzo-1,4-dioxan, 5 wt.% Imidazole, 0.1 wt.% Quinoline, 5 wt.% Methyl viologen, 0.1 wt.% Quinoxaline, 0.1 wt.% DMF, 5 wt.% of d-sorbitol and 0.1 wt.% Surfynol® 2502.

4.4 Characterization Instruments

4.4.1 Infrared Spectroscopy (FTIR)

- Institute of Materials Science and the Polymer Program at the University of Connecticut, USA.

Fourier transform infrared spectroscopy (FTIR) model MAGNA-IR560 was used in these experiments. Spectra was taken on ground powder in a KBr matrix with a scanning range of 500 – 4000 cm^{-1} , 64 scans at a resolution of 4 cm^{-1} [104-105].

- Center of Excellence on Catalysis and Catalytic Reaction Engineering.

Infrared spectra are recorded with Nicolet 6700 FTIR spectrometer using a scanning ranged from 400 to 4000 cm^{-1} with scanning 64 times [104-105].



Figure 4.8 Fourier transform infrared spectroscopy (FT-IR) Equipment [104-105].

4.4.2 Thermogravimetric analysis (TGA)

- Institute of Materials Science and the Polymer Program at the University of Connecticut, USA.

Thermogravimetric Analysis (TGA) is analyzed by a Perkin-Elmer TGA 7 series analysis system with the heating rate of 20°C/min under air at the flow rate of 60 mL/min [104-105].

- Center of Excellence on Catalysis and Catalytic Reaction Engineering.

Thermogravimetric analysis (TGA) is analyzed by a SDT Analyzer model Q600 from TA Instruments, USA. The sample weights were 3-10 mg. and the temperature range of 30-700°C with the heating rate of 20 °C/min under air at the flow rate of 400 mL/min [104-105].



Figure 4.9 Thermogravimetric analysis (TGA) Equipment [104-105].

4.4.3 Gel Permeation Chromatography (GPC)

- Institute of Materials Science and the Polymer Program at the University of Connecticut, USA.

Gel Permeation Chromatography (GPC) was performed by a millipore model 150-C GPC system. The mobile phase that used for the system was DMAC. The results were calibrated using standards of poly(methyl methacrylate) [104-105].

4.4.4 Nuclear Magnetic Resonance (NMR)

- Institute of Materials Science and the Polymer Program at the University of Connecticut, USA.

Nuclear Magnetic Resonance (NMR) ^1H NMR spectra are recorded by a Bruker DMX-500 NMR Spectrometer [104-105].

- Center of Excellence on Catalysis and Catalytic Reaction Engineering.

Nuclear Magnetic Resonance (NMR) ^1H NMR spectra are recorded by Bruker Biospin DPX400 NMR spectrometer (Switzerland) operating at 400 MHz with deuterated dimethyl sulfoxide ($\text{DMSO-}d_6$) [104-105].

4.4.5 Conductivity

- Institute of Materials Science and the Polymer Program at the University of Connecticut, USA.

Conductivities are measured by a four-line collinear array utilizing a Keithley Instruments 224 constant current source and a 2700 Multimeter. The polymer is coated on the glass substrate and laid to the holder which having four gold coated leads on the surface across the entire width of the polymer and 0.25 cm apart from each other. The current is applied across the outer leads while the voltage is measured across the inner leads [104-105].

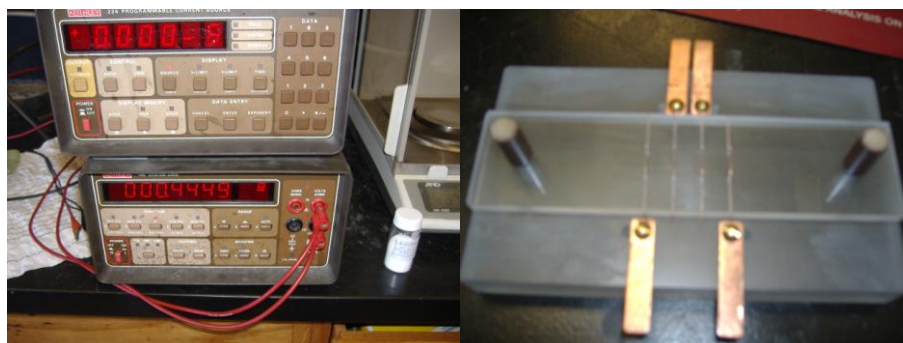


Figure 4.10 Current generator and Multimeter (left), Four-point probe (Gold wires) (right) [104-105].

- Center of Excellence on Catalysis and Catalytic Reaction Engineering.

Conductivities are measured by a four-line collinear array utilizing a Keithley Instruments 6221 DC and AC current source and a Keithley 2182A Nanovoltmeter. Conductivity is calculated from the equation of $\sigma = l/twR$ (S/cm) where l is the distance between platinum wires, t is the thickness of the film and w is the width of the film [104-105].



Figure 4.11 Current generator and Nanovoltmeter equipped with Four-point probe (Platinum wires) [104-105].

4.4.6 Transmission electron microscope (TEM)

- Institute of Materials Science and the Polymer Program at the University of Connecticut, USA.

The synthesized polymers are imaged by a JEOL 2010 Fas and Philips EM420 transmission electron microscope [104-105].

- Center of Excellence on Catalysis and Catalytic Reaction Engineering.

The synthesized polymers are imaged by a JEOL JEM 2010 transmission electron microscope that employed a LaB₆ electron gun in the voltage range of 80–200 kV with an optical point-to-point resolution of 0.23 nm [104-105].

4.4.7 Tensile testing machine

- Center of Excellence on Catalysis and Catalytic Reaction Engineering.

Tensile properties are characterized by using an Instron universal testing machine with a test speed of 5 mm/min and sample size of 2 x 10 cm. The tests were conducted follow to ASTM D 882-02 [104-105].

The tensile testing machine of a constant-rate-of-crosshead movement is used in these experiments. It has a fixed member grip and a moveable member grip. Self-aligning grips were employed for holding the test specimen between the fixed member and moveable member to prevent the alignment problem. An extension

indicator was used in determining the distance between two designated points located within the length of the test specimen as the specimen is stretched [104-105].



Figure 4.12 Tensile testing machine equipment [104-105].

CHAPTER V

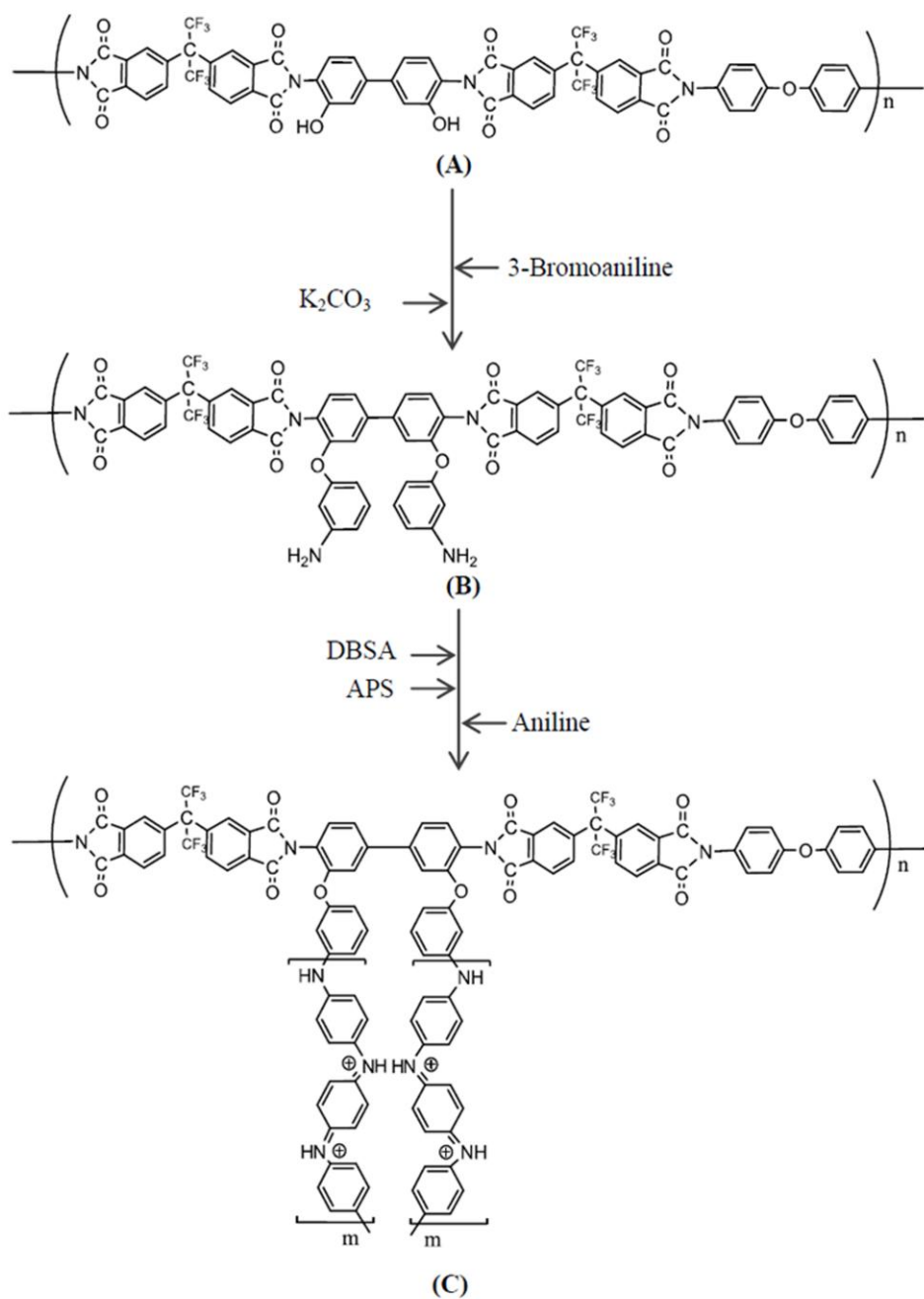
RESULTS AND DISCUSSION

The results and discussion in this chapter are divided into 4 parts. The first part (section 5.1) shows the preparation and characterization of conductive polyimide-graft-polyaniline. The second part (section 5.2) shows the organic surface conductive polyimide. The fourth part (section 5.3) shows the comparison of the thermally stable conducting polymers PEDOT, PANI, and PPy using sulfonated poly(imide) templates via poly(amic acid) and the third part (section 5.4) shows the secondary dopants modified PEDOT-Sulfonated poly(imide)s for high temperature range application.

5.1 Preparation and characterization of conductive polyimide-graft-polyaniline

5.1.1 Grafting of polyaniline on polyimide chains

In order to graft polyaniline to polyimide, polyimide molecules needed to have special functional group along the molecules. Using DHBD, two hydroxyl functional groups per molecule of DHBD were laid along the molecule of polyimide. The number of hydroxyl functional groups per molecule of polyimide, which the graft aniline could attach to, could be controlled by adjusting the incorporated DHBD per molecule of polyimide. The hydroxyl group could react with 3-bromoaniline releasing HBr and had the ether linkage between polyimide molecule and aniline as shown in Scheme 5.1. The grafting process could be further done by the addition of DBSA and APS with gradually adding aniline monomer to the solution [96-97]. The length of grafting aniline could be controlled by controlling the addition of the proper quantity of aniline. In order to obtain a high strength of the soluble copolymer, it was necessary to regulate and optimize the amount of DHBD and the length of polyimide. From the experiments, to make the single film from appropriated monomers, the ratio of 6FDA: ODA: DHBD equal to 10.03:9:1 was employed. This ratio gave the optimum properties both for completely soluble polyimide products before preceded to reaction with polyaniline segments and for high free-standing film strength even after grafting with polyaniline.



Scheme 5.1 The preparation of conductive polyimide.

In order to test the reaction between the OH group of DHBD and the Br group of BA, the direct reaction between DHBD and excess amount of BA was performed at 120 °C using K_2CO_3 as a catalyst [98-100]. The results showed that the reaction was plausible and that the aniline could be attached to the DHBD through the ether bond.

Table 5.1 Molar ratio of compositions on the reaction mixtures.

| Code | Molar ratio of the composition | | | | | Conductivities (S/cm) | |
|------------|--------------------------------|-----|------|----|---------|-----------------------|---------------|
| | 6FDA | ODA | DHBD | BA | Aniline | 20°C | 250°C, 15 min |
| PI | 10.03 | 9 | 1 | 0 | 0 | 0 | 0 |
| PANI | 0 | 0 | 0 | 0 | 12 | 71.31 | 0 |
| PI-PANI(1) | 10.03 | 9 | 1 | 2 | 12 | 2.96 | 1.47 |
| PI-PANI(2) | 10.03 | 9 | 1 | 2 | 36 | 6.12 | 2.11 |
| PI-PANI(3) | 10.03 | 9 | 1 | 2 | 60 | 16.2 | 0.18 |

Fig. 5.1 shows the ^1H NMR spectrums of DHBD, BA and DHBD-BA. In the ^1H NMR spectroscopy studies, the signals appearing at 9, 6.6-6.8, and 4.5 ppm (see Fig. 5.1(a)) could be assigned to the hydroxyl protons (-OH), aromatic protons, and primary amine protons (-NH₂) of DHBD, respectively. The ^1H NMR signals appearing at 6.6-7.2 and 5.1 ppm in Fig. 5.1(b) could be assigned to the aromatic protons and primary amine protons (-NH₂) of BA. For the ^1H NMR spectrum in Fig. 5.1(c), all of the combination spectra between DHBD and BA were shown except the spectrum of OH groups of DHBD at 9 ppm. This suggested that DHBD could react completely with BA.

The polymerization reaction of aniline in DMF was also tested. The aniline was dissolved in DMF at room temperature. The mixture of DBSA and APS was added to the solution under stirring. The solution acquired a deep dark green color and became highly viscous. The product of the reaction was precipitated in methanol and examined by FTIR, as showed in Fig. 5.3.

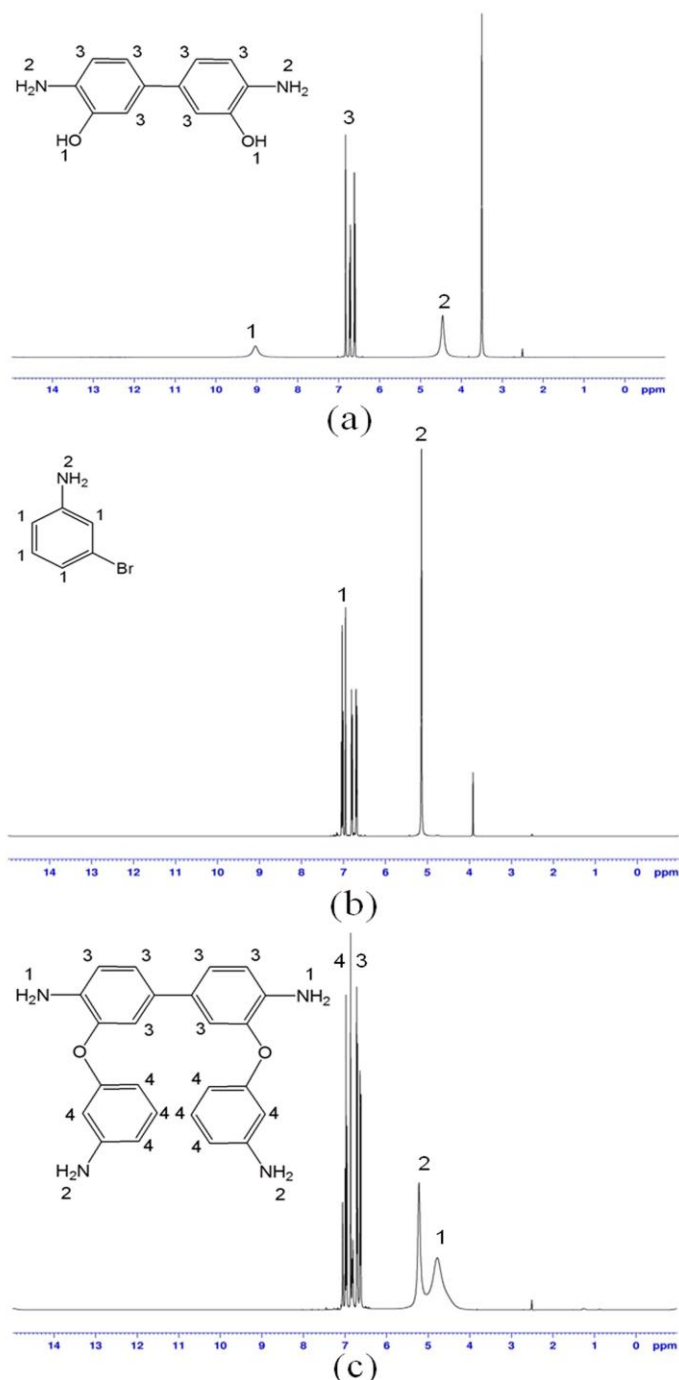


Figure 5.1 ^1H NMR spectrum of DHBD(a), BA(b) and DHBD-BA(c).

Polyimide made by reacting one hundred part of DHBD with nine hundred part of ODA and one thousand and three part of 6FDA, because of the unbalance mole ratio of acid and amine, the polyimide products become more soluble. The polymerization was conducted without initiator because the reaction was self-acid

catalyzed and could proceed autonomously. The reaction with BA was performed and the attachment of aniline to polyimide at DHBD was confirmed by $^1\text{H-NMR}$ spectra as in Fig. 5.2. The $^1\text{H-NMR}$ peak at 9 ppm, which represented the hydroxyl group in back bone polyimide, had completely disappeared after BA was attached to the main chain. The reaction of aniline monomer to aniline that attached to polyimide was performed by APS and DBSA in DMF, while keeping as low concentration of aniline as possible. This was achieved by drop-wise addition of aniline monomer in certain time. After the addition of aniline was completed, the particles were filtrated from the solution and washed several times with toluene, common solvent for polyaniline, before undergoing GPC measurements. The free chain of polyaniline that did not attach to the polyimide would be dissolved in toluene and washed away while the remained was the polyimide graft with polyaniline, which was not dissolved in toluene. The single peak of GPC resulted with larger molecular weight obtained confirmed that polyaniline could be grafted on polyimide chains.

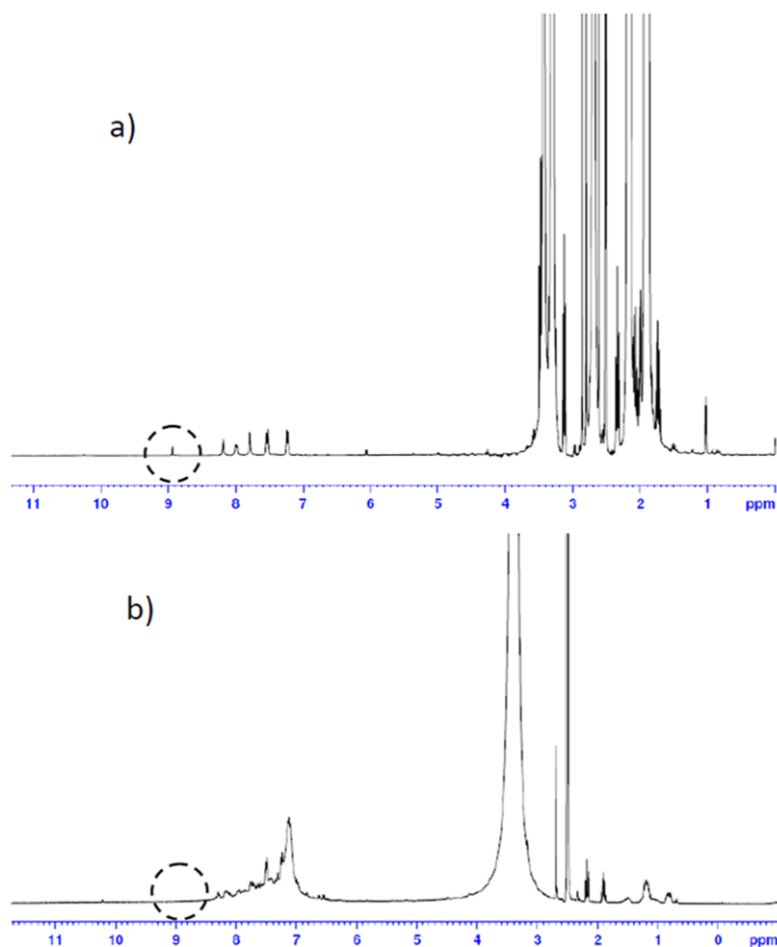


Figure 5.2 (a) ^1H NMR spectrum of Main Chain Polyimide before grafting, (b) ^1H NMR spectrum of Graft Copolymer Obtained. The circles focus the disappearance of hydrogen peak of alcohol group after grafting.

The FTIR of the copolymer combined the characteristic peak of polyimide and polyaniline as expected. As shown in the FTIR spectra in Fig. 5.3, the band observed at 1778 cm^{-1} and 1726 cm^{-1} are attributed to C=O symmetrical and C=O asymmetrical stretching of imide groups, whereas the bands at 1380 cm^{-1} was associated with the C–N stretching modes, represented the polyimide [101]. The characteristic peaks of polyaniline were observed at approximately 1552 , 1463 , 1289 , and 1123 cm^{-1} , respectively, with C=C stretching of the quinoid ring, C=C stretching of the benzenoid ring, C–N stretching, and N=Q=N stretching (Q representing the quinoid ring) [102-103]. The FTIR of three synthesized copolymers was the combination between peaks of polyimide and polyaniline. However, the heights of characteristic

peaks of polyaniline in the synthesized copolymers were different. The highest peaks belong to the longest lengths of the polyaniline graft chain and the peaks were gradually lower in shorter polyaniline graft chain because three different amount of aniline monomer were each attached to the same polyimide molecule. Three different amount of reacted aniline per one mole DHBD was 12, 36 and 60 mole aniline corresponded to PI-PANI(1), PI-PANI(2) and PI-PANI(3), respectively. The results of PI-PANI(3) had the higher polyaniline characteristic than those of PI-PANI(2) and PI-PANI(1) because of the higher polyaniline contents in copolymer.

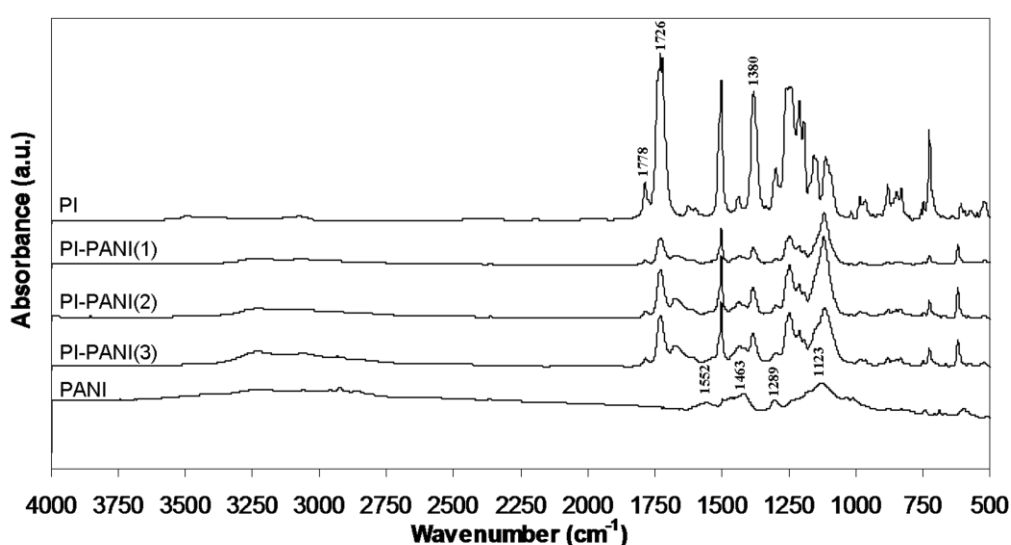


Figure 5.3 FTIR spectra of each PANI-g-PI samples in comparison with pure PI and pure PANI for comparison.

Fig. 5.4 shows the molecular weight distribution of PI-PANI(1), PI-PANI(2) and PI-PANI(3). The molecular weight distribution of all samples showed only one peak and thus confirmed that polyanilines were completely grafted on the polyimide chains. Moreover, this also confirmed that the unattached polyaniline was completely washed away by toluene. The molecular weight (M_n) of PI, PI-PANI(1), PI-PANI(2), and PI-PANI(3) were 12.43, 14.83, 15.42 and 16.88 kDa, respectively. The molecular weight (M_n) of PI-PANI(3) was higher than that of PI-PANI(2) and PI-PANI(1), because it had higher polyaniline segments than the others (in the same length of polyimide molecule). Polyaniline contents in copolymer matrix could be calculated by comparing the molecular weight (M_n) of samples with nascent PI. Percent weight of

Polyaniline segments in PI-PANI(1) is 19.30% while the results from PI-PANI(2) and PI-PANI(3) are 24.05% and 35.80%, respectively.

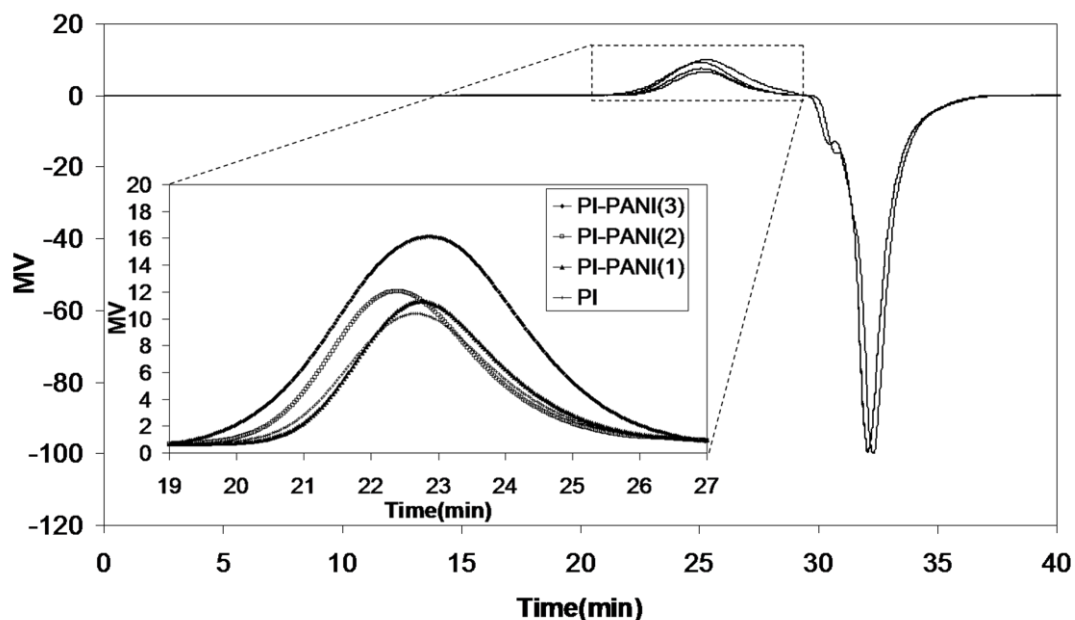


Figure 5.4 GPC of PI, PI-PANI(1), PI-PANI(2), and PI-PANI(3). The small window expanded the focus area of the single curve of each samples for closely observation easily.

5.1.2 Thermal stability

Thermal properties of PI, PANI, PI-PANI(1), PI-PANI(2), and PI-PANI(3) can be shown in Fig. 5.5. The 10% weight loss temperatures or degradation temperature (T_d) of PI, PANI, PI-PANI(1), PI-PANI(2), and PI-PANI(3) appeared at 528, 180, 222, 213 and 201 °C, respectively. These results may be due to the polyaniline that grafted on polyimide chains retarding the weight loss at higher temperature than pure polyaniline. Thermal stability of PI-PANI(1) was higher than that of PI-PANI(2) and PI-PANI(3). The lower polyaniline segments exhibited a higher thermal stability than the longer segments. Polyaniline contents in copolymers could be calculated from the data of weight loss of aniline which was about 400-500°C compared to polyimide weight loss at above 600°C. Percent weight of polyaniline segments as calculated from ratio of weight loss in PI-PANI(1), PI-PANI(2), and PI-PANI(3) are 17.64%, 25.00% and 33.33%, respectively, which were

similar to the results from GPC. These confirmed the incorporation of different length of graft aniline controlled by amount of monomer added.

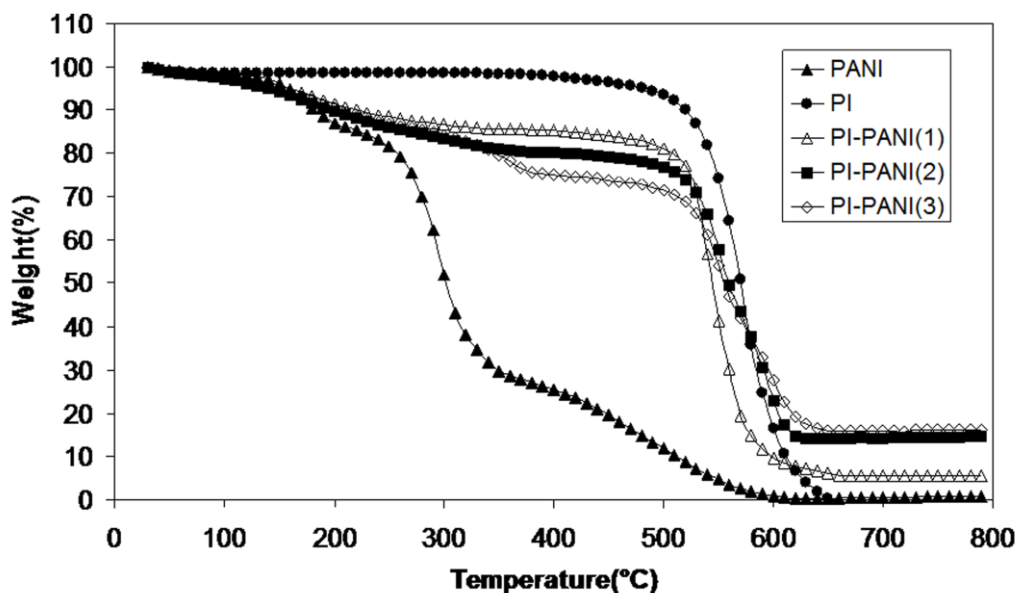


Figure 5.5 TGA of PI, PANI, PI-PANI(1), PI-PANI(2), and PI-PANI(3) as a function of annealing temperature in air.

5.1.3 Conductivity

As can be seen in Table 5.1, the conductivities of PANI, PI-PANI(1), PI-PANI(2), and PI-PANI(3) at 20°C are 71.31, 2.96, 6.12, and 16.20 S/cm, respectively. The results showed that the higher contents of polyaniline in grafted polymer might significantly enhance the conductivity of materials, but, however, less enhance than the pure PANI. Moreover, to anneal at 250 °C, 15 min diminished the conductivity of pure PANI, while the conductivities of PI-PANI(1), PI-PANI(2) and PI-PANI(3) were reduced to 1.47, 2.11 and 0.18 S/cm, respectively. It showed that, polyaniline that grafted in polyimide chains were partly decomposed after annealed at high temperature, but still function as conductive films and also exhibited conductivity. However, the more Polyaniline in PI-PANI, the more effects of temperature, so PI-PANI(3) had the highest decreasing in both weight loss and conductivity because of the posses of the highest polyaniline segments. As could be proven in this research, normally polyaniline cannot withstand high temperature as high as 250°C. The

grafted polymers were enabled higher thermal stability than pure PANI and the graft copolymer still have considerable conductivity after annealed at high temperature.

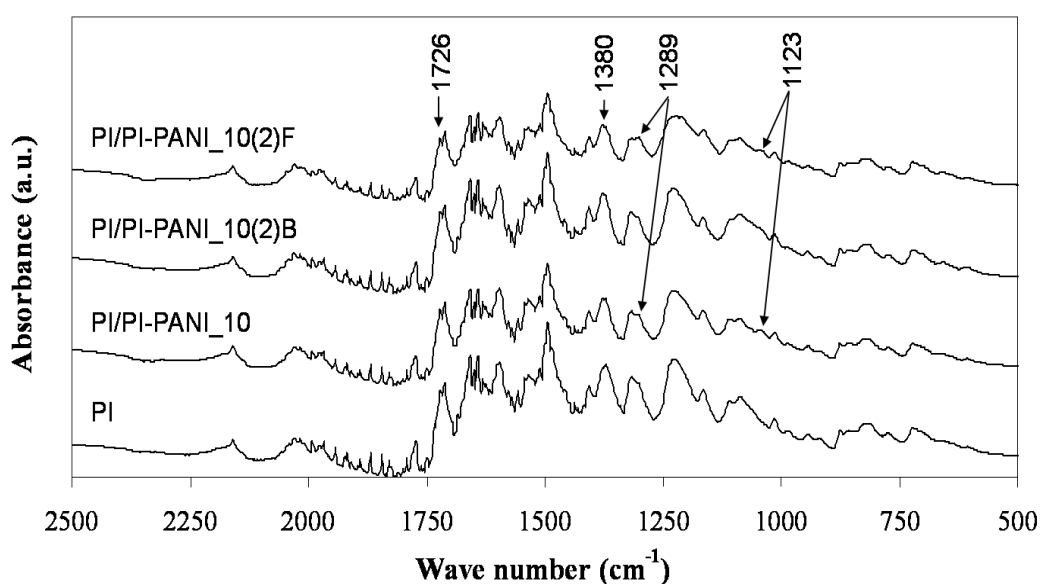
5.2 Organic Surface Conductive Polyimide

5.2.1 Polymer characterization

The FTIR of surface-conductive polyimides and conductive polyimide composites were the combination of the characteristic peaks of polyimide and polyaniline, but surface-conductive polyimides had two layers (conductive polymer on top layer and lower layer was polyimide), while composites were the mixed combination of conductive polymer and nascent polyimide (only one layer, all mixed). As shown in the FTIR spectra in Fig. 5.6, the band observed at 1726 cm^{-1} was attributed to the C=O symmetrical stretching of imide groups, whereas the bands at 1380 cm^{-1} was associated with the C–N stretching modes, presented in the polyimide. Polyaniline characteristic peaks were observed at approximately 1289 and 1123 cm^{-1} , with C–N stretching, and N=Q=N stretching (Q representing the quinoid ring) [96,102-103]. The FTIR spectra of PI/PI-PANI₁₀₍₂₎ of the front surface (F) and back surface (B) were exhibited the different peaks, because of the differences segregation of different materials. The result of PI/PI-PANI₁₀₍₂₎F could show that polyaniline characteristic peaks were located at the same places as PI/PI-PANI₁₀ peaks at 1289 and 1123 cm^{-1} while PI/PI-PANI₁₀₍₂₎B was exhibited the similar location of characteristic peaks as polyimide(PI).

Table 5.2 Films compositions on the reaction mixtures.

| Code | Film composition (wt%) | |
|------------------|------------------------|---------|
| | PI | PI-PANI |
| PI | 100 | 0 |
| PI/PI-PANI_2.5 | 97.5 | 2.5 |
| PI/PI-PANI_5 | 95 | 5 |
| PI/PI-PANI_7.5 | 92.5 | 7.5 |
| PI/PI-PANI_10 | 90 | 10 |
| PI/PI-PANI_10(2) | 90 | 10 |
| PI/PI-PANI_15(2) | 85 | 15 |
| PI/PI-PANI_20(2) | 80 | 20 |

**Figure 5.6** FTIR spectra of PI, PI/PI-PANI₁₀, PI/PI-PANI_{10(2)B}, and PI/PI-PANI_{10(2)F}.

5.2.2 Thermal stability

Thermal properties of PI, PI/PI-PANI₅, PI/PI-PANI₁₀, PI/PI-PANI₁₀₍₂₎ and PI/PI-PANI₂₀₍₂₎ can be shown in Fig. 5.7. The overall weight residue of PI, PI/PI-PANI₅, PI/PI-PANI₁₀₍₂₎, PI/PI-PANI₁₀ and PI/PI-PANI₂₀₍₂₎ after heated at 300 °C for 180 min are 86%, 84%, 83.7%, 82% and 79%, respectively. These

results showed that composite polyimides had lower thermal stabilities than pure polyimide. The higher PANI segments led to the lower thermal stability of the composites. Thermal stability of PI/PI-PANI₁₀₍₂₎ was higher than PI/PI-PANI₁₀, which showed that surface-conductive polyimide had higher thermal stability than that the conductive polyimide composite.

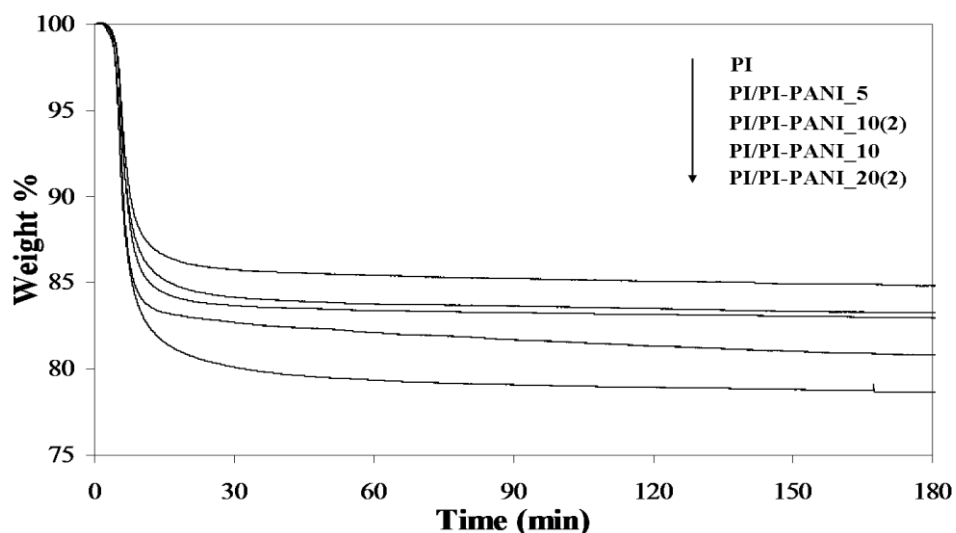
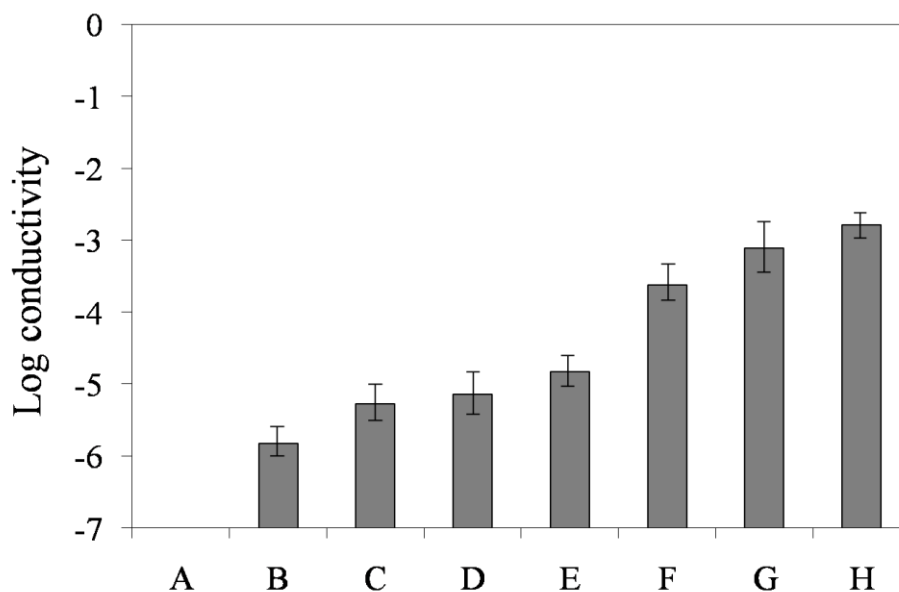


Figure 5.7 Isothermal TGA at 300 °C for PI, PI/PI-PANI₅, PI/PI-PANI₁₀, PI/PI-PANI₁₀₍₂₎ and PI/PI-PANI₂₀₍₂₎.

5.2.3 Conductivity

Fig. 5.8 shows the conductivities of all samples. The results showed that the higher PANI contents would enhance the higher conductivities. Moreover, the conductivity of surface-conductive polyimide was higher than conductive polyimide composite.



*A = non conductive material

Figure 5.8 Conductivities of PI[A], PI/PI-PANI_2.5[B], PI/PI-PANI_5[C], PI/PI-PANI_7.5[D], PI/PI-PANI_10[E], PI/PI-PANI_10(2)[F], PI/PI-PANI_15(2)[G], PI/PI-PANI_20(2)[H].

5.2.4 Mechanical property

Mechanical properties of all samples can be shown in Fig. 5.9. The higher PANI segments showed the lower mechanical properties. Tensile stress of PI/PI-PANI_10(2) was 12.5 MPa, but PI/PI-PANI_10 film was brittle and could not measure the free standing film properties, which confirmed that the surface-conductive polyimide had higher strength than that the conductive polyimide composite.

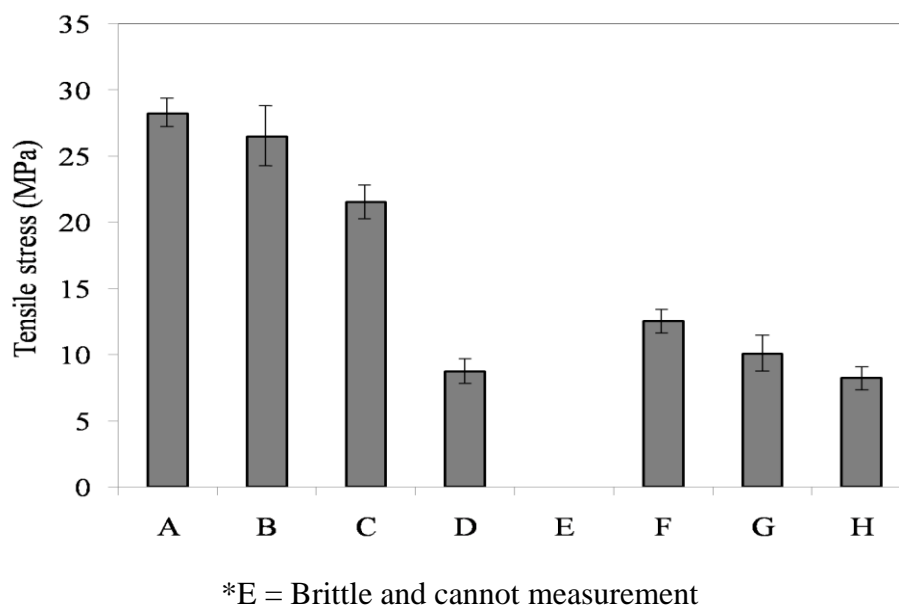


Figure 5.9 Tensile stresses of PI[A], PI/PI-PANI_2.5[B], PI/PI-PANI_5[C], PI/PI-PANI_7.5[D], PI/PI-PANI_10[E], PI/PI-PANI_10(2)[F], PI/PI-PANI_15(2)[G], PI/PI-PANI_20(2)[H].

5.2.5 Morphology and particles distribution

To investigate the effects of formation, diameter and distribution of PANI particles in polyimide matrix, SEM measurements were conducted. Fig. 5.10a-e showed the SEM images of polyimide, composite polyimide and surface-conductive polyimide. The bare polyimide displayed a smooth surface while the other samples showed distribution of PANI particles in polyimide matrix. Although the same amount of PANI in PI/PI-PANI_10 and PI/PI-PANI_10(2) were controlled, PI/PI-PANI_10(2) morphology showed higher intensity of PANI distribution on the conductive surface than PI/PI-PANI_10 (Fig. 5.10b-c). This indicated that PANI segments in PI/PI-PANI_10(2) were laid only on top layer of conductive films laminate. Because of higher PANI contents, intensity of PANI distribution in PI/PI-PANI_20(2) film was higher than that the result of PI/PI-PANI_10(2) film and led to some more accumulation of PANI in polyimide matrix as showed in bigger particle sizes, *ca* 0.5 μm (Fig. 5.10c-d). Fig. 5.10e showed the cross section image of PI/PI-PANI_10(2) film, which confirmed that surface-conductive polyimide comprises two

layers, all of PANI small particles were laid in the top layer and some large particles were laid in bottom layer, because of the segregation of heavier particles.

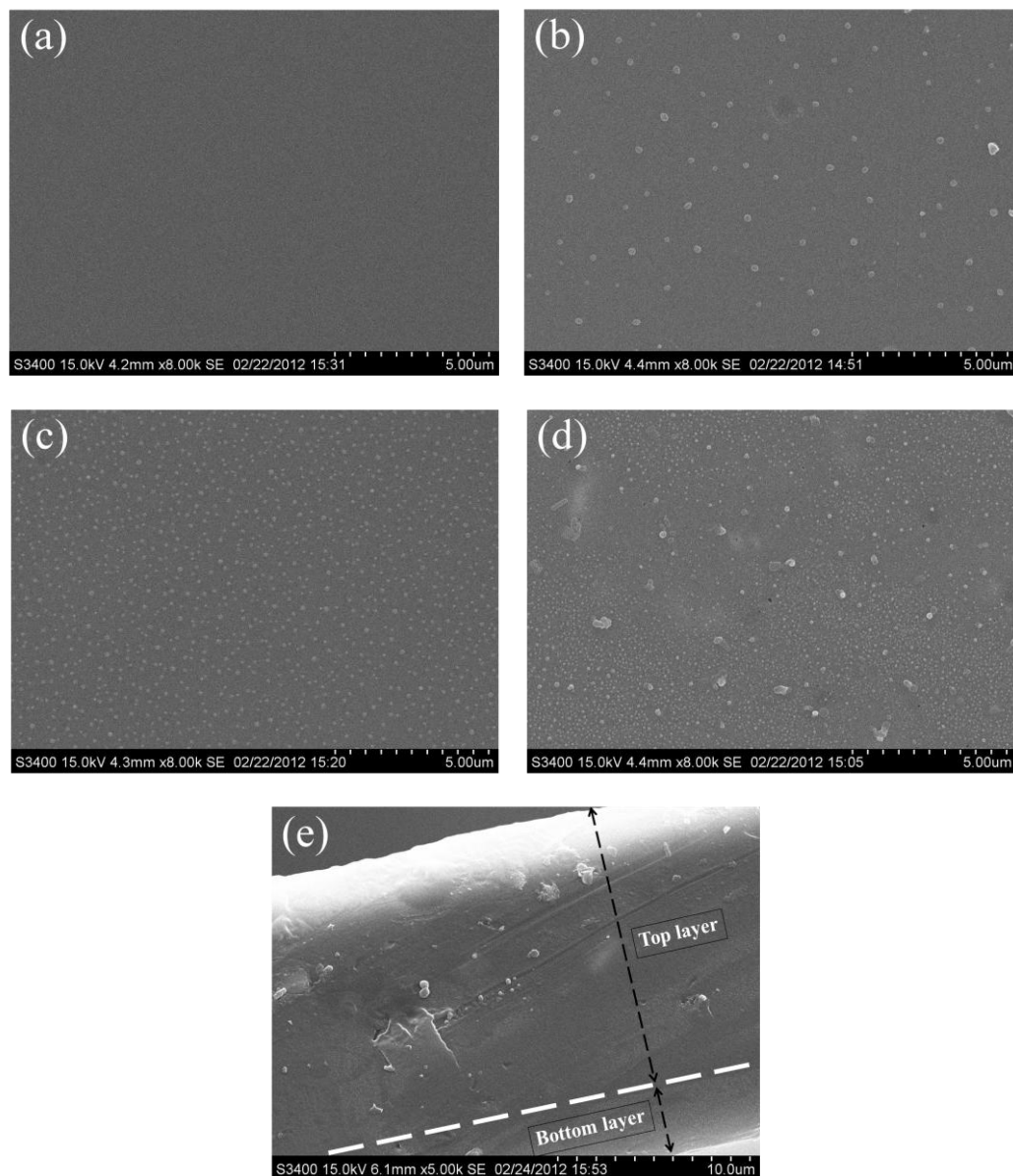


Figure 5.10 SEMs of PI [a], PI/PANI₁₀ [b], PI/PANI₁₀₍₂₎ [c], PI/PANI₂₀₍₂₎ [d] and cross section of PI/PANI₁₀₍₂₎ [e].

5.3 Comparison of the Thermally Stable Conducting Polymers PEDOT, PANI, and PPy Using Sulfonated Poly(imide) Templates via Poly(amic acid)

5.3.1 Diamine monomer and PEDOT, PANI, PPy with sulfonated poly(amic acid) templates

4,4'-diaminodiphenyl ether-2,2'-disulfonic acid (4,4'-ODADS) is synthesized by using fuming sulfuric acid as a sulfonated agent resulting in the sulfonated diamine monomer for making sulfonated poly(amic acid). We have synthesized the new template, sulfonated poly(amic acid) with two different dianhydrides (Fig. 5.11). 4,4'-oxydiphthalic anhydride (O-DPDA) is used as a dianhydride monomer to synthesize the first template (SPAA1), which has an ether bond (R-O-R) between two aromatic positions and led to a flexible system. The second template (SPAA2) was used 4,4'-hexafluoroisopropylidene-oxydiphthalic anhydride (6FDA) as a dianhydride monomer resulting in more thermally stable than that the first template (SPAA1) [105].

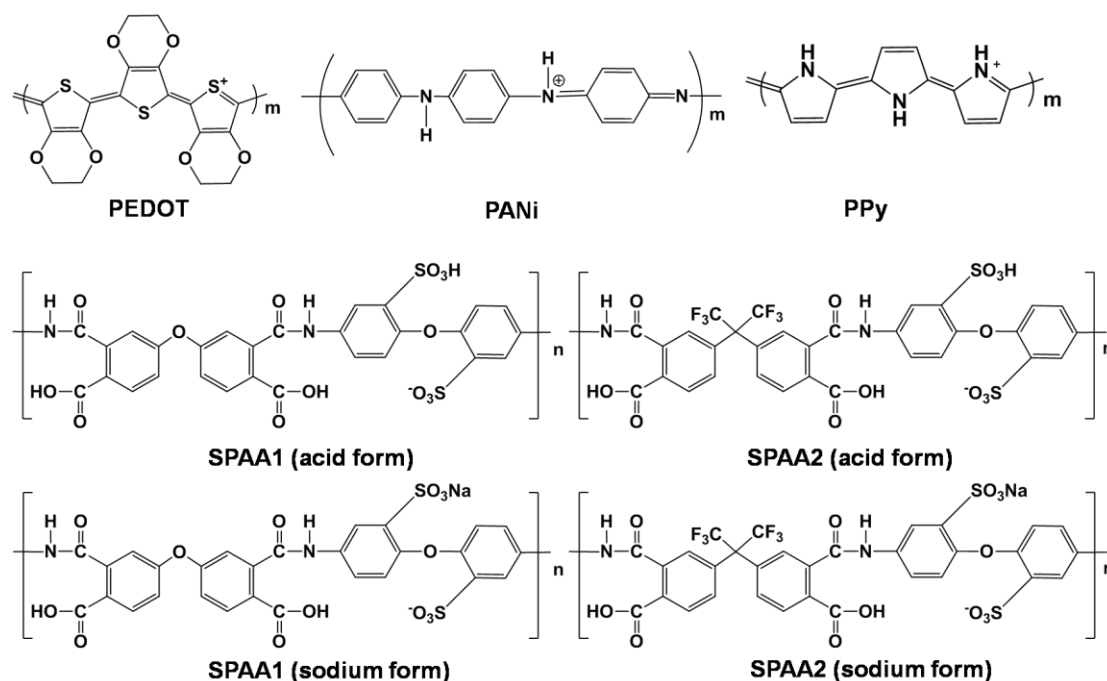


Figure 5.11 Chemical structures of the various conducting polymers and the various templates used in this study, with their corresponding abbreviations [105].

FTIR spectrums were confirmed the structure of poly(amic acid)s. The absorbed water in the sample were represented the broad absorption band at 3476.9 cm^{-1} . The absorption bands of carbonyl group (CONH) were represented the peak at 1663.3 cm^{-1} while the peak at *ca.* $2500\text{-}3500\text{ cm}^{-1}$ were indicated the absorption bands of the carboxylic acid (COOH). The peak at 1029.0 cm^{-1} was indicated the sulfonic acid groups (SO_3H) in the structure of sulfonated poly(amic acid)s. After shot time annealing at 180°C , the symmetric imide C=O stretching and the asymmetric imide C=O stretching were represented the peak around 1719.7 cm^{-1} and 1778.6 cm^{-1} , respectively, which confirmed the complete imidization from sulfonated poly(amic acid)s to sulfonated poly(imide)s as shown in Fig. 5.12 [105].

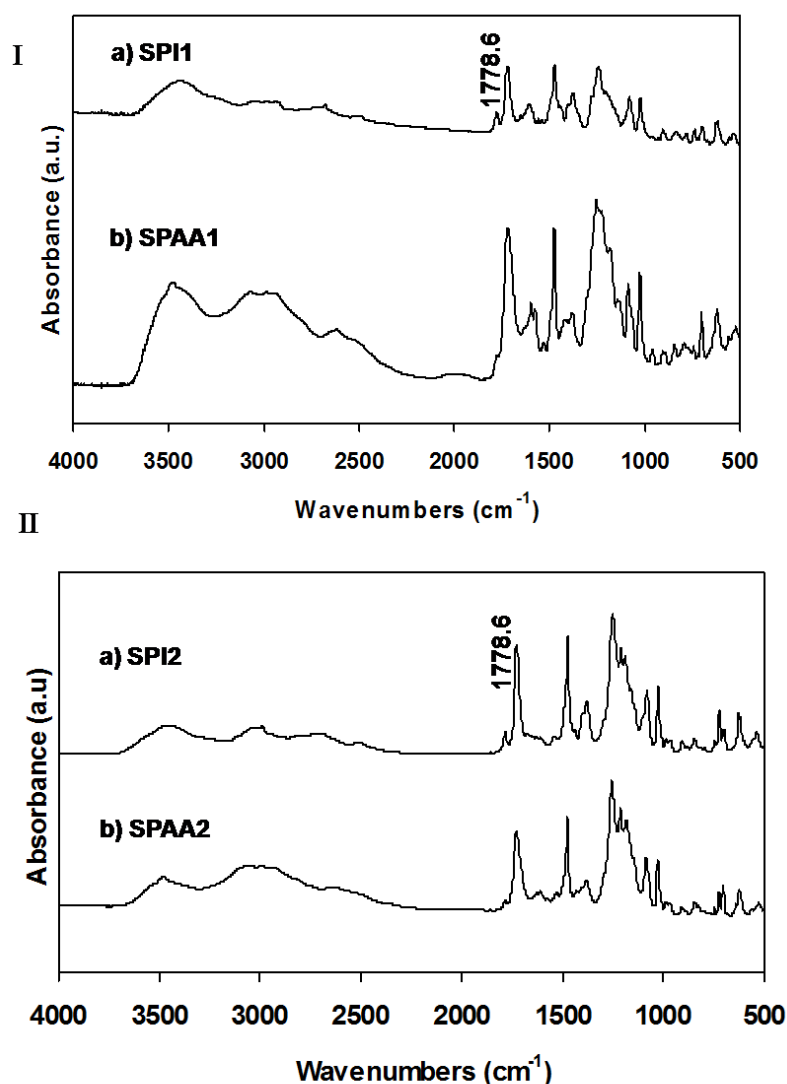


Figure 5.12 (I) FTIR spectrum of a) SPI1, b) SPAA1. (II) FTIR spectrum of a) SPI2, b) SPAA2 [105].

The conducting polymers are selected because of their widespread popularity in academia and industry. The templates are selected on the basis of differences in rigidity. The selected templates should not too-rigid because it will dissolve easily in water and ease to connect with conducting polymers. We have tried to polymerize conducting polymer with sulfonated Kapton template, but the result was shown the failure. We have selected PSSA, SPAA1 and SPAA2 to use as the sulfonated templates. Although SPAA2 was more rigid than SPAA1 and PSSA, it was not too rigid and allowed formation of the templated CP in all cases. The difference systems

led to the results in difference reaction times. The control reaction for each CP using PSSA template (PEDOT-PSS) takes 24 h while PEDOT-SPAA1 and PEDOT-SPAA2 takes 7 days and 5 days, respectively. In term of conducting polymers, regardless of the template, PANI was faster, which taking reaction time 12 h. PPy systems were shown the completed templating in 5 days [105].

5.3.2 Conductivity

The conductivities of all conducting polymers (PEDOT, PANI, and PPy with SPAA1, SPAA2, and PSS templates) were measured to compare the results each other. In cases of annealing, only 5-10 min is needed to convert the template from the amic acids to the imides (SPI1 and SPI2). SPAA1 template is more water soluble than SPAA2 template because the results of the samples using SPAA2 template were shown a slight decrease in conductivity. However, PEDOT-SPAA1 became a dark blue dispersion slower than PEDOT-SPAA2 (7 days as opposed to 5 days). In case of using the same template (SPAA1) at room temperature, the conductivities of PANI-SPAA1, PPy-SPAA1 and PEDOT-SPAA1 were 7.74 S/cm, 3.47×10^{-2} S/cm and 2.04×10^{-4} S/cm, respectively. In case of using SPAA2, the conductivities of PANI-SPAA2, PPy-SPAA2 and PEDOT-SPAA2 at room temperature were 7.34×10^{-1} S/cm, 3.63×10^{-3} S/cm and 1.96×10^{-4} S/cm, respectively. The results show that PANI systems have higher conductivities than PEDOT and PPy systems.

The chain alignment in the films after heat treatment will change because the differences in rigidity of the poly(amic acid) and the poly(imide) resulting modified morphologies and led to conductivity enhancement. For example, after annealing at 180°C for 10 minutes, PEDOT-SPI1 was shown conductivity enhancement from 2.04×10^{-4} S/cm to 5.83×10^{-3} S/cm, a 10-fold increasing, but the result of PANI-SPI1 was shown slightly decreasing from 7.74 S/cm to 2.88 S/cm. The conductivities of PPy-SPI1 were slightly increased from 3.47×10^{-2} S/cm to 5.00×10^{-2} S/cm. The chain rearrangements after heat treatment leading to the conductivity enhancement was more affected to PEDOT systems than PANI and PPy systems. The conductivities results of all samples, including all annealing and doping studies using d-sorbitol and other common additives are shown in Table 5.3 to 5.11 [105].

Table 5.3 Conductivities of PEDOT-PSS (in house) and PEDOT-SPAA. Upon annealing, PEDOT-SPAA imidizes to PEDOT-SPI [105].

| Processing Temperature | | PEDOT-PSS | PEDOT-SPAA1 | PEDOT-SPAA2 |
|-------------------------------|---------------------|-----------------------|-----------------------|-----------------------|
| 20°C | Conductivity (S/cm) | 3.15×10^{-4} | 2.04×10^{-4} | 1.96×10^{-4} |
| | Std. Dev. | 4.03×10^{-5} | 3.42×10^{-5} | 3.58×10^{-5} |
| 180°C (90 min) | Conductivity (S/cm) | 2.65×10^{-4} | 2.96×10^{-4} | 4.91×10^{-4} |
| | Std. Dev. | 3.32×10^{-5} | 5.49×10^{-6} | 1.42×10^{-4} |
| 300°C (10 min) | Conductivity (S/cm) | $< 1 \times 10^{-5}$ | 6.06×10^{-4} | 5.23×10^{-4} |
| | Std. Dev. | $< 1 \times 10^{-5}$ | 4.84×10^{-5} | 5.76×10^{-5} |

Table 5.4 Conductivities of secondary-doped PEDOT-SPAA1 at various processing temperatures. Upon annealing, PEDOT-SPAA1 imidizes to PEDOT-SPI1 [105].

| Processing Temperature | | PEDOT-SPAA1 | DMF 0.1 wt.% | |
|-------------------------------|---------------------|--------------------------|--------------------------|-----------------------|
| 20°C | Conductivity (S/cm) | 2.04×10^{-4} | 5.76×10^{-4} | |
| | Std. Dev. | 3.42×10^{-5} | 6.09×10^{-5} | |
| 180°C (10 min) | Conductivity (S/cm) | 5.83×10^{-3} | 8.99×10^{-2} | |
| | Std. Dev. | 1.18×10^{-3} | 8.28×10^{-2} | |
| 300°C (10 min) | Conductivity (S/cm) | 6.47×10^{-4} | 4.25×10^{-2} | |
| | Std. Dev. | 3.73×10^{-5} | 2.03×10^{-2} | |
| Processing Temperature | | surfynol 0.1 wt.% | d-sorbitol 5 wt.% | Combination |
| 20°C | Conductivity (S/cm) | 1.82×10^{-4} | 4.22×10^{-2} | 3.78×10^{-4} |
| | Std. Dev. | 2.51×10^{-5} | 5.84×10^{-3} | 9.33×10^{-5} |
| 180°C (10 min) | Conductivity (S/cm) | 3.33×10^{-4} | 2.00×10^{-2} | 4.34×10^{-3} |
| | Std. Dev. | 3.59×10^{-5} | 3.51×10^{-3} | 8.54×10^{-4} |
| 300°C (10 min) | Conductivity (S/cm) | 5.68×10^{-3} | 6.56×10^{-3} | 3.74×10^{-3} |
| | Std. Dev. | 1.48×10^{-3} | 1.50×10^{-3} | 1.13×10^{-3} |

Table 5.5 Conductivities of secondary-doped PEDOT-SPAA2 at various processing temperatures. Upon annealing, PEDOT-SPAA2 imidizes to PEDOT-SPI2 [105].

| Processing Temperature | | PEDOT-SPAA2 | DMF 0.1 wt.% | |
|-------------------------------|---------------------|--------------------------|--------------------------|-----------------------|
| 20°C | Conductivity (S/cm) | 1.96×10^{-4} | 1.72×10^{-4} | |
| | Std. Dev. | 3.58×10^{-5} | 2.55×10^{-5} | |
| 180°C (10 min) | Conductivity (S/cm) | 2.50×10^{-3} | 5.34×10^{-3} | |
| | Std. Dev. | 4.39×10^{-4} | 1.79×10^{-4} | |
| 300°C (10 min) | Conductivity (S/cm) | 5.21×10^{-4} | 3.91×10^{-3} | |
| | Std. Dev. | 4.28×10^{-5} | 5.48×10^{-4} | |
| Processing Temperature | | surfynol 0.1 wt.% | d-sorbitol 5 wt.% | Combination |
| 20°C | Conductivity (S/cm) | 3.14×10^{-4} | 6.44×10^{-2} | 2.78×10^{-4} |
| | Std. Dev. | 6.14×10^{-5} | 6.06×10^{-3} | 2.95×10^{-5} |
| 180°C (10 min) | Conductivity (S/cm) | 3.57×10^{-4} | 2.25×10^{-2} | 2.96×10^{-3} |
| | Std. Dev. | 1.94×10^{-5} | 3.11×10^{-3} | 8.17×10^{-4} |
| 300°C (10 min) | Conductivity (S/cm) | 2.10×10^{-3} | 2.10×10^{-3} | 1.70×10^{-3} |
| | Std. Dev. | 4.65×10^{-4} | 4.65×10^{-4} | 1.15×10^{-4} |

Table 5.6 Conductivities of PANI-PSS (in house) and PANI-SPAA. Upon annealing, PANI-SPAA imidizes to PANI-SPI [105].

| Processing Temperature | | PANI-PSS | PANI-SPAA1 | PANI-SPAA2 |
|-------------------------------|---------------------|-----------------------|----------------------|-----------------------|
| 20°C | Conductivity (S/cm) | 12.6 | 7.74 | 7.34×10^{-1} |
| | Std. Dev. | 4.79×10^{-1} | 2.76 | 1.12×10^{-1} |
| 180°C (90 min) | Conductivity (S/cm) | 3.9 | $< 1 \times 10^{-5}$ | $< 1 \times 10^{-5}$ |
| | Std. Dev. | 8.46×10^{-1} | $< 1 \times 10^{-5}$ | $< 1 \times 10^{-5}$ |
| 300°C (10 min) | Conductivity (S/cm) | $< 1 \times 10^{-5}$ | $< 1 \times 10^{-5}$ | $< 1 \times 10^{-5}$ |
| | Std. Dev. | $< 1 \times 10^{-5}$ | $< 1 \times 10^{-5}$ | $< 1 \times 10^{-5}$ |

Table 5.7 Conductivities of secondary-doped PANI-SPAA1 at various processing temperatures. Upon annealing, PANI-SPAA1 imidizes to PANI-SPII[105].

| Processing Temperature | | PANI-SPAA1 | DMF 0.1 wt.% | |
|-------------------------------|---------------------|--------------------------|--------------------------|-----------------------|
| 20°C | Conductivity (S/cm) | 7.74 | 2.98 | |
| | Std. Dev. | 2.76 | 6.67×10^{-1} | |
| 180°C (10 min) | Conductivity (S/cm) | 2.88 | 9.00×10^{-1} | |
| | Std. Dev. | 6.88×10^{-1} | 4.17×10^{-2} | |
| 300°C (10 min) | Conductivity (S/cm) | $< 1 \times 10^{-5}$ | $< 1 \times 10^{-5}$ | |
| | Std. Dev. | $< 1 \times 10^{-5}$ | $< 1 \times 10^{-5}$ | |
| Processing Temperature | | surfynol 0.1 wt.% | d-sorbitol 5 wt.% | Combination |
| 20°C | Conductivity (S/cm) | 2.83 | 9.75×10^{-2} | 1.83×10^{-1} |
| | Std. Dev. | 1.56×10^{-1} | 5.72×10^{-2} | 3.38×10^{-2} |
| 180°C (10 min) | Conductivity (S/cm) | 1.37 | 7.85×10^{-2} | 3.13×10^{-2} |
| | Std. Dev. | 7.72×10^{-2} | 8.26×10^{-3} | 9.20×10^{-3} |
| 300°C (10 min) | Conductivity (S/cm) | $< 1 \times 10^{-5}$ | $< 1 \times 10^{-5}$ | $< 1 \times 10^{-5}$ |
| | Std. Dev. | $< 1 \times 10^{-5}$ | $< 1 \times 10^{-5}$ | $< 1 \times 10^{-5}$ |

Table 5.8 Conductivities of secondary-doped PANI-SPAA2 at various processing temperatures. Upon annealing, PANI-SPAA2 imidizes to PANI-SPI2 [105].

| Processing Temperature | | PANI-SPAA2 | DMF 0.1 wt.% | |
|-------------------------------|---------------------|--------------------------|--------------------------|-----------------------|
| 20°C | Conductivity (S/cm) | 7.34×10^{-1} | 1.47 | |
| | Std. Dev. | 1.12×10^{-1} | 1.14×10^{-1} | |
| 180°C (10 min) | Conductivity (S/cm) | 5.45×10^{-1} | 1.13 | |
| | Std. Dev. | 6.95×10^{-3} | 5.83×10^{-2} | |
| 300°C (10 min) | Conductivity (S/cm) | $< 1 \times 10^{-5}$ | $< 1 \times 10^{-5}$ | |
| | Std. Dev. | $< 1 \times 10^{-5}$ | $< 1 \times 10^{-5}$ | |
| Processing Temperature | | surfynol 0.1 wt.% | d-sorbitol 5 wt.% | Combination |
| 20°C | Conductivity (S/cm) | 1.28 | 5.41×10^{-2} | 1.66×10^{-2} |
| | Std. Dev. | 4.66×10^{-2} | 2.09×10^{-2} | 7.83×10^{-3} |
| 180°C (10 min) | Conductivity (S/cm) | 8.69×10^{-1} | 1.08×10^{-1} | 3.48×10^{-2} |
| | Std. Dev. | 3.27×10^{-2} | 1.34×10^{-2} | 1.01×10^{-2} |
| 300°C (10 min) | Conductivity (S/cm) | $< 1 \times 10^{-5}$ | $< 1 \times 10^{-5}$ | $< 1 \times 10^{-5}$ |
| | Std. Dev. | $< 1 \times 10^{-5}$ | $< 1 \times 10^{-5}$ | $< 1 \times 10^{-5}$ |

Table 5.9 Conductivities of PPy-PSS (in house) and PPy-SPAA. Upon annealing, PPy-SPAA imidizes to PPy-SPI [105].

| Processing Temperature | | PPy-PSS | PPy-SPAA1 | PPy-SPAA2 |
|-------------------------------|---------------------|-----------------------|-----------------------|-----------------------|
| 20°C | Conductivity (S/cm) | 2.74 | 3.47×10^{-2} | 3.63×10^{-3} |
| | Std. Dev. | 6.23×10^{-1} | 2.27×10^{-3} | 8.39×10^{-5} |
| 180°C (90 min) | Conductivity (S/cm) | 6.17×10^{-1} | 2.00×10^{-2} | 1.79×10^{-3} |
| | Std. Dev. | 2.29×10^{-2} | 5.41×10^{-4} | 3.68×10^{-4} |
| 300°C (10 min) | Conductivity (S/cm) | 1.19×10^{-1} | 8.33×10^{-3} | 6.28×10^{-4} |
| | Std. Dev. | 2.31×10^{-3} | 7.43×10^{-5} | 2.64×10^{-5} |

Table 5.10 Conductivities of secondary-doped PPy-SPAA1 at various processing temperatures. Upon annealing, PPy-SPAA1 imidizes to PPy-SPI1 [105].

| Processing Temperature | | PPy-SPAA1 | DMF 0.1 wt.% | |
|-------------------------------|---------------------|-----------------------|-----------------------|--|
| 20°C | Conductivity (S/cm) | 3.47×10^{-2} | 3.97×10^{-1} | |
| | Std. Dev. | 2.27×10^{-3} | 1.91×10^{-2} | |
| 180°C (10 min) | Conductivity (S/cm) | 5.00×10^{-2} | 1.98×10^{-1} | |
| | Std. Dev. | 9.02×10^{-3} | 6.74×10^{-3} | |
| 300°C (10 min) | Conductivity (S/cm) | 8.33×10^{-3} | 1.73×10^{-3} | |
| | Std. Dev. | 7.43×10^{-5} | 1.40×10^{-4} | |

| Processing Temperature | | surfynol 0.1 wt.% | d-sorbitol 5 wt.% | Combination |
|-------------------------------|---------------------|--------------------------|--------------------------|-----------------------|
| 20°C | Conductivity (S/cm) | 2.41×10^{-1} | 3.89×10^{-3} | 1.35×10^{-2} |
| | Std. Dev. | 6.83×10^{-3} | 1.81×10^{-3} | 3.30×10^{-4} |
| 180°C (10 min) | Conductivity (S/cm) | 1.61×10^{-1} | 1.79×10^{-1} | 1.72×10^{-1} |
| | Std. Dev. | 5.07×10^{-3} | 1.09×10^{-2} | 2.25×10^{-3} |
| 300°C (10 min) | Conductivity (S/cm) | 7.37×10^{-4} | $< 1 \times 10^{-5}$ | $< 1 \times 10^{-5}$ |
| | Std. Dev. | 3.00×10^{-4} | $< 1 \times 10^{-5}$ | $< 1 \times 10^{-5}$ |

Table 5.11 Conductivities of secondary-doped PPy-SPAA2 at various processing temperatures. Upon annealing, PPy-SPAA2 imidizes to PPy-SPI2 [105].

| Processing Temperature | | PPy-SPAA2 | DMF 0.1 wt.% | |
|-------------------------------|---------------------|-----------------------|-----------------------|--|
| 20°C | Conductivity (S/cm) | 3.63×10^{-3} | 7.80×10^{-3} | |
| | Std. Dev. | 8.39×10^{-5} | 5.85×10^{-4} | |
| 180°C (10 min) | Conductivity (S/cm) | 5.98×10^{-3} | 1.36×10^{-1} | |
| | Std. Dev. | 2.78×10^{-5} | 1.76×10^{-2} | |
| 300°C (10 min) | Conductivity (S/cm) | 6.28×10^{-4} | 3.92×10^{-3} | |
| | Std. Dev. | 2.64×10^{-6} | 5.32×10^{-5} | |

| Processing Temperature | | surfynol 0.1 wt.% | d-sorbitol 5 wt.% | Combination |
|-------------------------------|---------------------|--------------------------|--------------------------|-----------------------|
| 20°C | Conductivity (S/cm) | 9.99×10^{-3} | 2.03×10^{-4} | 3.40×10^{-4} |
| | Std. Dev. | 7.39×10^{-4} | 1.25×10^{-5} | 6.25×10^{-5} |
| 180°C (10 min) | Conductivity (S/cm) | 3.46×10^{-2} | 2.67×10^{-2} | 3.46×10^{-2} |
| | Std. Dev. | 2.05×10^{-3} | 3.89×10^{-3} | 7.33×10^{-3} |
| 300°C (10 min) | Conductivity (S/cm) | $< 1 \times 10^{-5}$ | $< 1 \times 10^{-5}$ | $< 1 \times 10^{-5}$ |
| | Std. Dev. | $< 1 \times 10^{-5}$ | $< 1 \times 10^{-5}$ | $< 1 \times 10^{-5}$ |

For ease of comparison, the conductivity for every system is shown in Figure 5.13 to 5.18 [105].

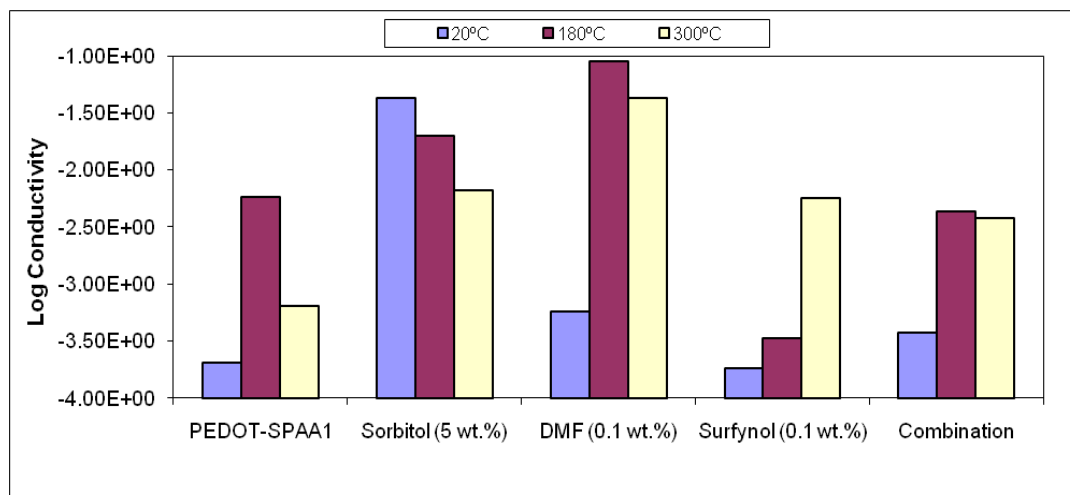


Figure 5.13 Conductivities of PEDOT-SPAA1 [105].

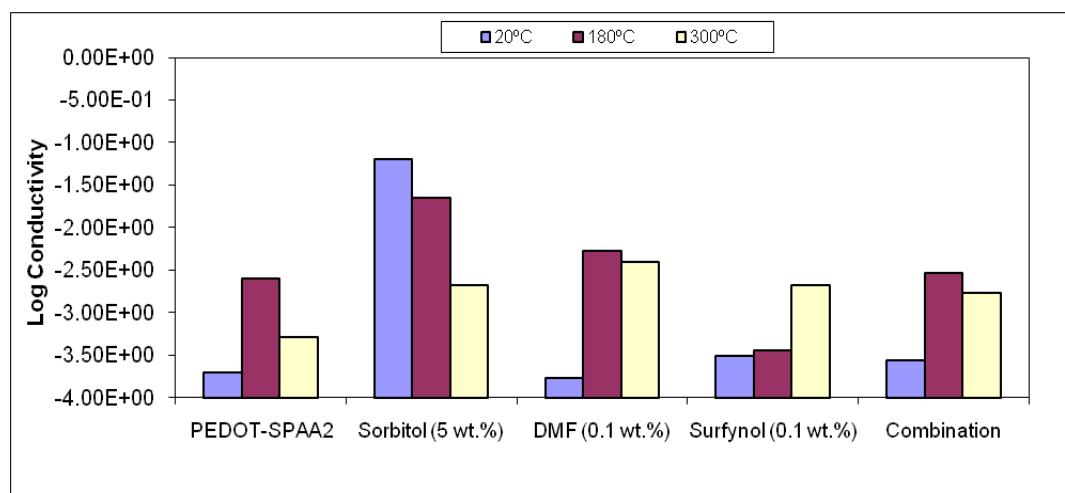


Figure 5.14 Conductivities of PEDOT-SPAA2 [105].

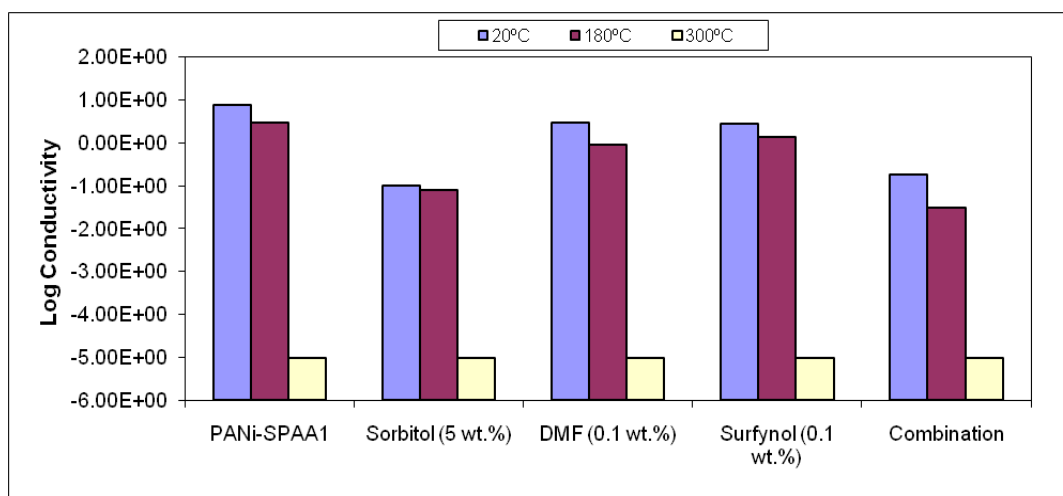


Figure 5.15 Conductivities of PANI-SPAA1 [105].

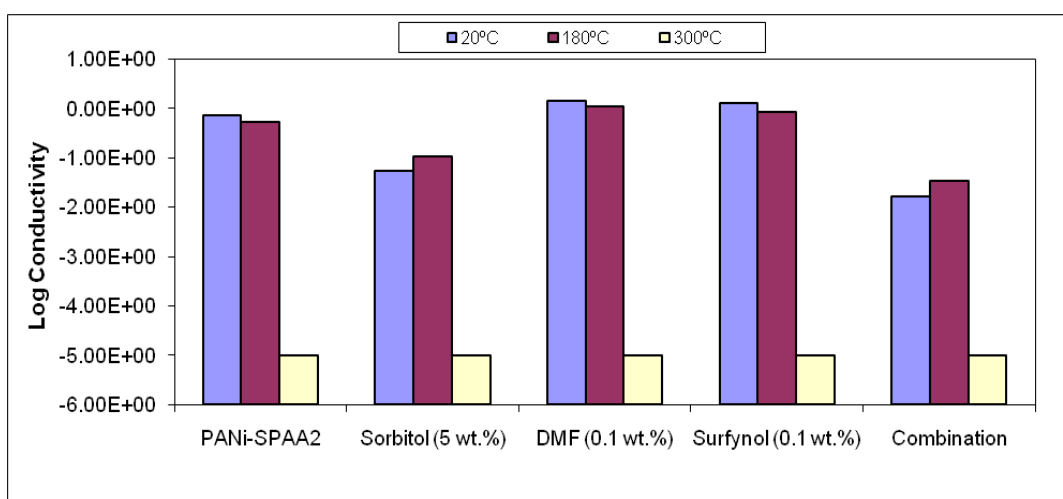


Figure 5.16 Conductivities of PANI-SPAA2 [105].

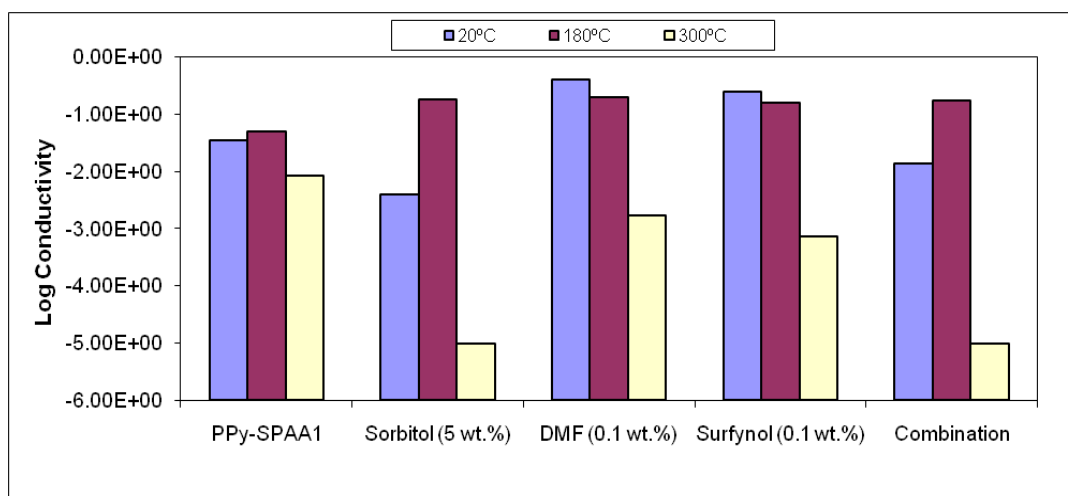


Figure 5.17 Conductivities of PPy-SPAA1 [105].

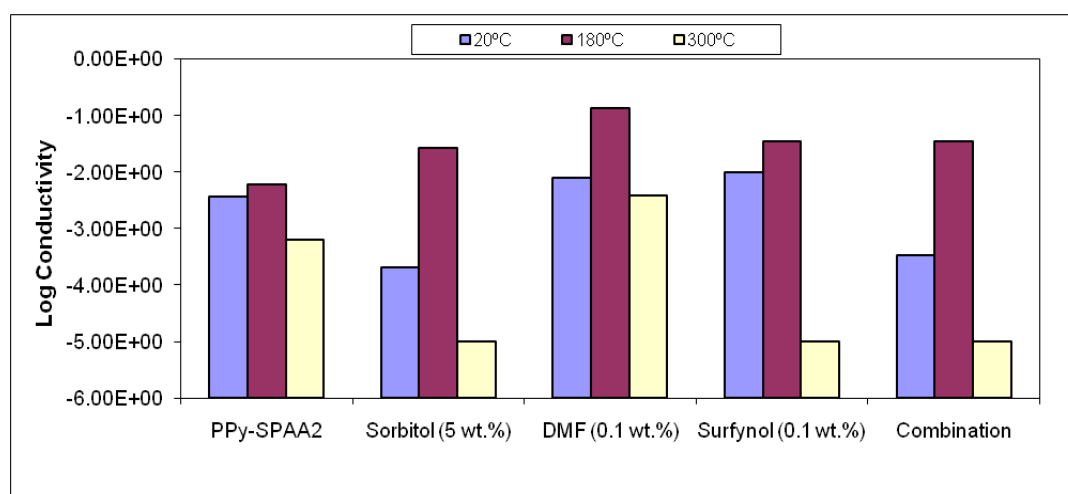


Figure 5.18 Conductivities of PPy-SPAA2 [105].

From the results, we found that the conductivities of PANI systems were higher than PPy and PEDOT systems. After annealing at 180°C for 10 min, the conductivities of PEDOT systems were increased from 2.04×10^{-4} S/cm to 5.83×10^{-3} S/cm, and increased to 6.47×10^{-4} S/cm after annealing at 300°C for 10 min. In the results of PPy systems, after annealing at 180°C for 10 min, the conductivities were increased from 3.47×10^{-2} S/cm to 5.00×10^{-2} S/cm while the conductivity after annealing at 300°C for 10 min was decreased to 8.33×10^{-3} S/cm. In term of PANI systems, after heat treatment, the conductivities were decreased. After annealing at 300°C, PANI-SPI1 and PANI-SPI2 could not be measured while the conductivities of

PPy-SPI1 and PPy-SPI2 were slightly decreased. The conductivities of PPy-PSS, PPy-SPAA1 and PPy-SPAA2 at room temperature were 2.47 S/cm, 3.47×10^{-2} S/cm and 3.63×10^{-3} S/cm, respectively. The result from secondary doped PEDOT-SPAA1, which was doped with DMF (0.1 wt.%) and annealed at 180°C for 10 min showed the highest conductivity value of 8.99×10^{-2} S/cm (so, in reality, it was the PEDOT-SPI1). In the case of secondary doped PEDOT-SPAA2, the highest value of conductivity was 6.44×10^{-2} S/cm, which was doped with d-sorbitol (5 wt.%). For PANI systems, the highest conductivity of PANI-SPAA1 was 7.74 S/cm, which was without thermal annealing and secondary doping while the highest conductivity of PANI-SPAA2 was 1.47 S/cm, which was doped with DMF (0.1 wt.%). For PPy systems, the result showed the similar trends to the PEDOT systems. The highest conductivity of PPy-SPAA1 was 3.97×10^{-1} S/cm belong to the sample which was doped with DMF (0.1 wt.%) without thermal annealing while the highest conductivity of PPy-SPAA2 was 1.36×10^{-1} S/cm, which was doped with DMF (0.1 wt.%) and annealed at 180°C for 10 min (so, in reality, it was the PEDOT-SPI2). The highest conductivities results for all of the various samples are shown in Fig. 5.19 [105].

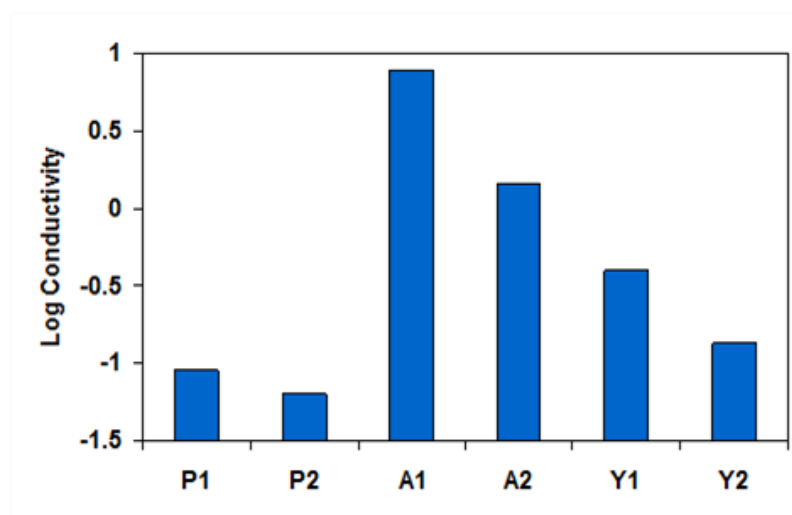


Figure 5.19 Conductivities of each system. (**P1** = PEDOT-SPAA1 doped with DMF 0.1 wt.% at 180°C, **P2** = PEDOT-SPAA2 doped with d-sorbitol 5 wt.% at 20°C, **A1** = PANI-SPAA1 at 20°C, **A2** = PANI-SPAA2 doped with DMF 0.1 wt.% at 20°C, **Y1** = PPy-SPAA1 doped with DMF 0.1 wt.% at 20°C, **Y2** = PPy-SPAA2 doped with DMF 0.1 wt.% at 180°C) [105].

5.3.3 Thermal stability of films

Thermal properties of PEDOT-SPI, PANI-SPI and PPy-SPI are summarized in Fig. 5.20. PEDOT-SPI1 had higher thermal stability than PPy-SPI1 and PANI-SPI1, respectively. The systems using SPI2 template showed the higher thermal stability when compared with the other systems using the SPI1. The initial weight loss around 100°C was represented the absorbed water in the sample. The decomposition of the sulfonic acid groups was shown the weight loss at 250°C. The weight loss at 420°C was indicated the degradation of the polyimide backbone. PANI system showed the lowest thermal stability, and could not retain its conductivity with high temperature or long term annealing [105].

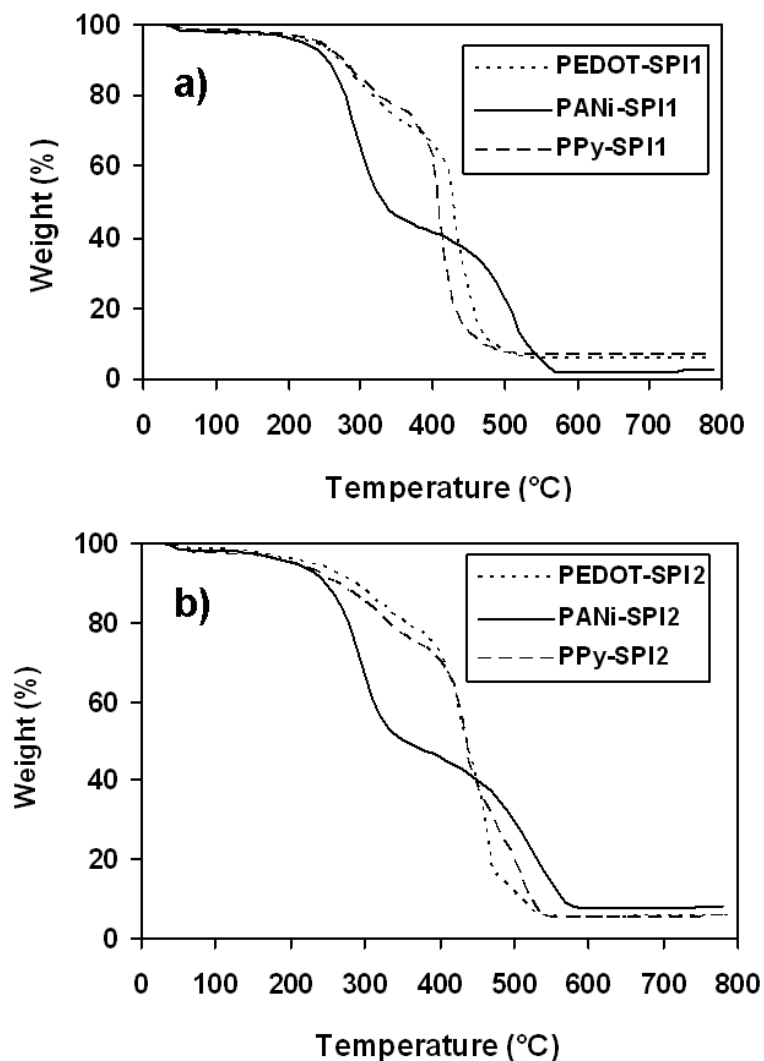


Figure 5.20 Overlaid TGAs of a) PEDOT, PANI, PPy with SPI1 and b) PEDOT, PANI, PPy with SPI2 [105].

The thermal stabilities of PEDOT, PANI, PPy using sulfonated poly(imide)s were investigated in air to compare the results with the control systems of PEDOT, PANI, PPy using conventional template (PSSA). Fig. 5.21 to 5.29 showed the longer-term mass stabilities for each system with running isothermal TGAs in 5 h. The results showed that the SPI2 template had higher thermal stability than every system of SPI1, which corresponded to the normal TGAs as shown in fig. 5.20 [105].

The weight retention after heating at 300 °C for 5 h is 38.57% for PEDOT-PSS as shown in Figure 5.21 [105].

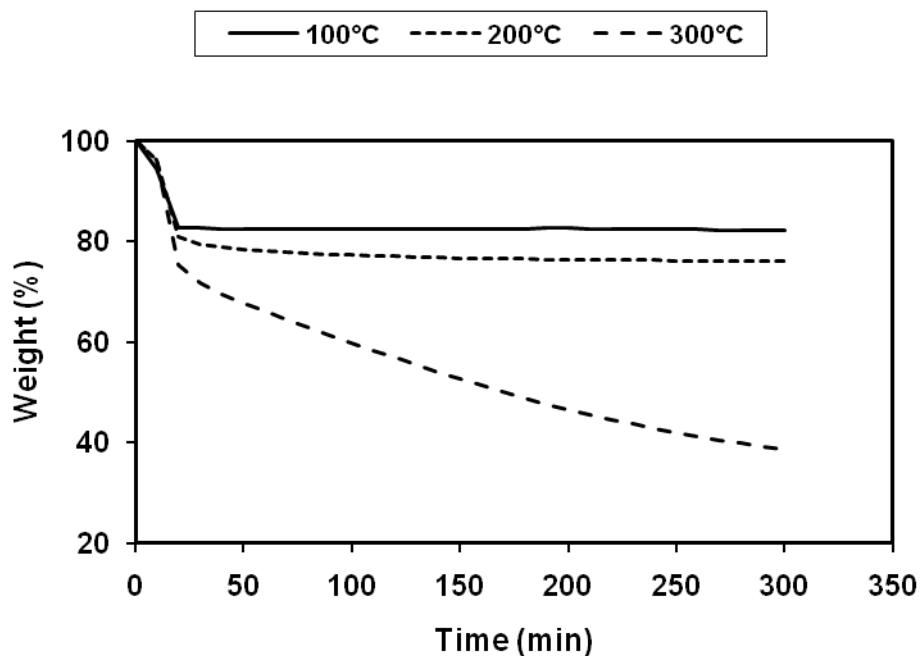


Figure 5.21 Isothermal TGA of PEDOT-PSS [105].

The weight retention after heating at 300 °C for 5 h is 54.74% for PEDOT-SPI1 as shown in Figure 5.22 [105].

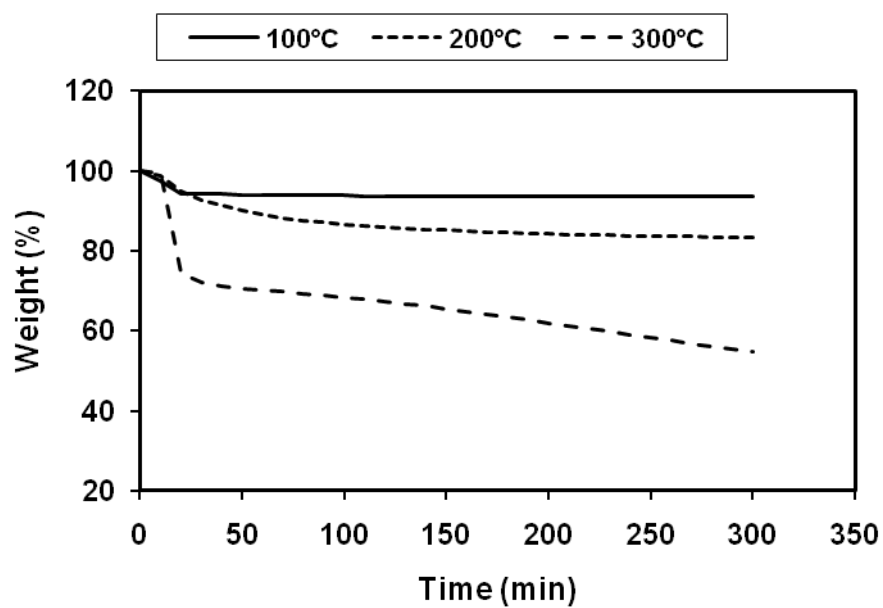


Figure 5.22 Isothermal TGA of PEDOT-SPI1 [105].

The weight retention after heating at 300 °C for 5 h is 55.96% for PEDOT-SPI2 as shown in Figure 5.23 [105].

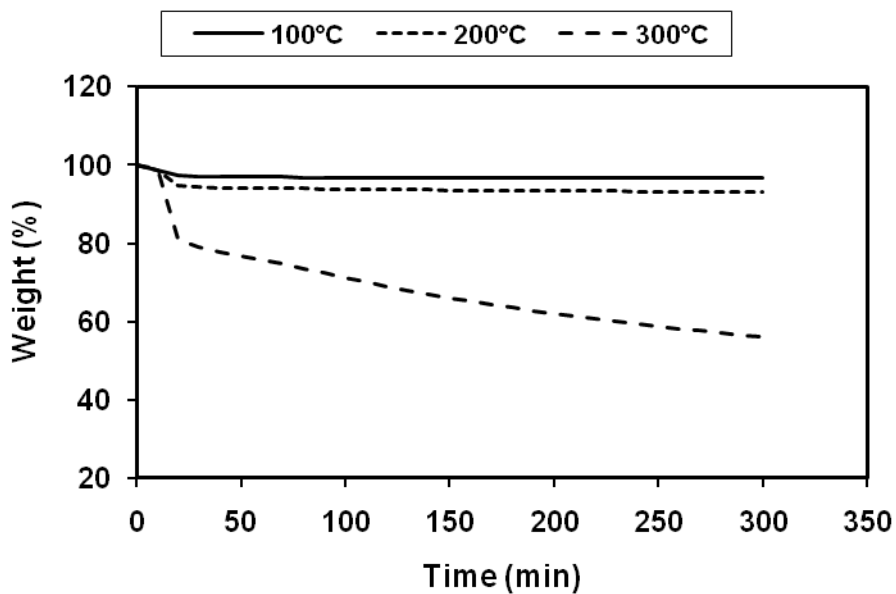


Figure 5.23 Isothermal TGA of PEDOT-SPI2 [105].

The weight retention after heating at 300 °C for 5 h is 32.16% for PANI-PSS as shown in Figure 5.24 [105].

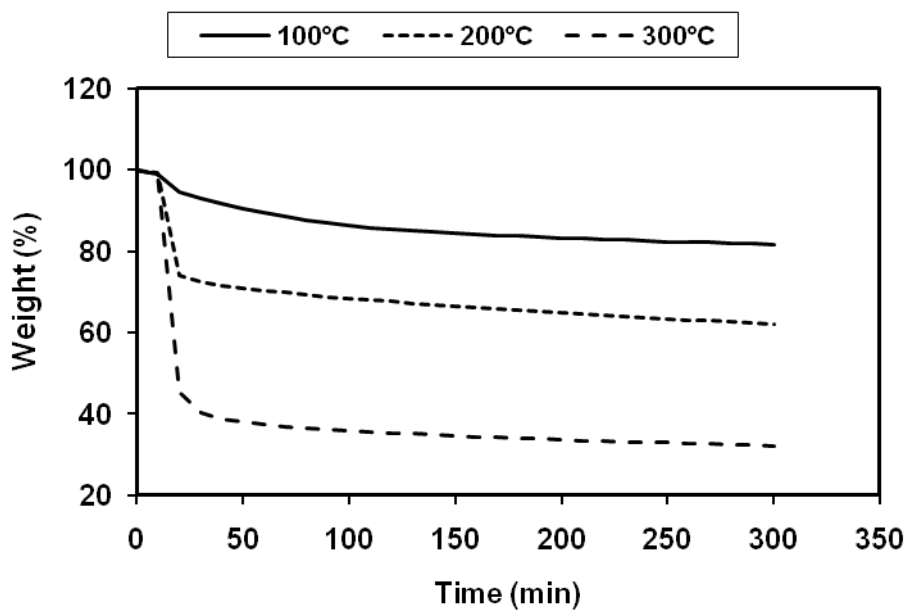


Figure 5.24 Isothermal TGA of PANI-PSS [105].

The weight retention after heating at 300 °C for 5 h is 37.49% for PANI-SPI1 as shown in Figure 5.25 [105].

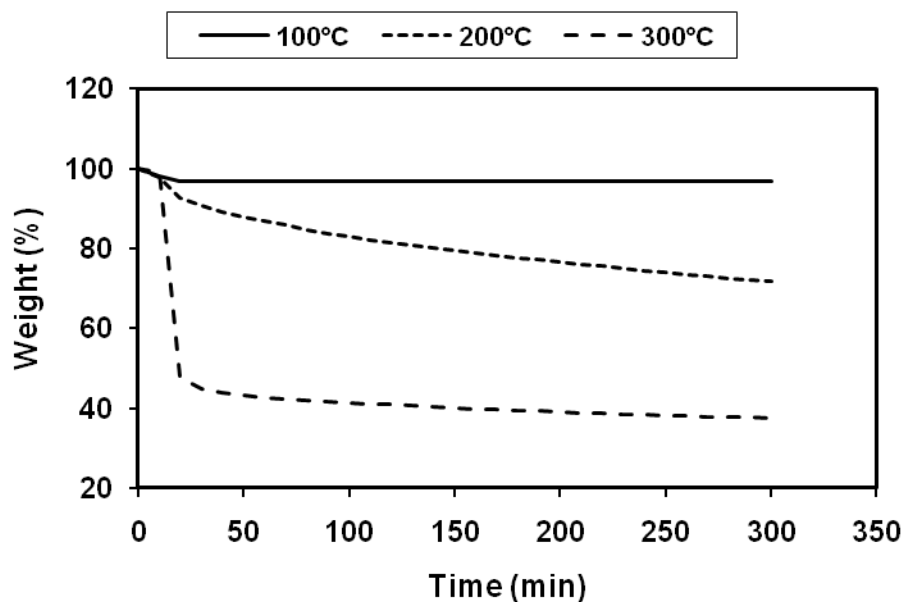


Figure 5.25 Isothermal TGA of PANI-SPI1 [105].

The weight retention after heating at 300 °C for 5 h is 40.21% for PANI-SPI2 as shown in Figure 5.26 [105].

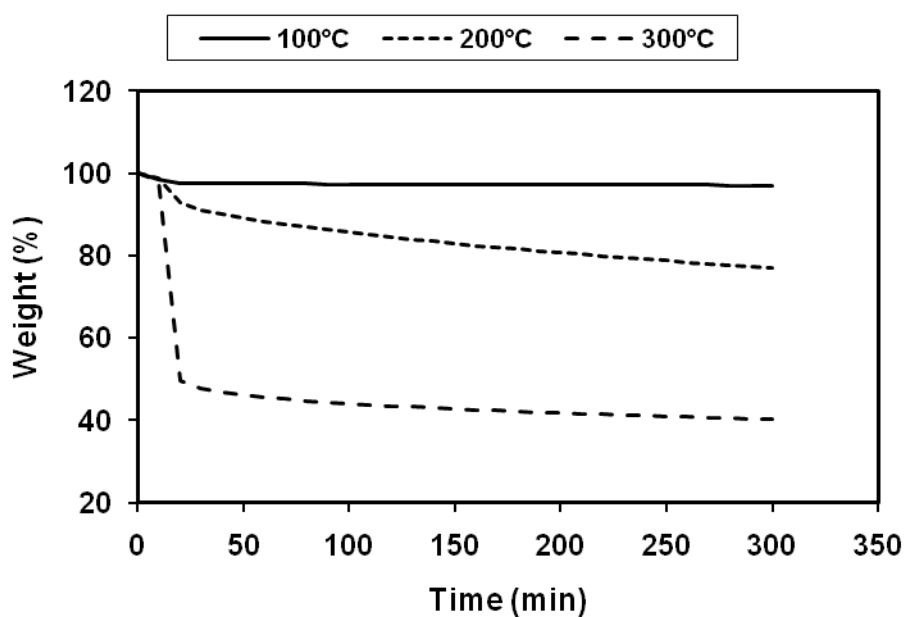


Figure 5.26 Isothermal TGA of PANI-SPI2 [105].

The weight retention after heating at 300 °C for 5 h is 31.57% for PPy-PSS as shown in Figure 5.27 [105].

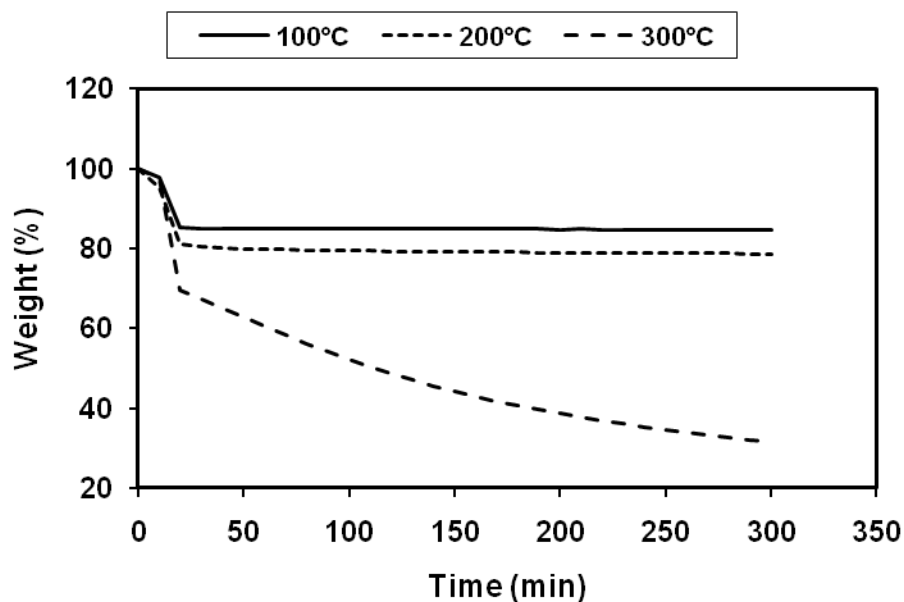


Figure 5.27 Isothermal TGA of PPy-PSS [105].

The weight retention after heating at 300 °C for 5 h is 42.72% for PPy-SPI1 as shown in Figure 5.28 [105].

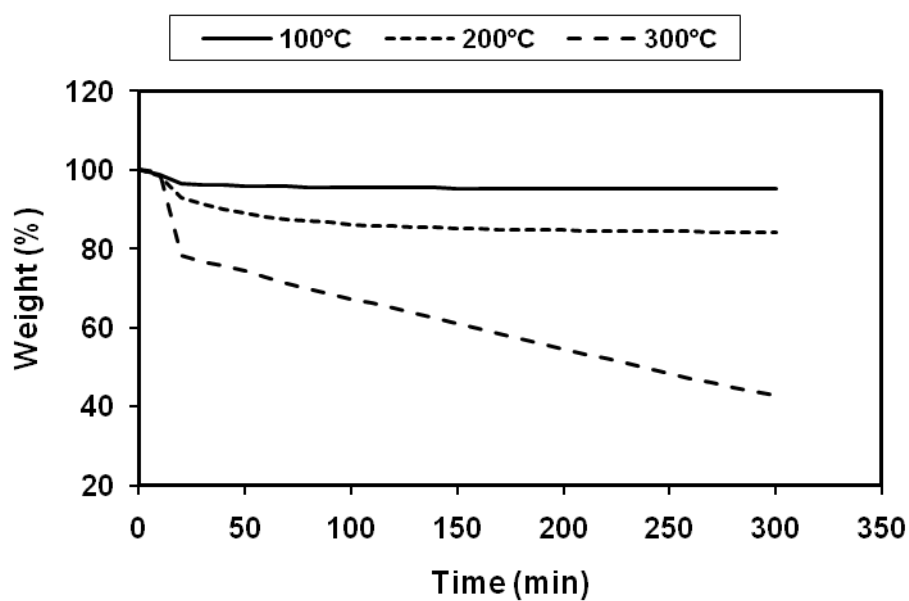


Figure 5.28 Isothermal TGA of PPy-SPI1 [105].

The weight retention after heating at 300 °C for 5 h is 62.84% for PPy-SPI2 as shown in Figure 5.29 [105].

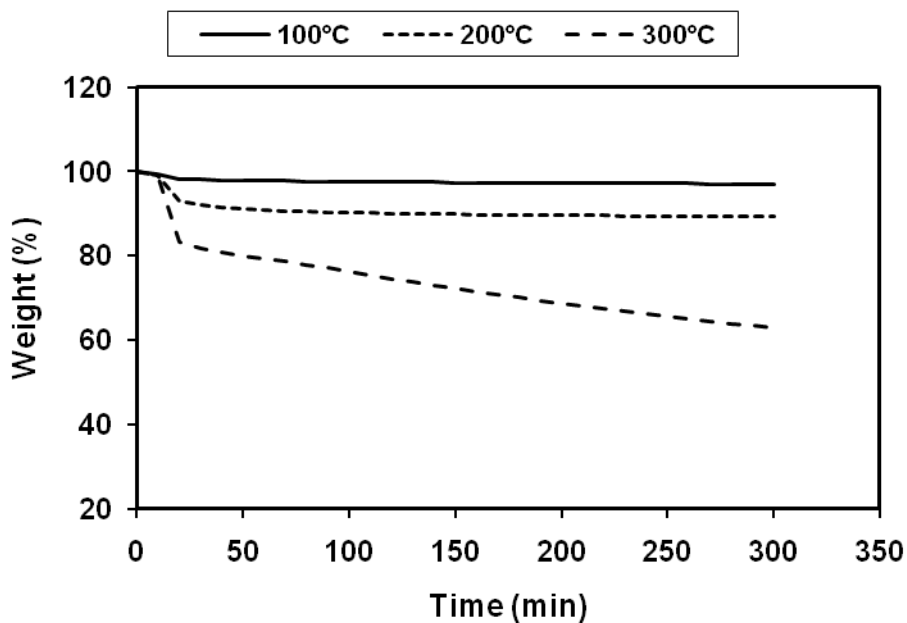


Figure 5.29 Isothermal TGA of PPy-SPI2 [105].

From the results, conducting polymers using SPI2 template were higher longer-term mass stabilities than every system of SPI1 and PSS. SPI1 has an ether bond (R-O-R) between two aromatic positions in the structure, which means this system has more flexible than using SPI2 template. Because of SPI2 has two groups of the rigidity of fluorine bond (CF₃) in the structure, which affect to the strength of chain. However, the property in term of solubility in water is another important reason for choosing the template, because the resultant polymer from template polymerization should be stand in water medium [105].

5.4 Secondary Dopants Modified PEDOT-Sulfonated Poly(imide)s for High Temperature Range Application

5.4.1 Synthesis 4,4'-ODADS monomer

4,4'-diaminodiphenyl ether (4,4'-ODA) is reacted directly with fuming sulfuric acid to synthesize 4,4'-Diaminodiphenyl ether-2,2'-disulfonic acid (4,4'-ODADS). Firstly, 4,4'-ODA was reacted with concentrated sulfuric acid (H_2SO_4) to form the sulfuric acid salt of 4,4'-ODA. Secondly, SO_3 in fuming sulfuric acid reacted with 4,4'-ODA at 80°C . FTIR and ^1H NMR spectrums were confirmed the structure of 4,4'-ODADS monomer. Fig. 5.30 showed the FTIR spectrum in absorptions at a) 1031.8 and b) 1088.3 cm^{-1} , represented to the sulfonic acid group, and at c) 3481.7 cm^{-1} , represented to NH_2 of the diamine. ^1H NMR spectrum was confirmed that the sulfonation primarily occurred at the meta position of 4,4'-ODA as shown in Fig. 5.31, [104-106].

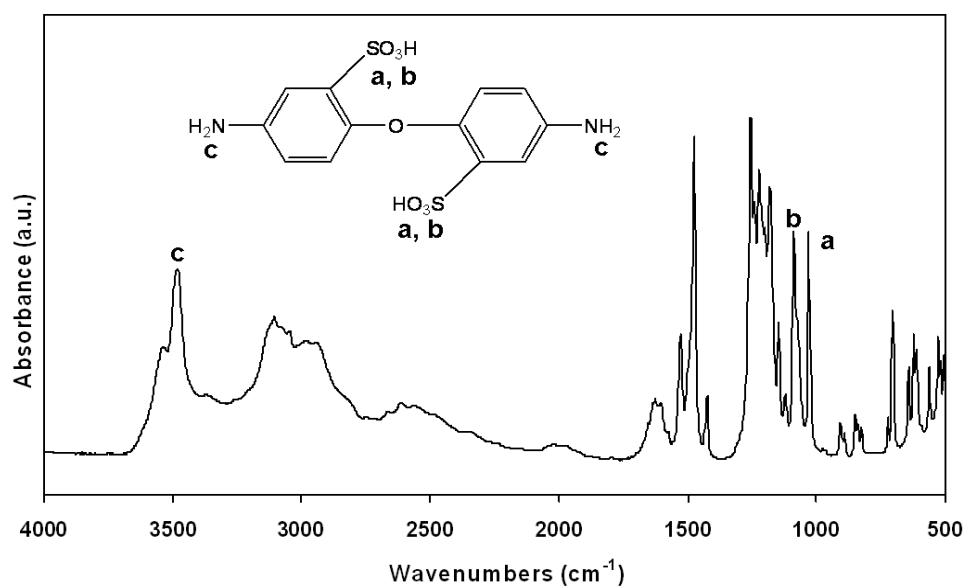


Figure 5.30 FTIR spectrum of 4,4'-ODADS [105].

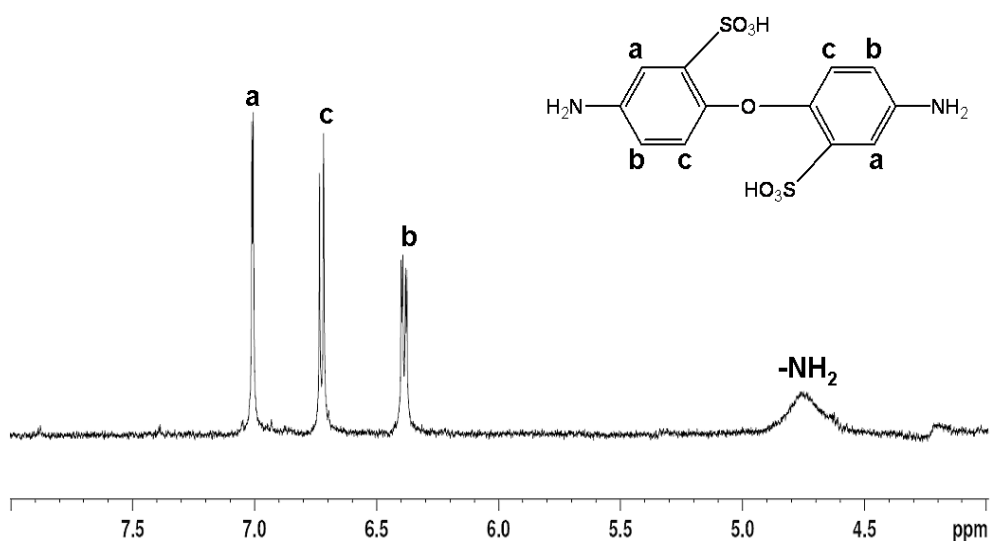


Figure 5.31 ^1H NMR spectrum of 4,4'-ODADS [105].

5.4.2 Sulfonated poly(amic acid) templates

FTIR spectrums have confirmed the structure of poly(amic acid)s as shown in Fig. 5.32. The absorbed water in the sample were represented the broad absorption band at 3476.9 cm^{-1} . The absorption bands of carbonyl group (CONH) were represented the peak at 1663.3 cm^{-1} while the peak at *ca.* $2500\text{-}3500\text{ cm}^{-1}$ were indicated the absorption bands of the carboxylic acid (COOH). The peak at 1029.0 cm^{-1} was indicated the sulfonic acid groups (SO_3H) in the structure of sulfonated poly(amic acid)s. After shot time annealing at 180°C , the symmetric imide C=O stretching and the asymmetric imide C=O stretching were represented the peak around 1720 cm^{-1} and 1780 cm^{-1} , respectively, which confirmed the complete imidization from sulfonated poly(amic acid)s to sulfonated poly(imide)s. The stretching of ethylenedioxy group was indicated at 1192 cm^{-1} while the stretching of C=C and C-C bonds in thiophene were represented at 1515 , 1473 , 1388 and 1311 cm^{-1} [104-105].

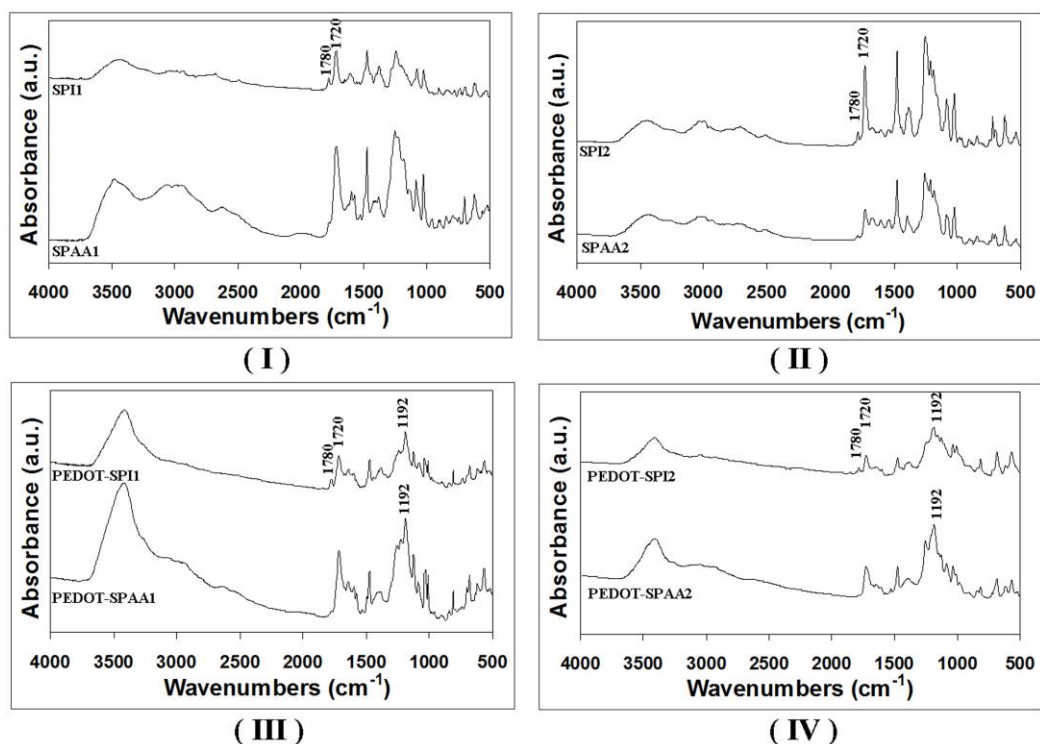


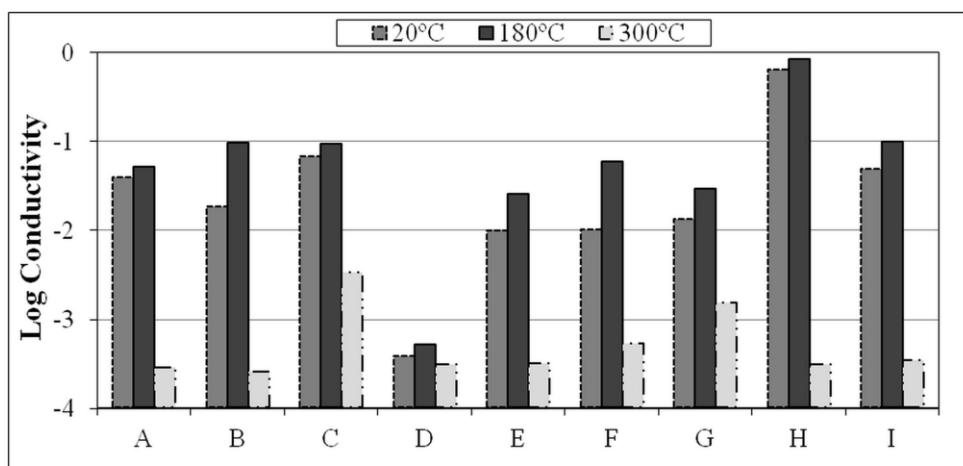
Figure 5.32 (I) FTIR spectrum of SPAA1 and SPI1, (II) SPAA2 and SPI2, (III) PEDOT-SPAA1 and PEDOT-SPI1, (IV) PEDOT-SPAA2 and PEDOT-SPI2.

5.4.3 Conductivity

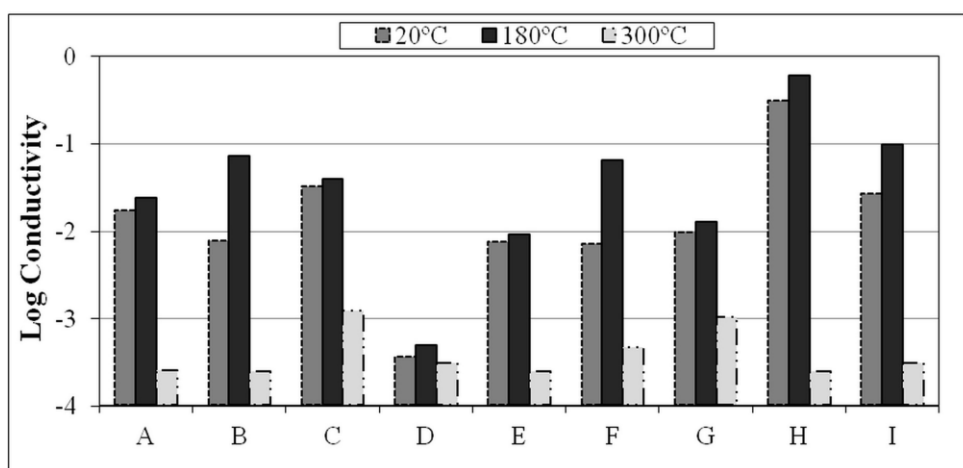
Conductivities from the new method (mechanical stirrer) were higher than that the old method (magnetic stirrer) [104-105], *ca.* 100-2,000 fold. This was attributed to the highly shear-force exerted by mechanical stirrer, exerted during polymerization. The observed aqueous dispersion of conducting polymers showed the particles size in nano-scale (Fig. 5.34). The new method can not only increase the batch size but also reduced the reaction time from 7 days to 3 days in order to obtain the same dark blue colored solution.

The conductivities of PEDOT-PSS were decreased after annealed at 180°C or at 300°C, resulted in less thermally stable than PEDOT-SPAA1 and PEDOT-SPAA2. However, un-doped PEDOT-SPAA1 and PEDOT-SPAA2 showed the lower conductivity than that PEDOT-PSS, which drove the needs to use the secondary doping technique to enhance the conductivity. The effects from new dopants (benzo-1,4-dioxan, imidazole, quinoline, methyl viologen and quinoxaline) of PEDOT-SPAA1 and PEDOT-SPAA2 were investigated and compared with the common

dopants (DMF, d-sorbitol and surfynol) at room temperature, 180°C and 300°C, respectively (Fig. 5.33). The results of doping with imidazole were exhibited more conductivities than un-doped PEDOT-SPAA1 and PEDOT-SPAA2, and still higher than doped with DMF and surfynol at room temperature. Moreover, the further increased in conductivity of 20-30% when annealing at 180°C, 10 minutes (Table 5.12) were observed with imidazole doping system. Although the conductivities of the systems doping with benzo-1,4-dioxan and quinoxaline were lower than un-doped PEDOT-SPAA1 and PEDOT-SPAA2 at room temperature, surprisingly their conductivities were enhanced 428-828% after annealed at 180°C for 10 minutes. After heat treatment, the chain alignment within the films would be changed due to the differences in rigidity of the poly(amic acid), before heated, and the poly(imide), after heated, leading to the modified morphologies, which caused the enhancement in the observed conductivities [105]. On the other hands, doping with quinoline and methyl viologen showed the decrease in conductivity due to the accumulated particles of PEDOT-SPAA1 and PEDOT-SPAA2 in aqueous solution after doping, indicated the poor alignment of structure when cast as films on glass template. The conductivity results from using the first template (SPAA1) were higher than that using the SPAA2. However, after heat treatment at 300°C, 10 minutes, the conductivities of PEDOT-SPAA1 and PEDOT-SPAA2 systems were decreased due to decomposition of the structures of the conducting polymers at higher temperature.



PEDOT-SPAA1



PEDOT-SPAA2

Figure 5.33 Conductivities of each system at 20°C, 180°C and 300°C. (A = Un-doped conducting polymers, B = Doped with benzo-1,4-dioxan (0.1 wt.%), C = Doped with imidazole (5 wt.%), D = Doped with quinoline (0.1 wt.%), E = Doped with methyl viologen (5 wt.%), F = Doped with quinoxaline (0.1 wt.%), G = Doped with DMF (0.1 wt.%), H = Doped with d-sorbitol (5 wt.%), I = Doped with surfynol (0.1 wt.%).

Table 5.12 Comparison conductivities of conducting polymers before and after annealing at 180°C, 10 minutes.

| Sample | PEDOT-SPAA1 | | | PEDOT-SPAA2 | | |
|--------|-----------------------|-----------------------|------------|-----------------------|-----------------------|------------|
| | Conductivities (S/cm) | | Increasing | Conductivities (S/cm) | | Increasing |
| | at RT | after 180°C | (%) | at RT | after 180°C | (%) |
| A | 3.82×10^{-2} | 5.11×10^{-2} | 33.77 | 1.72×10^{-2} | 2.37×10^{-2} | 37.79 |
| B | 1.80×10^{-2} | 9.51×10^{-2} | 428.33 | 7.64×10^{-3} | 7.09×10^{-2} | 828.01 |
| C | 6.72×10^{-2} | 9.30×10^{-2} | 38.39 | 3.19×10^{-2} | 3.84×10^{-2} | 20.38 |
| D | 3.80×10^{-4} | 5.05×10^{-4} | 32.89 | 3.60×10^{-4} | 4.83×10^{-4} | 34.17 |
| E | 9.63×10^{-3} | 2.50×10^{-2} | 167.09 | 7.40×10^{-3} | 9.12×10^{-3} | 23.24 |
| F | 9.91×10^{-3} | 5.79×10^{-2} | 484.26 | 6.98×10^{-3} | 6.43×10^{-2} | 821.20 |
| G | 1.32×10^{-2} | 2.84×10^{-2} | 115.15 | 9.51×10^{-3} | 1.24×10^{-2} | 30.39 |
| H | 6.26×10^{-1} | 8.30×10^{-1} | 32.59 | 3.06×10^{-1} | 5.85×10^{-1} | 91.18 |
| I | 4.85×10^{-2} | 9.80×10^{-1} | 102.06 | 3.99×10^{-2} | 9.71×10^{-2} | 143.36 |

5.4.4 Particle size distribution analysis and morphology

The particle sizes of the colloidal dispersions PEDOT-PSS and PEDOT-SPAA1 and PEDOT-SPAA2 were investigated by TEM, as shown in Fig. 5.14. TEM images of the samples clearly indicated that the materials had uniform solid nanoparticles network and their diameters of PEDOT-PSS(a), PEDOT-SPAA1(b) and PEDOT-SPAA2(c) samples were about 54, 45 and 78 nm, respectively.

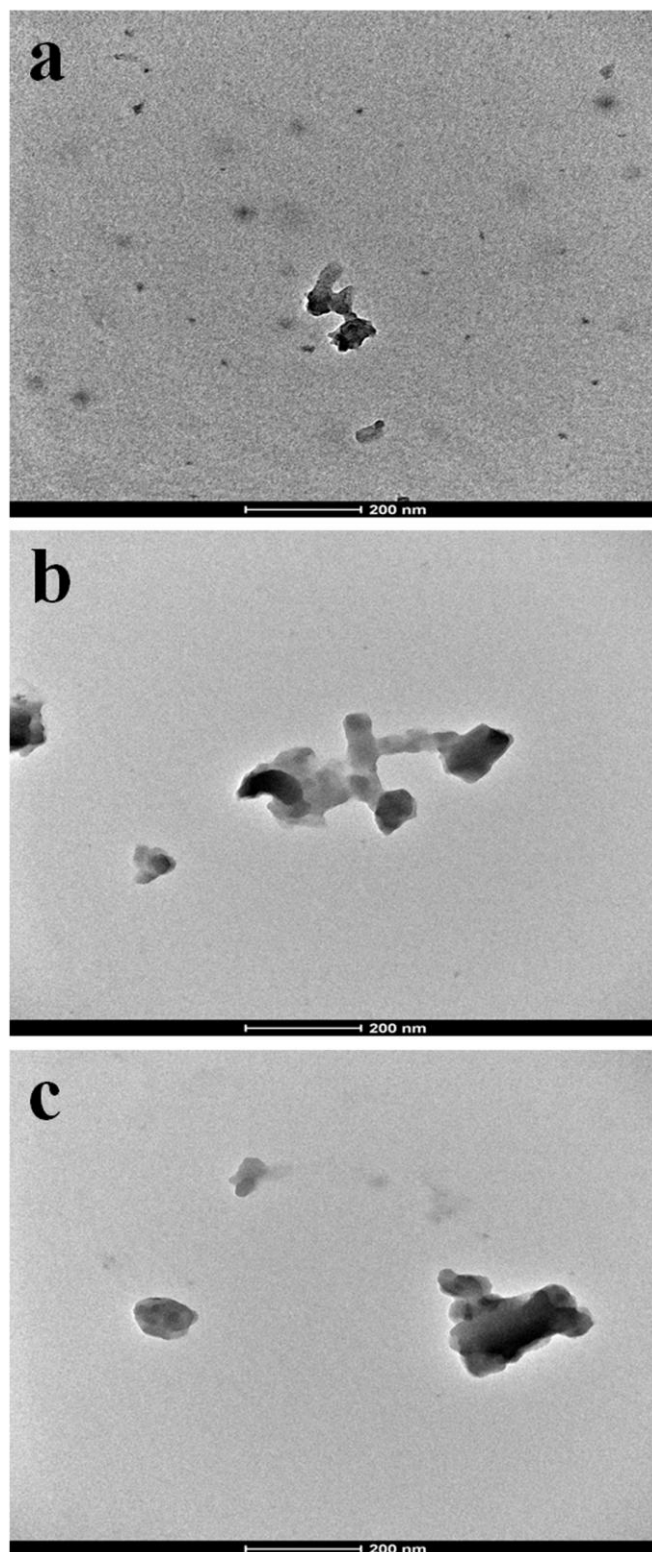


Figure 5.34 TEM images of PEDOT-PSS (a), PEDOT-SPAA1 (b) and PEDOT-SPAA2 (c).

CHAPTER VI

CONCLUSIONS & RECOMMENDATIONS

6.1 Conclusions

6.1.1 Preparation and Characterization of Conductive Polyimide-graft-Polyaniline

1. Polyimide copolymer molecules can be made conductively by cooperation of grafted polyaniline.
2. The conductivities of polyimide copolymers were in the range of 2.96-16.20 S/cm, depended on the chain length of graft polyaniline.
3. The thermal stability of the polyimides copolymer was higher than the nascent polyaniline.
4. At high temperature, polyaniline lost its conductivity but copolymers were still conductive, which proved the success of preparation of heat resisted graft-copolymer.

6.1.2 Organic Surface Conductive Polyimide

1. The mechanical properties of polyaniline-g-polyimides could be improved via two methods. The first method is casting polyaniline-g-polyimides on polyimide substrate resulting in surface-conductive polyimide. The second method is mixing polyaniline-g-polyimides together with polyimide solution resulting in conductive polyimide composites.
2. The conductivities, thermal stabilities and mechanical properties of surface-conductive polyimides (one conductive layer, one substrate layer) were higher than conductive polyimide composites (mixture of polyimide and polyaniline-g-polyimide).
3. This modification method could possibly make conductive photolithographic polyimide by further modification.

6.1.3 Comparison of the Thermally Stable Conducting Polymers PEDOT, PANI, and PPy Using Sulfonated Poly(imide) Templates via Poly(amic acid)

1. The conducting polymers: anilines, pyrroles, and thiophenes using two different poly(amic acid) templates have successfully been synthesized. The rigidity in the backbone of the new template leads to the conductivity enhancement, resulting in a 10-fold increasing for PEDOT systems.

2. PEDOT-SPAA took seven days to complete the reaction of polymerization, but it had the highest thermal stability and retained high conductivity after annealing at high temperature.

3. PANI-SPAA took less the reaction time than PEDOT-SPAA (12 h versus 7 days) and had the highest conductivity at room temperature (ca. 10 S/cm). However, their thermal stability was not good as PEDOT-SPAA, resulting in conductivity decreasing after annealing at high temperature.

4. PPy-SPAA had more thermal stability than PANI-SPAA with slightly lower conductivity. When compare with PEDOT-SPAA, PPy-SPAA had higher conductivity than PEDOT-SPAA with lower thermal stability.

5. Conducting polymers using SPAA2 template had higher thermal stability than using SPAA1 template with slightly lower conductivity.

6.1.4 Secondary Dopants Modified PEDOT-Sulfonated Poly(imide)s (SPIs) for High Temperature Range Application

1. The new method (mechanical stirring) for the synthesis of PEDOT with sulfonated poly(amic acid) template was undertaken and caused less reaction time and more conductivity than our earlier systems (magnetic stirring).

2. The conductivities of PEDOT-SPAAAs could be further enhanced by using the secondary dopants in combination with heat treatment. After heat treatment, the structures of PEDOT-SPAAAs were changed to PEDOT-SPIs and their conductivities were increased as the same time.

3. Benzo-1,4-dioxan, imidazole and quinoxaline were investigated as the new dopants at high temperature and could be used as well as surfynol to improve the conductivity of PEDOT-SPIs (better than DMF dopant).

4. The high thermal stability and highly conductivity PEDOT-SPIs have successfully been synthesized in order to apply for higher application temperature or higher processing temperature without detrimental to the conductivity.

6.2 Recommendations

6.2.1 The condition of secondary doping with new dopants could be further improved in term of concentration and annealing time to enhance the maximum conductivity for PEDOT-SPIs.

6.2.2 The method of film formations should be prepared by spin-coating to obtain thinner, which has higher conductivity.

REFERENCES

- [1] Dahiya, R.S., Adami, A., Collini, C., and Lorenzelli, L. Fabrication of Single Crystal Silicon Mirco-/Nanostructures and Transferring them to Flexible Substrates. Microelectronic Engineering 98 (2012) : 502-507.
- [2] Watcharaphalakorn, S., Ruangchuay, L., Chotpattananont, D., Srivat, A., and Schwank, J. Polyaniline/polyimide blends as gas sensors and electrical conductivity response to CO–N₂ mixtures. Polymer International 54 (2005) : 1126–1133.
- [3] Su, T.M., Ball, I.J., Conklin, J.A., Huang, S.C., Larson, R.K., Song, L., Nguyen, S.L., Lew, B.M., and Kaner, R.B. Polyaniline/polyimide blends for pervaporation and gas separation studies. Synthetic Metal 84 (1997) : 801–802.
- [4] Wang, H.L., and Mattes, B.R. Gas transport and sorption in polyaniline thin film. Synthetic Metal 102 (1999) : 1333–1334.
- [5] Ball, I.J., Huang, S.C., Wolf, R.A., Shimano, J.Y., and Kaner, R.B. Pervaporation studies with polyaniline membranes and blends. Journal of Membrane Science 174 (2000) : 161–176.
- [6] Meloni, A.W., and Bernhard, Brian C. Polyimide based substrate comprising doped polyaniline. US patent (2008) : 7,316,791.
- [7] Moon, G.H., and Seung, S.I. Morphological study of conductive polyaniline/polyimide blends. I. Determination of compatibility by small-angle X-ray scattering method. Polymer 42 (2001) : 7449-7454.
- [8] Chao, D., Lu, X., Chen J., Liu, X., Zhang, W.J., and Wei, Y. Synthesis and characterization of electroactive polyamide with amine-capped aniline pentamer and ferrocene in the main chain by oxidative coupling polymerization. Polymer 47 (2006) : 2643-2648.
- [9] Kuan, Y.H., Yu, S.J., Pei, S.W., Chieh, H.L., Yuan, H.Y., and Jui, M.Y. Electrochemical studies for the electroactivity of amine-capped aniline trimer on the anticorrosion effect of as-prepared polyimide coatings. European Polymer Journal 45 (2009) : 485-493.

- [10] Tang, Z., Donohoe, S.T., Robinson, J.M., Chiarelli, P.A., and Wang, H.L. Film formation, surface character, and relative density for electrochromic PEI/(PSS:PEDOT) multilayered thin films. Polymer 46 (2005) : 9043-9052.
- [11] Huh, D.H., Chae, M., Bae, W.J., Jo, W.H., and Lee, T.W. A soluble self-doped conducting polyaniline graft copolymer as a hole injection layer in polymer light-emitting diodes. Polymer 48 (2007) : 7236-7240.
- [12] Tarkuc, S., Sahin, E., Toppare, L., Colak, D., Chianga, I., and Yagci, Y. Synthesis, characterization and electrochromic properties of a conducting copolymer of pyrrole functionalized polystyrene with pyrrole. Polymer 47 (2006) : 2001-2009.
- [13] Ghosh, M.K., and Mittal, K.L. Polyimides, fundamentals and applications. New York : Mercel-Dekker, 1996.
- [14] Sroog, C.E., Endrey, A.L., Abroma, S.V., Berr, C.E., Edward, W.M., and Oliver, K.L. Aromatic polypyromellitimides from aromatic polyamic acids. Journal of Applied Polymer Science, Part A 3 (1965) : 1373-1390.
- [15] Ardashnikov, A.Y., Kardash, I.Y., and Pravednmkov, A.N. The nature of the equilibrium in the reaction of aromatic anhydrides with aromatic amines and its role in synthesis of polyimides. Journal Polymer Science USSR 13 (1971) : 2092-2100.
- [16] Pmavcdnikov, A.N., Kardash, I.Y., Glukhovedov, N.P. and Ardasltmmtkov, A.Y. Some features of the synthesis of heat-resistant heterocyclic polymers. Journal Polymer Science USSR 15 (1973) : 399-410.
- [17] Nechayev, P.P., Vygodskii, Ya.S., Zaikov, G.Ye. and Vmnagradova, S.V. The mechanism of formation and decomposition of polyimides. Journal Polymer Science USSR 18 (1976) : 1903-1919.
- [18] Kolegov, V. I., Belen'kii, B. G. and Frenkel, S. Ya. Study of the formation of polyamido acids. Comparison of theoretical and experimental results. Journal Polymer Science USSR 19 (1977) : 2146-2152.
- [19] Kreuz, J.A., Endrey, A.L., Gay, F.P. and Smog, C.E. Journal of Applied Polymer Science, Part A 4 (1966) : 2607-2616.

- [20] Angelo, R.J., Golike, R.C., Tatum, W.E. and Kreuz, J.A., Recent Advance in Polyimide Science and Technology. Brookfield, CT, 1985.
- [21] Russel, B. High Temperature Polymers for Proton Exchange Membrane Fuel Cells. Doctoral Dissertation, Department of Macromolecular Science and Engineering, Faculty of Engineering, Virginia Tech, 2005.
- [22] Iojoiu, C., Marechal, M., and Chabert, F. Mastering sulfonation of aromatic polysulfones: crucial for membranes for fuel cell application. Fuel Cells 5 (2005) : 344-354.
- [23] Patil, A.O., Heeger, A.J., and Wudl, F. Optical-properties of conducting polymers. Chemical Reviews 88 (1988) : 183-200.
- [24] Seymour, R.B. Conductive Polymers; Polymer Science and Technology. 1st ed. New York : Plenum Press, 1981.
- [25] Maness, K.M., Terrill, R.H., Meyer, T.J., Murray, R.W., and Wightman, R.M. Solid state diode like chemiluminescence based on serial, immobilized concentration gradients in mixed-valent poly [Ru(vbpy)(3)] (PF6)(2) films. Journal of the American Chemical Society 118 (1996) : 10609-10616.
- [26] Dupon, R., Whitmore, D.H., and Shriver, D.F. Transference number measurements for the polymer electrolyte poly(ethylene oxide). Journal of the Electrochemical Society 128 (1981) : 715-716.
- [27] Huang, J.C. Carbon black filled conducting polymers and polymer blends. Advances in Polymer Technology 21 (2002) : 299-313.
- [28] Sichel, E.K. Carbon Black-Polymer Composites: the Physics of Electrically Conducting Composites (Plastics engineering). New York : Marcel Dekker, 1982.
- [29] Billingham, N.C., and Calvert, P.D. Electrically conducting polymers – a polymer science viewpoint. Advances in Polymer Science 90 (1989) : 1-104.
- [30] Fenton, D.E., Parker, J.M., and Wright, P.V. Complexes of alkali metal ions with poly(ethylene oxide). Polymer 14 (1973) : 589-590.
- [31] Bruce, P.G. Solid State Electrochemistry. new ed. Cambridge, UK : Cambridge University Press, 1997.

- [32] Gray, F.M. Polymer Electrolytes; RSC Materials Monographs. 1st ed. Cambridge, UK : The Royal Society of Chemistry, 1997.
- [33] Scrosati, B. Applications of Electroactive Polymers. London : Chapman and Hall, 1993.
- [34] Armand, M.B., Chabagno, J.M., and Duclot, M.J. Polyethers as solid electrolytes. Fast Ion Transparent Solids: Electrodes Electrolytes. Proceeding of the International Conference, 1979.
- [35] Gray, F.M. Solid Polymer Electrolytes: Fundamentals and Technological Applications. New York : Wiley-VCH Verlag GmbH, 1991.
- [36] Bruce, P.G. Rechargeable lithium batteries. Philosophical Transactions of the Royal Society of London 354 (1996) : 1577-1594.
- [37] Lightfoot, P., Mehta, M.A., and Bruce, P.G. Crystal- structure of the polymer electrolyte poly(ethylene oxide)₃LiCF₃SO₃. Science 262 (1993) : 883-885.
- [38] Macglashan, G.S., Andreev, Y.G., and Bruce, P.G. Structure of the polymer electrolyte poly(ethylene oxide) (6): LiAsF₆. Nature 398 (1999) : 792-794.
- [39] Skotheim, T.A. Handbook of Conducting Polymers. London : CRC Press, 1986.
- [40] Chiang, C.K., Druy, M.A., Gau, S.C., Heeger, A.J., Louis, E.J., Macdiarmid, A. G., Park, P.W., and Shirakawa, H. Synthesis of highly conducting film of derivatives of polyacetylene. Journal of the American Chemical Society 100 (1978) : 1013-1016.
- [41] Cao, Y., Qiu, J.J., and Smith, P. Effect of solvents and cosolvents on the processibility or polyaniline.1.Solubility and conductivity studies. Synthetic Metals 69 (1995) : 187-190.
- [42] Cao, Y., Smith, P., and Heeger, A.J. Counterion induced processibility of conducting polyaniline and of conducting polyblends of polyaniline in bulk polymers. Synthetic Metals 48 (1992) : 91-97.
- [43] Moore, W.J. Seven Solid States: An Introduction to the Chemistry and Physics of Solids. New York : Benjamin, 1967.
- [44] Diaz, A.F., Kanazawa, K., and Gardini, G.P. Electrochemical polymerization of pyrrole. Chemical Communications 14 (1979) : 635-636.

- [45] Polowinski, S. Template Polymerization. Ontario : ChemTec Publishing, 1997.
- [46] Elschner, A., Kirchmeyer, S., Lovenich, W., Merker, U., and Reuter, K. PEDOT Principles and Applications of an Intrinsically Conductive Polymer. New York : CRC Press, 2011.
- [47] Atkins, P.W. Physical Chemistry. 5th ed. Oxford, UK : Oxford University Press, 1994.
- [48] Perepichka, I.F., and Perepichka, D.F. Handbook of Thiophene-based Materials. West Sussex, UK : John Wiley&Sons Ltd, 2009.
- [49] Reuter, K., Kirchmeyer, S., and Elschner, A. PEDOT-Properties and Technical Relevance. West Sussex, UK : John Wiley&Sons Ltd, 2009.
- [50] Shirakawa, H. The discovery of polyacetylene film. The dawning of an era of conducting polymers. Synthetic Metals 125 (2002) : 3-10.
- [51] Macdiarmid, A.G. Synthetic metals: a novel role for organic polymers. Synthetic Metals 125 (2002) : 11-22.
- [52] Heeger, A.J. Semiconducting and metallic polymers: the fourth generation of polymeric materials. Synthetic Metals 125 (2002) : 23-42.
- [53] Kondo, H., Ono, S., and Irie, S. Pyrrole derivatives. IV. Condensation of β -bromovulnic ester with acetoacetic ester and ammonia. Yakugaku Zasshi 57 (1937) : 404-406.
- [54] Guha, P.C., and Iyer, B.H. Attempts towards the synthesis of cantharidin, part II. Journal of the Indian Institute of Science 21 (1938) : 115-118.
- [55] Gogte, V.N., Shah, L.G., Tilak, B.D., Gadekar, K.N., and Sahasrabudhe, M.B. Synthesis of potential anticancer agents-I, synthesis of substituted thiophenes. Tetrahedron 23 (1967) : 2437-2441.
- [56] Heywang, G., and Jonas, F. Poly(alkylenedioxythiophene)s-new, very stable conducting polymers. Advanced Materials 4 (1992) : 116-118.
- [57] Coffey, M., Mckellar, B.R., Reinhardt, B.A., Nijakowski, T., and Feld, W.A. A facile synthesis of 3,4-dialkoxythiophenes. Synthetic Communications 26 (1996) : 2205-2212.
- [58] Quintero, D.C., and Bauerle, P. Synthesis of the first enantiomerically pure and chiral, disubstituted 3,4-ethylenedioxythiophene (EDOTs) and corresponding stereo- and regioregular PEDOTs. Chemical Communications

- (2004) : 926-927.
- [59] Reuter, K. Transition metal-catalyzed nucleophilic substitution at thiophene halides. German Patent DE (2001) : 10,162,746.
- [60] Aasmundtveit, K.E., Samuelsen, E.J., Petterson, L.A.A., Inngas, O., Johansson, T., and Feidenhansl, R. Structure of thin films of poly (3,4-ethylenedioxythiophene). Synthetic Metals 101 (1999) : 561-564.
- [61] Reuter, K., Karbach, A., Ritter, H., and Wrubbel, N. Alkylendioxythiophene and Poly(alkylendioxythiophene) mit mesogenen Gruppen. European Patent EP (2004) : 1,440,974.
- [62] Ghosh, S., and Inngas, O. Self-assembly of a conducting polymer nanostructure by physical crosslinking: applications to conducting blends and modified electrodes. Synthetic Metals 101 (1999) : 413-416.
- [63] Weast, R.C. Handbook of Chemistry and Physics. 66th ed. Boca Raton : CRC Press, 1985.
- [64] Zotti, G., Zecchin, S., Schiavon, G., Louwet, F., Groenendaal, L., Crispin, X., Osikowicz, W., Salaneck, W., and Fahlman, M. Electrochemical and XPS studies towards the role of monomeric and polymeric sulfonate counterions in the synthesis, composition and properties of poly(3,4-ethylenedioxythiophene). Macromolecules 36 (2003) : 3337-3344.
- [65] Hwang, J., Tanner, D.B., Schwendeman, I., and Reynolds, J.R. Optical properties of nondegenerate ground-state polymers: Three dioxythiophene-based conjugated polymers. Physical Review B 67 (2003) : 1-10.
- [66] Macdiarmid, A.G., and Epstein, A.J. The concept of secondary doping as applied to polyaniline. Synthetic Metals 65 (1994) : 103-106.
- [67] Jang, J. Conducting polymer nanomaterials and their applications. Advances in Polymer Science 199 (2006) : 189-259.
- [68] Chatzidaki, E.K., Favvas, E.P., Papageorgeou, S.K., Kanellopoulos, N.K. and Theophilou, N.V. New polyimide-polyaniline hollow fibers : Synthesis, characterization and behavior in gas separation. European Polymer Journal 43 (2007) : 5010-5016.

- [69] Han, M.G. and Im, S.S. Processable conductive blends of polyaniline/polyimide. Jornal of Applied Polymer Science 67 (1998) : 1863-1870.
- [70] Han, M.G. and Im, S.S. Electrical and structural analysis of conductive polyaniline/polyimide blends. Jornal of Applied Polymer Science 71 (1999) : 2169-2178.
- [71] Han, M.G. and Im, S.S. X-ray photoelectron spectroscopy study of electrically conducting polyaniline/polyimide blends . Polymer 41 (2000) : 3253-3262.
- [72] Han, M.G. and Im, S.S. Morphological study of conductive polyaniline/polyimide blends. I. Determination of compatibility by small angle X-ray scattering method. Polymer 42 (2001) : 7449-7454.
- [73] Lu, X.H., Xu, J.W. and Wong, L.M. Blends of polyimide and dodecylbenzene sulfonic acid-doped polyaniline: Effects of polyimide structure on electrical conductivity and its thermal degradation. Synthetic Metals 156 (2006) : 117-123.
- [74] Wang, Z.Y., Yang, C., Gao, J.P., Lin, J., Meng, X.S., Wei, Y. and Li, S. Electroactive Polyimides Derived from Amino-Terminated Aniline Trimer. Macromolecules 31 (1998) : 2702-2704.
- [75] Chao, D.M., Cui, L.L., Lu, X.F., Mao, H., Zhang, W.J. and Wei, Y. Electroactive polyimide with oligoaniline in the main chain via oxidative coupling polymerization. European Polymer Journal 43 (2007) : 2641-2647.
- [76] Kim, J.Y., Jung, J.H., Lee, D.E., and Joo, J. Enhancement of electrical conductivity of poly(3,4-ethylenedioxythiophene)/poly(4-styrenesulfonate) by a change of solvents. Synthetic Metals 126 (2002) : 311-316.
- [77] Ouyang, J., Xu, Q., Chu, C.W., Yang, Y., Li, G., and Shinar, J. On the mechanism of conductivity enhancement in poly (3,4-ethylenedioxythiophene):poly(styrene sulfonate) film through solvent treatment. Polymer 45 (2004) : 8443-8450.
- [78] Lee, B., Seshadri, V., and Sotzing, G.A. Poly(thieno[3,4-b]thiophene)-poly(styrene sulfonate): a low band gap, water dispersible conjugated polymer. Langmuir 21 (2005) : 10797-10802.

- [79] Ouyang, J., Chu, C.W., Chen, F.C., Xu, Q., and Yang, Y. High-conductivity poly(3,4-ethylenedioxythiophene):poly(styrene sulfonate) film and its application in polymer optoelectronic devices. Advanced Functional Materials 15 (2005) : 203-208.
- [80] Lee, B., Seshadri, V., and Sotzing, G.A. Water dispersible low band gap conductive polymer based on thieno[3,4-b]thiophene. Synthetic Metals 152 (2005) : 177-180.
- [81] Huang, J., Miller, P.F., Wilson, J.S., Mello, A.J., Mello, J.C., and Bradley, D.D.C. Investigation of the effects of doping and post-deposition treatments on the conductivity, morphology, and work function of poly(3,4-ethylenedioxythiophene)/poly(styrene sulfonate) films. Advanced Functional Materials 15 (2005) : 290-296.
- [82] Jang, J., Ha, J., and Cho, J. Fabrication of water dispersible polyaniline-poly(4-styrenesulfonate) nanoparticles for inkjet-printed chemical sensor applications. Advanced Materials 19 (2007) : 1772-1775.
- [83] Nardes, A.M., Kemerink, M., Kok, M.M., Vinken, E., Maturova, K., and Janssen, R.A. Conductivity, work function, and environmental stability of PEDOT:PSS thin films treated with sorbitol. Organic Electronics 9 (2008) : 727-734.
- [84] Kang, K.S., Chen, Y., Han, K.J., Yoo, K.H., and Kim, J. Conductivity enhancement of conjugated polymer after HCl-methanol treatment. Thin Solid Films 517 (2009) : 5909-5912.
- [85] Chen, Y., Kang, K.S., Han, K.J., Yoo, K.H., and Kim, J. Enhanced optical and electrical properties of PEDOT:PSS films by the addition of MWCNT-sorbitol. Synthetic Metals 159 (2009) : 1701-1704.
- [86] Wang, G.F., Tao, X.M., Xin, J.H., and Fei, B. Modification of conductive polymer for polymeric anodes of flexible organic light-emitting diodes. Nanoscale Research Letters 4 (2009) : 613-617.
- [87] Dimitriev, O.P., Grinko, D.A., Noskov, Y.V., Ogurtsov, N.A., and Pud, A.A. PEDOT:PSS films-effect of organic solvent additives and annealing on the film conductivity. Synthetic Metals 159 (2009) : 2237-2239.
- [88] Ner, Y., Invernale, M.A., Grote, J.G., Stuart, J.A., and Sotzing, G.A. Facile

- chemical synthesis of DNA- doped PEDOT. Synthetic Metals 160 (2010) : 351-353.
- [89] Yang, C., and Liu, P. Water-dispersed polypyrrole nanoparticles via chemical oxidative polymerization in the presence of a functional polyanion. Reactive & Functional Polymers 70 (2010) : 726-731.
- [90] Faure, S., Mercier, R., Aldebert, P., Pineri, M., and Sillion, B. French Patent (1996) : 9,605,707.
- [91] Gunduz, N. Synthesis and Characterization of Sulfonated Polyimides as Proton Exchange Membranes for Fuel Cells. Doctoral Dissertation, Department of Chemistry, Faculty of Science, Virginia Tech, 2001.
- [92] Genies, C. Stability study of sulfonated phthalic and naphthalenic polyimide structures in aqueous medium. Polymer 42 (2001) : 5097-5105.
- [93] Fang, J., Guo, X., Harada, S., Watari, T., Tanaka, K., Kita, H., and Okamoto, K. Novel sulfonated polyimides as polyelectrolytes for fuel cell application. 1. synthesis, proton conductivity, and water stability of polyimides from 4,4'-diaminodiphenyl ether-2,2'-disulfonic acid. Macromolecules 35 (2002) : 9022-9028.
- [94] Okamoto, K. Methanol permeability and proton conductivity of sulfonated copolyimide membranes. Journal of Membrane Science 258 (2005): 115-122.
- [95] Qiu, Z., Wu, S., Li, Z., Zhang, S., Xing, W., and Liu, C. Sulfonated poly(arylene-co-naphthalimide)s synthesized by copolymerization of primarily sulfonated monomer and fluorinated naphthalimide dichlorides as novel polymers for proton exchange membranes. Macromolecules 39 (2006) : 6425-6432.
- [96] Han, M.G., Cho, S.K., Oh, S.G., and Im, S.S. Preparation and characterization of polyaniline nanoparticles synthesized from DBSA micellar solution. Synthetic metals 126 (2002) : 53-60.
- [97] Lu, X., Xu, J., and Wong, L. Blends of polyimide and dodecylbenzene sulfonic acid-doped polyaniline: Effects of polyimide structure on electrical

- conductivity and its thermal degradation. Synthetic metals 156 (2006) : 117-123.
- [98] Chern, A.T., and Wang, J.J. Hydrolytic Stability and High Tg of Polyimides Derived from the Novel 4,9-Bis[4-(3,4-dicarboxyphenoxy)phenyl]-diamantane Dianhydride. Journal of Polymer Science Part A: Polymer Chemistry 47 (2009) : 1673-1684.
- [99] Chern, Y.T., Twu, J.T., and Chen, J.C. High Tg and high organosolubility of novel polyimides containing twisted structures derived from 4-(4-amino-2-chlorophenyl)-1-(4-aminophenoxy)-2,6-di-tert-butylbenzene. European Polymer Journal 54 (2009) : 1127-1138.
- [100] Xing, Y., Wang, D., Gao, H., and Jiang, Z. Synthesis and Properties of Novel Polyimide Optical Materials with Different Haloid Pendant. Journal of Applied Polymer Science 112 (2011) : 738-747.
- [101] Srisuwan, S., Thongyai, S., and Praserttham, P. Synthesis and characterization of low-dielectric photosensitive polyimide/silica hybrid materials. Journal of Applied Polymer Science 117 (2010) : 2422-2427.
- [102] He, Y. Synthesis of polyaniline/nano-CeO₂ composite microspheres via a solid-stabilized emulsion route. Materials Chemistry and Physics 92 (2005) : 134-137.
- [103] Lu, Y., Renb, Y., Wang, L., Wang, X., and Li, C. Template synthesis of conducting polyaniline composites based on honeycomb ordered polycarbonate film. Polymer 50 (2009) : 2035-2039.
- [104] Somboonsub, B., Invernale, M.A., Thongyai, S., Praserttham, P., Scola, D.A., and Sotzing, G.A. Preparation of the thermally stable conducting polymer PEDOT-Sulfonated poly(imide). Polymer 51 (2010) : 1231-1236.
- [105] Somboonsub, B., Srisuwan, S., Invernale, M.A., Thongyai, S., Praserttham, P., Scola, D.A., and Sotzing, G.A. Comparison of the Thermally Stable Conducting Polymers PEDOT, PANi, and PPy Using Sulfonated Poly(Imide) Templates. Polymer 51 (2010) : 4472-4476.
- [106] Fang, J., Guo, X., Harada, S., Watari, T., Tanaka, K., Kita, H., and Okamoto, K. Novel sulfonated polyimides as polyelectrolytes for fuel cell

application. 1. Synthesis, proton conductivity, and water stability of polyimides from 4,4'-diaminodiphenyl ether-2,2'-disulfonic acid. Macromolecules 35 (2002) : 9022-9028.

APPENDICES

APPENDIX A

CONDUCTIVITY CHARACTERIZATION

A-1 Conductivities of PEDOT-PSS, PEDOT-SPAA_s and PEDOT-SPI_s.

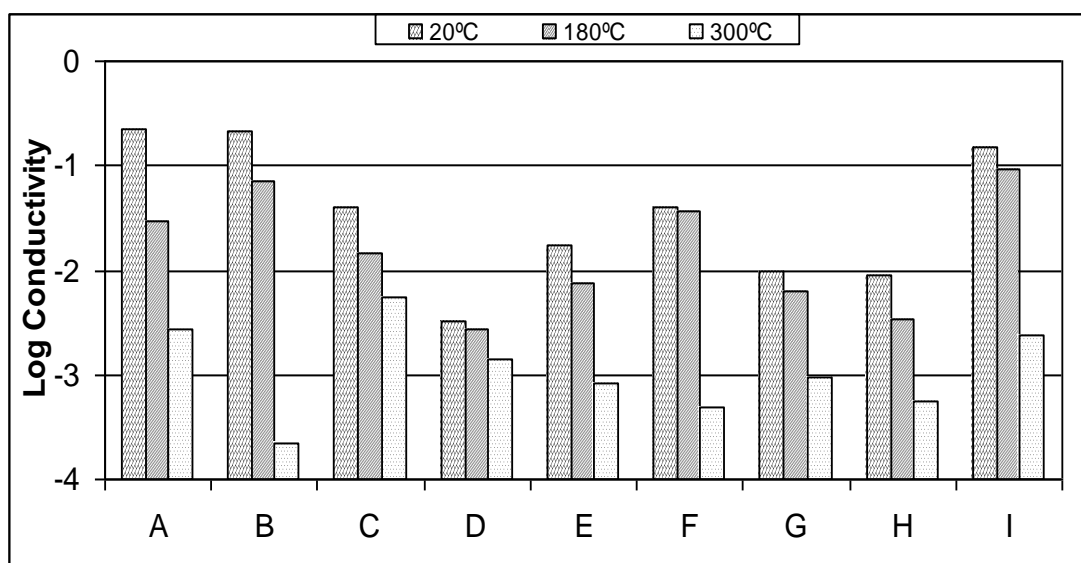
Table A-1 Conductivities of PEDOT-PSS (in house) and PEDOT-SPAA. Upon annealing, PEDOT-SPAA imidizes to PEDOT-SPI.

| Processing Temperature | | PEDOT-PSS | PEDOT-SPAA1 | PEDOT-SPAA2 |
|-------------------------------|----------------------------|-----------------------|-----------------------|-----------------------|
| 20°C | Conductivity (S/cm) | 2.28×10^{-1} | 5.80×10^{-2} | 1.72×10^{-2} |
| | Std. Dev. | 2.96×10^{-2} | 1.30×10^{-3} | 2.77×10^{-3} |
| 180°C (90 min) | Conductivity (S/cm) | 5.05×10^{-3} | 6.11×10^{-3} | 5.56×10^{-3} |
| | Std. Dev. | 1.89×10^{-3} | 2.09×10^{-3} | 2.24×10^{-3} |
| 300°C (10 min) | Conductivity (S/cm) | $< 1 \times 10^{-5}$ | 2.83×10^{-4} | 2.48×10^{-4} |
| | Std. Dev. | $< 1 \times 10^{-5}$ | 6.71×10^{-5} | 6.23×10^{-5} |

A-2 Conductivities of secondary-doped PEDOT-PSS.

Table A-2 Conductivities of secondary-doped PEDOT-PSS at various processing temperatures.

| Processing Temperature | | PEDOT-PSS | Benzo-1,4-dioxan 0.1 wt.% | Imidazole 5 wt.% |
|------------------------|---------------------|-----------------------|---------------------------|-----------------------|
| | 20°C | Conductivity (S/cm) | 2.28×10^{-1} | 2.12×10^{-1} |
| Std. Dev. | | 2.96×10^{-2} | 6.98×10^{-2} | 3.08×10^{-2} |
| 180°C (10 min) | Conductivity (S/cm) | 2.93×10^{-2} | 6.99×10^{-2} | 1.45×10^{-2} |
| | Std. Dev. | 2.37×10^{-2} | 4.28×10^{-2} | 1.32×10^{-2} |
| 300°C (10 min) | Conductivity (S/cm) | 2.73×10^{-3} | 2.23×10^{-4} | 5.56×10^{-3} |
| | Std. Dev. | 2.15×10^{-3} | 5.86×10^{-6} | 2.81×10^{-3} |
| Processing Temperature | | Quinoline 0.1 wt.% | Methyl viogen 5 wt.% | Quinoxaline 0.1 wt.% |
| 20°C | Conductivity (S/cm) | 3.27×10^{-3} | 1.72×10^{-2} | 3.94×10^{-2} |
| | Std. Dev. | 4.91×10^{-4} | 4.91×10^{-4} | 1.33×10^{-2} |
| 180°C (10 min) | Conductivity (S/cm) | 2.73×10^{-3} | 7.65×10^{-3} | 3.72×10^{-2} |
| | Std. Dev. | 1.70×10^{-3} | 5.44×10^{-3} | 2.07×10^{-2} |
| 300°C (10 min) | Conductivity (S/cm) | 1.43×10^{-3} | 8.39×10^{-4} | 4.91×10^{-4} |
| | Std. Dev. | 3.62×10^{-4} | 3.94×10^{-5} | 2.18×10^{-4} |
| Processing Temperature | | DMF 0.1 wt.% | d-sorbitol 5 wt.% | Surfynol 0.1 wt.% |
| 20°C | Conductivity (S/cm) | 9.72×10^{-3} | 9.03×10^{-3} | 1.50×10^{-1} |
| | Std. Dev. | 3.75×10^{-3} | 7.49×10^{-3} | 2.47×10^{-2} |
| 180°C (10 min) | Conductivity (S/cm) | 6.17×10^{-3} | 3.44×10^{-3} | 9.33×10^{-2} |
| | Std. Dev. | 2.92×10^{-3} | 1.35×10^{-3} | 6.53×10^{-2} |
| 300°C (10 min) | Conductivity (S/cm) | 9.67×10^{-4} | 5.64×10^{-4} | 2.36×10^{-3} |
| | Std. Dev. | 4.02×10^{-4} | 3.75×10^{-4} | 1.48×10^{-3} |



A = Un-doped PEDOT-PSS

B = Doped with Benzo-1,4-dioxan (0.1 wt.%)

C = Doped with Imidazole (5 wt.%)

D = Doped with Quinoline (0.1 wt.%)

E = Doped with Methyl viogen (5 wt.%)

F = Doped with Quinoxaline (0.1 wt.%)

G = Doped with DMF (0.1 wt.%)

H = Doped with d-sorbitol (5 wt.%)

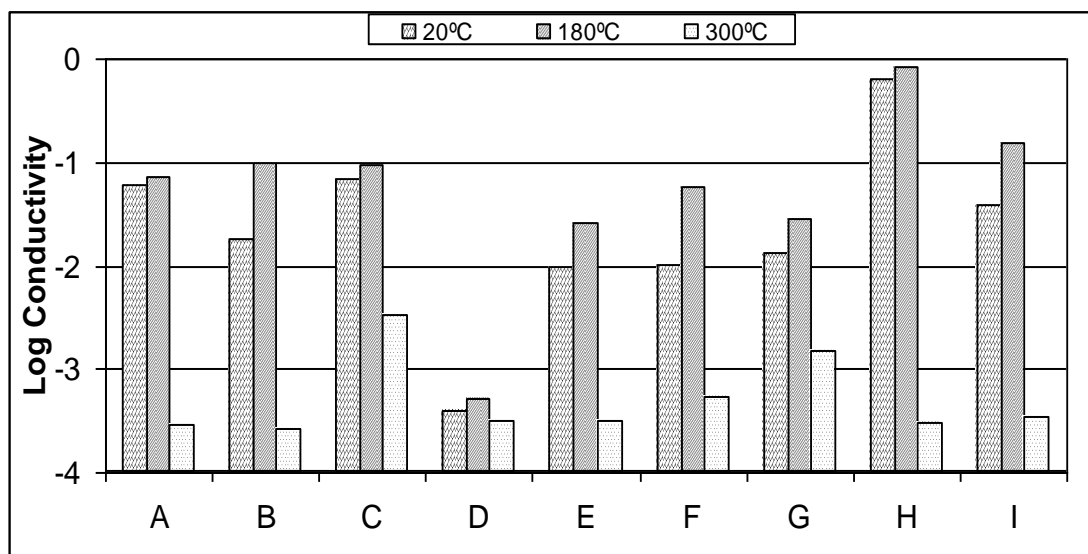
I = Doped with Surfynol (0.1 wt.%)

Figure A-1. Log conductivity of PEDOT-PSS.

A-3 Conductivities of secondary-doped PEDOT-SPAA1 and PEDOT-SPI1.

Table A-3 Conductivities of secondary-doped PEDOT-SPAA1 at various processing temperatures. Upon annealing, PEDOT-SPAA1 imidizes to PEDOT-SPI1.

| Processing Temperature | | PEDOT-SPAA1 | Benzo-1,4-dioxan 0.1 wt.% | Imidazole 5 wt.% |
|------------------------|---------------------|-----------------------|---------------------------|-----------------------|
| | 20°C | Conductivity (S/cm) | 5.80×10^{-2} | 1.80×10^{-2} |
| Std. Dev. | | 1.30×10^{-2} | 3.78×10^{-3} | 3.83×10^{-2} |
| 180°C (10 min) | Conductivity (S/cm) | 7.11×10^{-2} | 9.51×10^{-2} | 9.30×10^{-2} |
| | Std. Dev. | 2.46×10^{-2} | 6.33×10^{-2} | 6.91×10^{-2} |
| 300°C (10 min) | Conductivity (S/cm) | 2.83×10^{-4} | 2.55×10^{-4} | 3.31×10^{-3} |
| | Std. Dev. | 6.71×10^{-5} | 2.38×10^{-5} | 3.02×10^{-4} |
| Processing Temperature | | Quinoline 0.1 wt.% | Methyl viogen 5 wt.% | Quinoxaline 0.1 wt.% |
| 20°C | Conductivity (S/cm) | 3.80×10^{-4} | 9.63×10^{-3} | 9.91×10^{-3} |
| | Std. Dev. | 1.19×10^{-4} | 3.75×10^{-3} | 3.88×10^{-3} |
| 180°C (10 min) | Conductivity (S/cm) | 5.05×10^{-4} | 2.50×10^{-2} | 5.79×10^{-2} |
| | Std. Dev. | 2.34×10^{-4} | 4.28×10^{-3} | 1.25×10^{-2} |
| 300°C (10 min) | Conductivity (S/cm) | 3.09×10^{-4} | 3.12×10^{-4} | 5.25×10^{-4} |
| | Std. Dev. | 2.06×10^{-4} | 2.17×10^{-5} | 1.55×10^{-4} |
| Processing Temperature | | DMF 0.1 wt.% | d-sorbitol 5 wt.% | Surfynol 0.1 wt.% |
| 20°C | Conductivity (S/cm) | 1.32×10^{-2} | 6.26×10^{-1} | 3.85×10^{-2} |
| | Std. Dev. | 3.46×10^{-3} | 3.98×10^{-1} | 4.39×10^{-3} |
| 180°C (10 min) | Conductivity (S/cm) | 2.84×10^{-2} | 8.30×10^{-1} | 1.50×10^{-1} |
| | Std. Dev. | 6.25×10^{-3} | 5.21×10^{-1} | 2.47×10^{-2} |
| 300°C (10 min) | Conductivity (S/cm) | 1.49×10^{-3} | 3.03×10^{-4} | 3.45×10^{-4} |
| | Std. Dev. | 5.83×10^{-4} | 1.15×10^{-4} | 1.97×10^{-5} |



A = Un-doped PEDOT-SPAA1

B = Doped with Benzo-1,4-dioxan (0.1 wt.%)

C = Doped with Imidazole (5 wt.%)

D = Doped with Quinoline (0.1 wt.%)

E = Doped with Methyl viogen (5 wt.%)

F = Doped with Quinoxaline (0.1 wt.%)

G = Doped with DMF (0.1 wt.%)

H = Doped with d-sorbitol (5 wt.%)

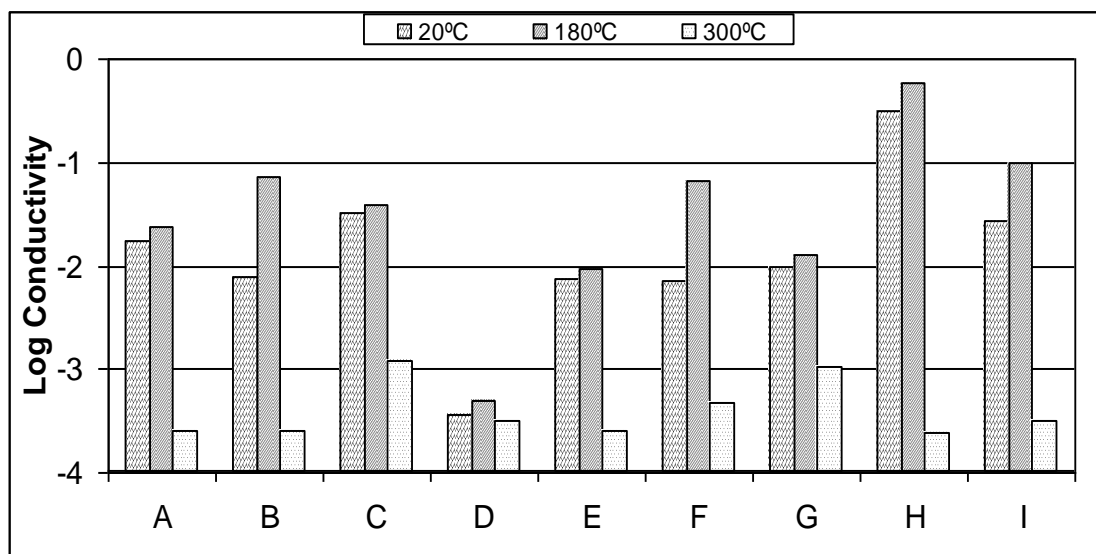
I = Doped with Surfynol (0.1 wt.%)

Figure A-2 Log conductivity of PEDOT-SPAA1.

A-4 Conductivities of secondary-doped PEDOT-SPAA2 and PEDOT-SPI2.

Table A-4 Conductivities of secondary-doped PEDOT-SPAA2 at various processing temperatures. Upon annealing, PEDOT-SPAA2 imidizes to PEDOT-SPI2.

| Processing Temperature | | PEDOT-SPAA2 | Benzo-1,4-dioxan 0.1 wt.% | Imidazole 5 wt.% |
|-------------------------------|----------------------------|---------------------------|----------------------------------|-----------------------------|
| 20°C | Conductivity (S/cm) | 1.72×10^{-2} | 7.64×10^{-3} | 3.19×10^{-2} |
| | Std. Dev. | 2.77×10^{-3} | 1.72×10^{-3} | 8.25×10^{-3} |
| 180°C (10 min) | Conductivity (S/cm) | 2.37×10^{-2} | 7.09×10^{-2} | 3.84×10^{-2} |
| | Std. Dev. | 3.10×10^{-3} | 4.14×10^{-2} | 2.40×10^{-2} |
| 300°C (10 min) | Conductivity (S/cm) | 2.48×10^{-4} | 2.45×10^{-4} | 1.20×10^{-3} |
| | Std. Dev. | 6.23×10^{-5} | 5.14×10^{-5} | 1.01×10^{-4} |
| Processing Temperature | | Quinoline 0.1 wt.% | Methyl viogen 5 wt.% | Quinoxaline 0.1 wt.% |
| 20°C | Conductivity (S/cm) | 3.60×10^{-4} | 7.40×10^{-3} | 6.98×10^{-3} |
| | Std. Dev. | 6.38×10^{-5} | 1.94×10^{-3} | 2.00×10^{-3} |
| 180°C (10 min) | Conductivity (S/cm) | 4.83×10^{-4} | 9.12×10^{-3} | 6.43×10^{-2} |
| | Std. Dev. | 2.28×10^{-4} | 3.47×10^{-3} | 2.06×10^{-2} |
| 300°C (10 min) | Conductivity (S/cm) | 3.06×10^{-4} | 2.44×10^{-4} | 4.63×10^{-4} |
| | Std. Dev. | 2.06×10^{-4} | 8.77×10^{-5} | 2.13×10^{-4} |
| Processing Temperature | | DMF 0.1 wt.% | d-sorbitol 5 wt.% | Surfynol 0.1 wt.% |
| 20°C | Conductivity (S/cm) | 9.51×10^{-3} | 3.06×10^{-1} | 8.99×10^{-3} |
| | Std. Dev. | 3.61×10^{-3} | 1.18×10^{-1} | 3.66×10^{-3} |
| 180°C (10 min) | Conductivity (S/cm) | 1.24×10^{-2} | 5.85×10^{-1} | 9.71×10^{-2} |
| | Std. Dev. | 2.88×10^{-3} | 3.47×10^{-1} | 7.31×10^{-2} |
| 300°C (10 min) | Conductivity (S/cm) | 1.02×10^{-3} | 2.42×10^{-4} | 7.05×10^{-4} |
| | Std. Dev. | 4.22×10^{-4} | 1.03×10^{-4} | 1.94×10^{-4} |



A = Un-doped PEDOT-SPAA2

B = Doped with Benzo-1,4-dioxan (0.1 wt.%)

C = Doped with Imidazole (5 wt.%)

D = Doped with Quinoline (0.1 wt.%)

E = Doped with Methyl viogen (5 wt.%)

F = Doped with Quinoxaline (0.1 wt.%)

G = Doped with DMF (0.1 wt.%)

H = Doped with d-sorbitol (5 wt.%)

I = Doped with Surfynol (0.1 wt.%)

Figure A-3 Log conductivity of PEDOT-SPAA2.

APPENDIX B
THERMOGRAVIMETRIC ANALYSIS (TGA)
CHARACTERIZATION

B-1 TGA of Poly(styrene sulfonic acid) (PSSA) [104-105].

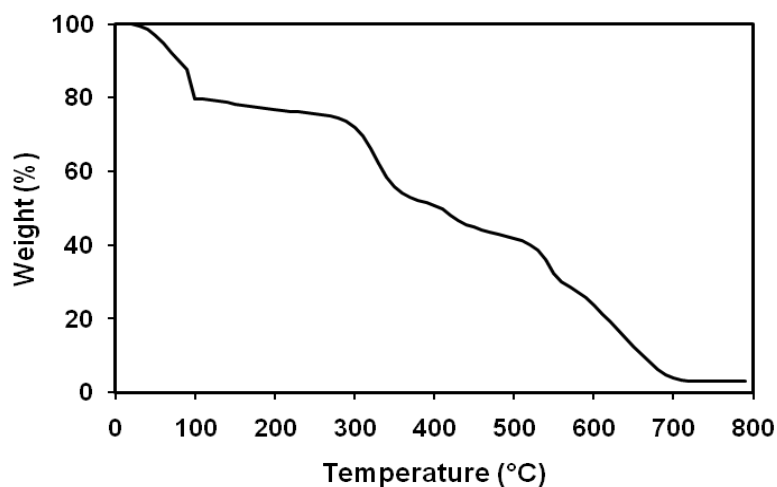


Figure B-1 TGA of Poly(styrene sulfonic acid) (PSSA) in air [104-105].

B-2 TGA of Poly(3,4-ethylenedioxythiophene) (PEDOT) [104-105].

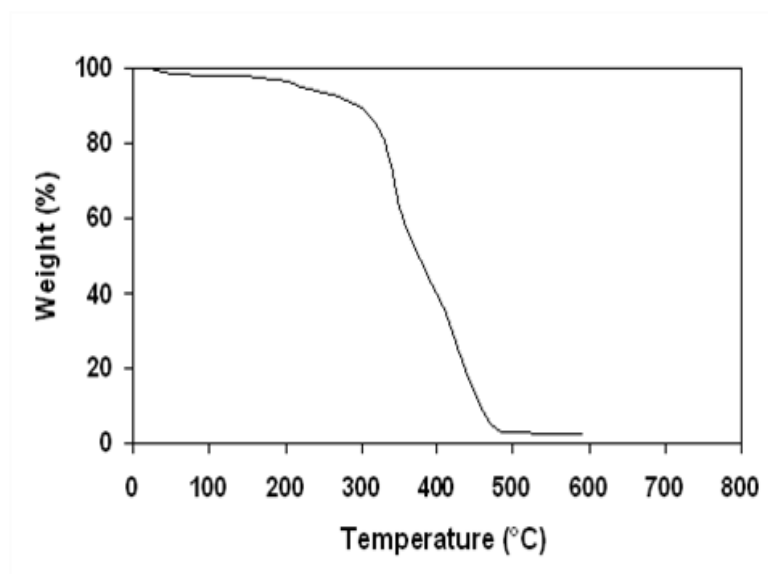


Figure B-2 TGA of Poly(3,4-ethylenedioxythiophene) (PEDOT) in air [104-105].

B-3 TGA of sulfonated poly(amic acid) (SPAA) [104-105].

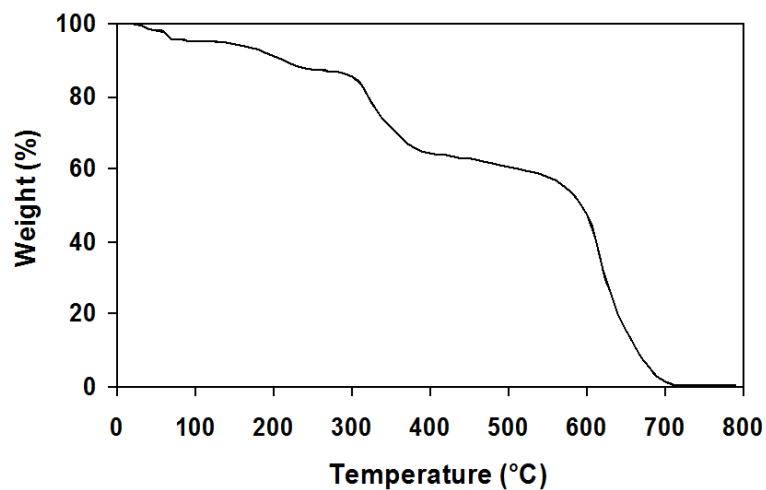


Figure B-3 TGA of sulfonated poly(amic acid) (SPAA) in air [104-105].

B-4 Isothermal TGA of Poly(3,4-ethylenedioxythiophene) (PEDOT) [104-105].

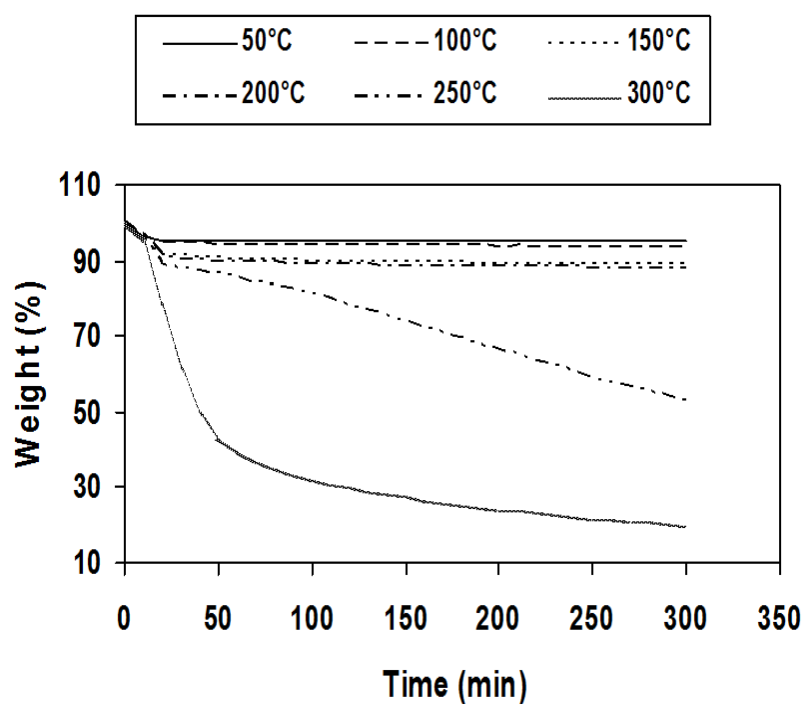
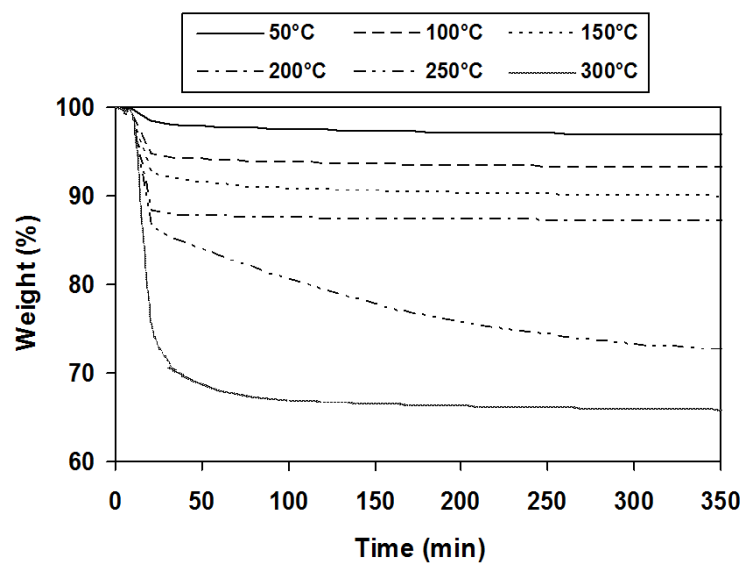


Figure B-4 Isothermal TGA of PEDOT [104-105].

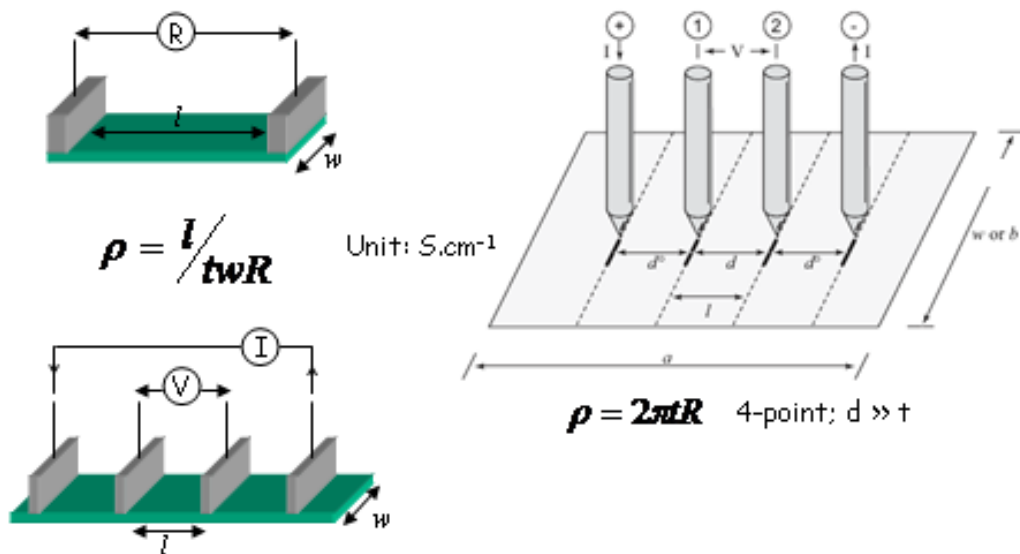
B- 5 Isothermal TGA of Sulfonated poly(amic acid) (SPAA) [104-105].

**Figure B-5** Isothermal TGA of SPAA [104-105].

APPENDIX C

CONDUCTIVITY CALCULATION

Conductivity



Definition

Conductivity is calculated from the equation of $\sigma = l/twR$ (S/cm) where l is the distance between gold or platinum wires, t is the thickness of the film, and w is the width of the film.

Resistance is calculated from the equation of $R = V/I$ (Ω) where V is the voltage measured and I is the current applied [104-105].

APPENDIX D

LIST OF PUBLICATIONS

Articles

1. Suttisak Srisuwan, Supakanok Thongyai, Gregory A. Sotzing and Piyasan Praserthdam, "Preparation and characterization of conductive polyimide-graft-polyaniline" Microelectronic Engineering 104 (2013) : 22-28.
2. Suttisak Srisuwan, Supakanok Thongyai, Gregory A. Sotzing and Piyasan Praserthdam, "Organic Surface Conductive Polyimide" to be submitted to Microelectronic Engineering.
3. Bongkoch Somboonsub, Suttisak Srisuwan, Michael A. Invernale, Supakanok Thongyai, Piyasan Praserthdam, Daniel A. Scola, and Gregory A. Sotzing, "Comparison of the thermally stable conducting polymers PEDOT, PANI, and PPy using sulfonated poly(imide) templates" Polymer 51 (2010) : 4472-4476.
4. Suttisak Srisuwan, Yujie Ding, Donna Mamangun, Supakanok Thongyai, Piyasan Praserthdam and Gregory A. Sotzing, "Secondary dopants modified PEDOT-sulfonated poly(imide)s for high-temperature range application" Applied Polymer Science 128 (2013) : 3840-3845.

Conference contributions

1. Poster: Suttisak Srisuwan, Bongkoch Somboonsub, Michael A. Invernale, Supakanok Thongyai, Piyasan Praserthdam, Daniel A. Scola, and Gregory A. Sotzing, "Template polymerization of conducting polymers using sulfonated poly(amic acid)", 240th American Chemical Society ACS National Meeting, Boston, USA August 22-26, 2010.

VITA

Mr. Suttisak Srisuwan was born on July 19, 1983 in Songkhla, Thailand. He received the Bachelor's Degree in Chemical Engineering from Department of Chemical Engineering, Faculty of Engineering, Prince of Songkhla University in April 2006. He received the Degree of Master of Engineering in Chemical Engineering at the Department of Chemical Engineering, Chulalongkorn University in 2008. After the M.Eng graduation, he has received a funding from Mektec Manufacturing Corporation (Thailand) Ltd. to study the Doctoral Degree of Engineering in Chemical Engineering at Chulalongkorn University in June 2008. He spent one year research at Institute of Materials Science and the Polymer program, University of Connecticut, USA.